Environmental extractability of chromium(III) and nickel from soils of South Africa's Eastern Highveld

by

Petrus Stephanus Rossouw

**Submitted in partial fulfilment of the requirements for the degree
MSc (Agric) Soil Science
In the Faculty of Natural and Agricultural Sciences
Department of Plant Production and Soil Science
University of Pretoria**

Supervisor: Mr P.C. de Jager

January 2009

UNIVERSITEIT VAN PRETORIA
UNIVERSITY OF PRETORIA
YUNIBESITHI YA PRETORIA

I, Petrus Stephanus Rossouw (ID: 8102095032088), declare that the thesis/desertation, which I hereby submit for the degree Msc (Agric) Soil Science at the University of Pretoria, is my own work and has not previously been submitted by me for a degree at this or any other tertiary institution.

Signature: ....

Date: ....

Table of contents

Table of contents i
List of figures iv
List of tables vi
Abstract viii
Introduction 1
References 3

Chapter 1 Chromium transformation on soil mineral surfaces: a review 5
1.1 Abstract 5
1.2 Introduction 5
1.3 Cr speciation in the soil environment 5
1.4 Sorption of Cr(VI) onto soil mineral surfaces 7
1.5 Reduction of Cr(VI) to Cr(III) 10
  1.5.1 Cr(VI) reduction by organic matter 11
  1.5.2 Cr(VI) reduction by Fe(II) 12
1.6 Sorption of Cr(III) onto soil mineral surfaces 14
1.7 Organic ligand induced dissolution of Cr(III) 18
1.8 Oxidation of Cr(III) to Cr(VI) by Mn-oxides 18
1.9 Inhibiting Cr(III) oxidation to Cr(VI) 21
1.10 Conclusion 21
1.11 References 23

Chapter 2 Nickel transformation on soil mineral surfaces: a review 29
2.1 Abstract 29
2.2 Introduction 29
2.3 Sorption of nickel onto iron oxide minerals 30
2.4 Sorption of Ni onto manganese oxides 34
2.5 Sorption of Ni onto aluminium oxides 35
2.6 Sorption of Ni onto clay minerals 36
2.7 Formation of Ni surface precipitates 40
2.8 Ageing of Ni surface precipitates 43
2.8 Ni surface precipitate stability 45

2.9 Conclusion 48
2.10 References 49

Chapter 3 Environmental extractability of chromium(III) and nickel correlated with soil water potential and the mineralogy of three South African Highveld soils 53
3.1 Abstract 53
3.2 Introduction 53
3.3 Materials and methods 56
  3.3.1 Soil characterisation 56
  3.3.2 Batch equilibration study 60
    3.3.2.1 Experimental setup 61
    3.3.2.2 Experimental approach 64
3.4 Results and discussion 66
  3.4.1 Cr(III) and Ni mobility correlated with soil water potential 66
  3.4.2 Cr(III) and Ni mobility correlated with soil mineralogy 75
  3.4.3 Predicting Cr(III) and Ni mobility 86
3.5 Conclusion 88
3.6 References 90

Chapter 4 Chromium(III) and nickel extractability as influenced by rewetting and drying cycles and an external source of silicon 97
4.1 Abstract 97
4.2 Introduction 97
4.3 Materials and methods 99
  4.3.1 Soil characterisation 100
  4.3.2 Batch equilibrium study 103
4.4 Results and discussion 105
  4.4.1 0.1 M $Mg(NO_3)_2$ extractable Cr(III) and Ni 105
  4.4.2 0.02 M diammonium EDTA extractable Cr(III) and Ni 107
  4.4.3 Cr(III) and Ni mobility linked to cation exchange and anion exchange capacity 112
  4.4.4 Effect of Si on Cr(III) stability 113
  4.4.5 Effect of Si on Ni stability 116
4.5 Conclusion 120

4.6 References 122

Chapter 5 Steel plant slag reactivity and heavy metal release in a highly buffered soil 128
5.1 Abstract 128
5.2 Introduction 128
5.3 Materials and methods 130
  5.3.1 Slag reactivity 131
  5.3.2 Slag heavy metal content 131
  5.3.3 Batch equilibration study: slag-amended soil 131
5.4 Results and discussion 134
  5.4.1 Slag reactivity 134
  5.4.2 Heavy metal release 136
5.5 Conclusion 143
5.6 References 145

Chapter 6 Summary and concluding remarks 150
6.1 Introduction 150
6.2 Salt-based study: Cr(III) and Ni extractability 151
6.3 Slag-based study: Cr and Ni extractability 151
6.4 Conclusion 152

List of figures

Figure 1.1 The sorption of Cr(VI) by a variety of mineral surfaces 7
Figure 1.2 The possible surface complexes formed by Cr(VI) on goethite...................8
Figure 1.3 Complexation of Cr(III) on a) silica and b) goethite 15

Figure 2.1 The effect of pH on the sorption of various heavy metals on hematite and goethite...30
Figure 2.2 Isotherms of Ni sorbed onto 1 g/L goethite at 25°C and an ionic strength of 10^{-3} 32
Figure 2.3 Solubility of heavy metals from a kaolinite system 37
Figure 2.4 Solubilisation of heavy metals from a mixed kaolinite-humic acid system (open symbols) and their theoretical solubilisation (filled symbols); (b) solubilisation of humic acid from the mixed kaolinite-humic acid system 38
Figure 2.5 Sorption of eight heavy metals onto Na-montmorillonite as a function of pH (initial metal concentration = 1×10^{-4}M)...39
Figure 2.6 The sorption of Ni by pyrophillite, talc, gibbsite and silica as a function of time 41
Figure 2.7 The structure and composition of α-Ni(OH)$_2$ in comparison to a Al-Ni LDH. The R_{Ni-Ni} of α-Ni(OH)$_2$ is 3.07 A, whereas that of Al-NI LDH is 3.05 – 3.08 A..42
Figure 2.8 Schematic illustration of a possible mechanism for the stabilization of an Al-Ni LDH precipitate over time...44
Figure 2.9 The rate of Ni desorption from Ni reacted minerals as a function of aging of surface precipitates. Replenishment steps with EDTA at pH 7.5 are shown on the left hand side, and replenishment steps with HNO_3 at pH 4.0 on the right hand side. Ni reacted minerals are from top pyrophillite (a & b), talc (c & d), and gibbsite (e & f) 46

Figure 3.1 The 0.1 M Mg(NO$_3$)$_2$ extractable Ni fraction correlated with soil water potential...67
Figure 3.2 The 0.02 M diammonium EDTA extractable Cr(III) fraction correlated with soil water potential...69

Figure 3.3 The 0.02 M diammonium EDTA extractable Ni fraction correlated with soil water potential 71

Figure 3.4 The EDTA extractable Ni fraction correlated with Al, Fe and Mn concentrations 76

Figure 3.5 Cr(III) extractability correlated with extractants 79

Figure 3.6 The pH 2.0, 0.1 M $NH_2OH.HCl$ extractable Cr(III) fraction correlated with Al, Fe and Mn concentrations 79

Figure 3.7 The pH 2.0, 0.1 M $NH_2OH.HCl$ extractable Ni fraction correlated with Al, Fe and Mn concentrations 80

Figure 3.8 Ni extractability correlated with extractants 82

Figure 3.9 The Tamm's reagent extractable Cr(III) fraction correlated with Al, Fe and Mn concentrations 83

Figure 4.1 $Mg(NO_3)_2$ extractable Ni. 106

Figure 4.2 0.02 M diammonium EDTA extractable Cr(III). 108

Figure 4.3 0.02 M diammonium EDTA extractable Ni. 110

Figure 4.4 0.02 M diammonium EDTA extractable Cr(III) from the E-horizon (White). 114

Figure 4.5 0.02 M diammonium EDTA extractable Cr(III) from the yellow brown apedal B-horizon (Yellow). 115

Figure 4.6 0.02 M diammonium EDTA extractable Cr(III) from the red apedal B-horizon (Red). 115

Figure 4.7 0.1 M $Mg(NO_3)_2$ extractable Ni from the E-horizon (White) – plus Si treatment. 116

Figure 4.8 0.1 M $Mg(NO_3)_2$ extractable Ni from the red apedal B-horizon (Red) – plus Si treatment. 117

Figure 4.9 0.1 M $Mg(NO_3)_2$ extractable Ni from the yellow brown apedal B-horizon (Yellow) – plus Si treatment. 118

Figure 4.10 0.02 M diammonium EDTA extractable Ni - plus Si treatment............ 119

Figure 5.1 Environmental extractability of Cr 137

Figure 5.2 Environmental extractability of Ni 140

List of tables

Table 2.1 Total sorption capacity of Na-montmorillonite towards certain heavy metals. 40

Table 3.1 Soil form, colour and texture as determined under field conditions...........57
Table 3.2 Soil clay content and mineralogy expressed as a percentage of the bulk soil composition. 57
Table 3.3 Cation exchange and anion exchange capacity determined at three pH values for each of the soils investigated. 60
Table 3.4 Gravimetric soil water content (%) of the investigated three Highveld soils linked to soil water potential (J.kg^{-1}). 61
Table 3.5 0.1 M $Mg(NO_3)_2$ extractable Ni at certain soil water potential levels.........68
Table 3.6 0.02 M diammonium EDTA extractable Cr(III) at certain soil water potential levels. 69
Table 3.7 0.02 M diammonium EDTA extractable Ni at certain soil water potential levels. 72
Table 3.8 The concentrations of Cr(III), Ni, Al, Fe, and Mn extrated from three Eastern Highveld soils at a soil water potential level of -3100 J.kg^{-1} using various extractants. 77
Table 3. 9 Cr(III) and Ni extracted as a percentage of the total concentrations added and correlated to extractants used at a soil water potential of -3100 J.kg^{-1}. 85
Table 3.10 The Cr(III) and Ni fraction not extracted from the three investigated soils. 86

Table 4.1 Soil form, colour and texture as determined under field conditions..........100
Table 4.2 Soil clay content and mineralogy expressed as a percentage of the bulk soil composition. 101
Table 4.3 Cation exchange and anion exchange capacity determined at three pH values for each of the soils investigated. 103
Table 4.4 0.1 M $Mg(NO_3)_2$ extractable Cr(III) and Ni after five rewetting and drying cycle. 106
Table 4.5 0.02 M diammonium EDTA extractable Cr(III) and Ni after five rewetting and drying cycles. 110

Table 5.1 Relative neutralising capacity (RS) of the slag samples used 135
Table 5.2 Determined pH for each treatment after an equilibration period of three months 135
Table 5.3 1.0 M HNO_3 extractable metals from the slag samples used 135
Table 5.4 Environmental extractability of Cr and the contribution of slag 139
Table 5.5 Environmental extractability of Ni and the contribution of slag 141
Table 5.6 Supernatant pH determined for each treatment after being subjected to the various extractants 142

Abstract

Amid a growing world population and diminishing living space, the discerning and beneficial use of steel plant slag as liming material in agriculture has become a viable option. However, until the potentially detrimental effect on human health and environmental quality of heavy metals contained within the matrixes of slag has been assessed, the use of slag in agriculture cannot be deemed sustainable.

This study aims to correlate the mechanisms by which chromium(III) and nickel are sorbed in Eastern Highveld soils to easily classifiable soil constituents. In addition, the influence of an external source of silicon, as would be the case in dissolving slag, on Cr(III) and Ni mobility was investigated. The study consisted of an investigation into the mechanisms by which Cr(III) and Ni are sequestered in soil within a single wetting and drying cycle, as well as over a period of five rewetting and drying cycles. The effect of Si was observed for the latter and a detailed mineralogical study conducted as part of the former. Additionally, the reactivity of and heavy metal (Cr and Ni) release from two commercially available slag samples used as liming material in a highly buffered soil was investigated.

Five main conclusions were drawn: (i) whereas Cr(III) is effectively sorbed (even at near water saturated conditions) and precipitation ascribed to bulk-solution saturation, Ni is not sequestered as effectively, and initially precipitates owing to the influence of soil mineralogy; (ii) conclusive evidence could not be gathered for the further immobilisation after sorption of Cr(III) and Ni over a short time period; (iii) both Cr(III) and Ni associate mainly with the amorphous Fe oxide mineral phase; (iv) an external source of Si renders Ni less mobile in soil that does not sequester the element effectively, but more mobile in soil that does tend to sequester the element to some degree; and (v) although neither Cr(III) nor Ni mobility could be explained using field classifiable soil characteristics (soil colour and texture), soil mineralogical and detailed surface charge characterisation did provide explanations for sorption behaviour.

Introduction

Although the use of steel plant slag as an agricultural liming agent may seem viable, such an option cannot be considered without a detailed investigation into the possible detrimental effects on human health and environmental quality of heavy metals contained in the slag. Steel plant slag, among other industrial by-products, has been used for decades in agriculture and dumped without proper precautionary measures, which is testimony that environmental legislation has come into play only in the last few years.

Assessing the suitability of steel plant slag for use in agriculture should entail at least four areas of research: (i) the characterisation of slag with regards to reactivity, solubility and subsequent rate of dissolution and release of heavy metals; (ii) the interaction of these solubilised heavy metals with soil constituents in an attempt to predict metal mobility; (iii) the rate of removal of these heavy metals from soil profiles which might lead to their accumulation in lower lying areas; and (iv) the extent to which heavy metals influence the environment, especially soil microbial activity and plant uptake of heavy metals.

This study focused on the second area of research, albeit only on Cr(III) and Ni and their interactions with soil constituents. As the presence of Cr(VI) in slag is likely to disqualify the use of that specific slag in agriculture, Cr(III) will dominate the Cr speciation in the slag used to amend agricultural soils. Although not toxic in itself, Cr(III) can be oxidised to the hazardous Cr(VI) ion by numerous Mn oxide minerals (Stepniewska, Bucior and Bennicelli, 2004; Cooper, 2002; Fendorf, 1994), thus warranting an investigation into the mobility of the trivalent ion. Cr(VI) and Ni are both toxic, and are known carcinogens (Baytak and Tűrker, 2005; Christensen *et al.*, 1996). Cr(III) is known to predominantly form inner-sphere complexes with numerous soil minerals and precipitate as a hydrous chrome oxide (Fendorf, Li and Gunter, 1996; Fendorf and Sparks, 1994; Charlet and Manceau, 1992). The stability of these precipitates is a function of morphology and is influenced by soil mineral characteristics (Fendorf, 1994; Charlet and Manceau, 1992). Ni is regarded as one of the most mobile transition elements in the soil environment, forming outer-sphere and weakly held inner-sphere complexes (Christensen *et al.*, 1996). Ni precipitates predominantly as a hydroxide or layered double hydroxide. Si dissolving from mineral surfaces has been shown to stabilise these precipitates through anionic interlayer exchange. The latter process leads to cementation and the formation of a phyllosilicate precursor (Scheckel *et al.*, 2000; Ford *et al.*, 1999b; Scheidegger, Lamble and Sparks, 1996).

The aim of this study is to investigate the interactions of Cr(III) and Ni with certain soil mineral phases in an attempt to identify soil characteristics which could aid the prediction of Cr(III) and Ni mobility in the soil environment. For these purposes Eastern Highveld soils formed the basis. Investigating the interactions of Cr(III) and Ni with certain soil constituents entailed the following areas of research: (i) the environmental extractability of Cr(III) and Ni within a single wetting and drying cycle, as well as the effect of soil water potential on it; (ii) the extractability of Cr(III) and Ni over a period of five rewetting and drying cycles as influenced by an external source of Si; and (iii) the solubility and subsequent release of heavy metals (Cr and Ni) from two commercially available slag samples in a highly buffered soil. The thesis is structured accordingly and is introduced by chapters dealing with the available literature on Cr and Ni in the soil environment. The concluding chapter summarises the findings.

References

BAYTAK, S. and TűRKER, R.A. 2005. Determination of lead and nickel in environmental samples by flame atomic absorption spectrometry after column solid-phase extraction on ambersorb-572 with EDTA. *Journal of Hazardous Material,* 129 (2005):30–36.

CHARLET, L. and MANCEAU, A.A. 1992. X-Ray adsorption spectroscopy study of the sorption of Cr(III) at the oxide-water interface: I. Molecular mechanisms of Cr(III) oxidation by Mn oxides. *Journal of Colloidal Interface Science,* 148:425–442.

CHRISTENSEN, T.H., LEHMANN, N., JACKSON, T. and HOLM, P.E. 1996. Cadmium and nickel distribution coefficients for sandy aquifer materials. *Journal of Contaminant Hydrology,* 24(1996):75–84.

COOPER, G.R.C. 2002. Oxidation and toxicity of chromium in ultramafic soils of Zimbabwe. *Applied Geochemistry,* 17:981–986.

FENDORF, S.E. 1994. Surface reactions of chromium in soils and waters. *Geoderma,* 67:55–71.

FENDORF, S.E., LI, G. and GUNTER, M.E. 1996. Micromorphologies and stabilities of chromium(III) surface precipitates elucidated by scanning force microscopy. *Soil Science Society of America Journal*, 60:99–106.

FENDORF, S.E. and SPARKS, D.L. 1994. Mechanisms of chromium(III) sorption onto silica. II: Effect of reaction conditions. *Environmental Science and Technology,* 28:290–297.

FORD, R.G., SCHEINOST, A.C., SCHECKEL, K.G. and SPARKS, D.L. 1999b. The link between clay mineral weathering and structural transformation in Ni surface precipitates. *Journal of Environmental Science and Technology*,18:3140–3144.

SCHECKEL, K.G., SCHEINOST, A.C., FORD, R.G. and SPARKS, D. 2000. Stability of layered Ni hydroxide surface precipitates – a dissolution kinetic study. *Geochimica et Cosmochimica Acta,* 64:2727–2735.

SCHEIDEGGER, A.M., LAMBLE, G.M. and SPARKS, D.L. 1996. Spectroscopic analysis for the formation of mixed cation hydroxide phases upon metal sorption on clay and aluminum oxides. *Journal of Colloid and Interface Science,* 186:118– 28.

STEPNIEWSKA, Z., BUCIOR, K. and BENNICELLI, R.P. 2004. The effect of MnO_2 on sorption and oxidation of Cr(III) by soils. *Geoderma,* 122:291–296.

Chapter 1 Chromium transformation on soil mineral surfaces: a review

1.1 Abstract

Chromium is a redox active element, persisting in the natural soil environment either as Cr(III) or Cr(VI). Whereas Cr(III) is rather benign and immobile, Cr(VI) is regarded as extremely toxic and easily transported. The reaction mechanisms and interaction of both Cr(III) and Cr(VI) with soil constituents must be known and researched in an attempt to predict the hazard Cr might pose to human health and environmental quality. This paper summarises the surface reactions that influence Cr chemistry in soil, with specific emphasis on retention reactions regarding Cr(III) and Cr(VI), Cr(III) oxidation to Cr(VI), and Cr(VI) reduction to Cr(III).

Key words: oxidation, reduction, silica, goethite, hematite, ferrihydroxide, gibbsite, Mn oxide minerals, Fe(II), sulphides, organic matter, montmorillonite, kaolinite

1.2 Introduction

Chromium is the tenth most abundant element in the earth's mantle, and is used in many industrial processes, including electroplating, tanning of animal hides, and as an anti-corrosion and alloying substance in the steel industry. The adsorption and precipitation behaviour of chromium in soils is governed by an array of factors, among others, redox potential, oxidation state, pH, soil minerals, competing ions and complexing agents (Fendorf, 1994; Bradl, 2004). The most important of these factors are perhaps the hydrolysis of Cr(III) and Cr(VI), redox reaction of Cr(III) and Cr(VI), and adsorption and precipitation of Cr(III) and Cr(VI) (Bradl, 2004; Fendorf, 1994).

1.3 Cr speciation in the soil environment

The oxidation states of chromium range from –2 to +6, but only the +3 and +6 states of Cr are stable under most soil environment conditions (Fendorf, 1994; Bradl, 2004; Reddy *et al*., 1997). Cr(VI) occurs as oxyanions $HCrO_4^-$ (bichromate), CrO_4^{2-} (chromate) and $Cr_2O_7^{2-}$ (dichromate), under a wide range of soil pH conditions (Reddy *et al*., 1997). Cr(VI) is most stable at pH values above 6 and Eh values surpassing 600 mV (James, 1994), whereas Cr(III) is most stable under reduced conditions, being present as a cation with the first [$Cr(OH)^{2+}$] or second [$Cr(OH)^{2+}$] hydrolysis product dominating at pH values of 4 to 8 (Fendorf, 1994) and Eh values of –200 to 500 mV (Stepniewska, Bucior and Bennicelli, 2004). Nonetheless, Cr(III) may also form hydroxides such as $Cr(OH)_2^{+}$, $Cr_2(OH)_4^{2+}$, $Cr(OH)_3^{0}$, $Cr(OH)_4^{-}$ $Cr_6(OH)_{12}^{6+}$ and $Cr_6(OH)_{15}^{3+}$ in solution. Cr(III) is insoluble over a wide pH range and, apart from forming stable complexes with soil mineral surfaces, readily precipitates as amorphous $Cr(OH)_3$ (Reddy *et al*., 1997).

Being a strong oxidising agent, corrosive, and a potential carcinogen, coupled with its ability to penetrate biological membranes, Cr(VI) is toxic to all living organisms (Hu and Deming, 2005; Reddy *et al*., 1997; Turner and Rust, 1971) in concentrations as low as 0.5 parts per million (ppm) in solution and 5 ppm in soils (Fendorf, 1994). The World Health Organization (WHO), however, has established a limit of 0.05 ppm Cr(VI) in drinking water (WHO, 1996). On the contrary, Cr(III) is not toxic and is an essential nutrient for mammals to maintain normal glucose, cholesterol and fatty acid metabolism (Hu and Deming, 2005; Bartlett and James, 1988).

The formation of Cr(III) hydrolysis products at low pH values has important implications for the reactivity, sorption and solubility of the Cr(III) ion (Fendorf, 1994; Rai, Sass and Moore, 1987). The sorption of hydrolysable metal ions, owing to the disruption of their symmetric water coordination sphere, is highly correlated with the hydrolysis product of formation. The disruption of an ion's water coordination sphere greatly enhances its reactivity (Schindler and Stumm, 1987). The retention of Cr(III) on soil minerals should, therefore, be appreciable under most pH conditions. The strong retention of Cr(III) by mineral surfaces, coupled with its low hydroxyl solubility, limits the bioavailability and mobility of Cr(III) in soils and water (Fendorf, 1994).

Cr(VI) is commonly very mobile in soils and water owing to the formation of anionic species. Cr(VI) is therefore not appreciably sorbed by negatively charged soil colloids; it is sorbed by many hydrous oxides, however (Fendorf, 1994). In addition to potential immobilisation, Cr(VI) can be reduced to Cr(III) by organic matter, Fe(II), and sulphides. The reduction of Cr(VI) to Cr(III) by Fe(II) has the added advantage that Cr(III) and Fe(III), being products of the redox reaction, can readily form co-precipitates, which then stabilise the reduced Cr in an immobile state (Fendorf, 1994; Sass and Rai, 1987). It is therefore important to determine not only the total amount of Cr in a system and its oxidation state, but also the possible retention of these valence states by soil minerals (Fendorf, 1994).

Although not a significant hazard in itself, Cr(III) can be oxidised to Cr(VI) by manganese oxides, making it a serious threat to living matter (Bartlett and James, 1979; Eary and Rai, 1987; Johnson and Xyla, 1991, Fendorf and Zasoski, 1992; Stepniewska *et al.*, 2004; Cooper, 2004;). Many solution and surface factors may influence the transformation of Cr(III) to Cr(VI) by manganese oxides. These factors include processes such as adsorption and precipitation, organic complexation, and surface coatings on manganese oxides (Fendorf, 1994; Stepniewska *et al.*, 2004).

1.4 Sorption of Cr(VI) onto soil mineral surfaces

Cr(VI) species are sorbed by a variety of mineral phases with hydroxyl groups on their surfaces. These mineral phases include Fe, Mn, and Al oxides as well as clays such as kaolinite and montmorillonite (Zachara, Girvin, Cowen and Resch, 1989; Zachara, Ainsworth and Cowen and Resch, 1989). Figure 1.1 depicts the adsorption of Cr(VI) as a function of pH by a variety of surfaces (Zachara *et al.*, 1989).

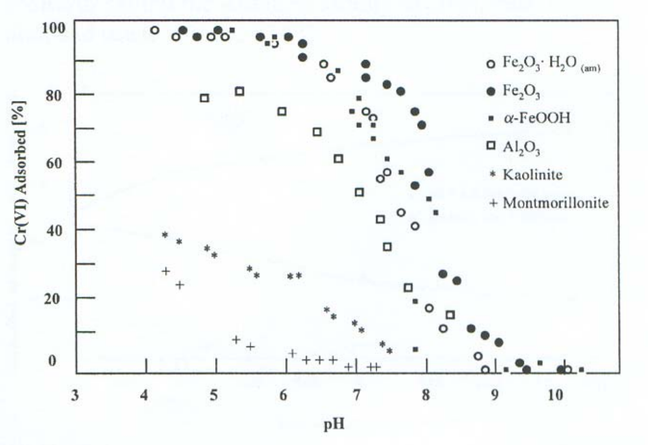

Figure 1.1 The sorption of Cr(VI) by a variety of mineral surfaces

Source: Bradl, 2004

The sorption of Cr(VI) onto mineral surfaces decreases as pH increases, owing to the protonation of surface hydroxyl groups. Sorption of Cr(VI) is favoured if the mineral surfaces exhibit a high point of zero charge (PZC), leaving the mineral surface mainly positively charged at low to neutral pH values (Sparks, 2003; Bradl, 2004). The reaction between the Cr(VI) ion and the mineral surface hydroxyl group can be seen as surface complexation reactions (Bradl, 2004; Zachara *et al.,* 1987; Zachara *et al.,* 1989; Benjamin and Bloom, 1981; Reddy *et al*., 1997; Deng, Stjernstrom and Banwat, 1996). Kaolin and montmorillonite are reported to exhibit PZC values of approximately 3.5 and 2.0 respectively. At pH values surpassing these PZC values, predominantly negatively charged surfaces will dominate and the sorption of Cr(VI) will consequently be rendered less effective. Fe oxides, however, tend to exhibit the highest sorption affinity for Cr(VI), followed by Al_2O_3, kaolinite and montmorillonite (Bradl, 2004; Reddy *et al*., 1997). Hydrous oxides of Fe and Al are often present in significant amounts in soils, being commonly positively charged (Fendorf, 1994). Cr(VI) sorption was found to be exceptional in lower pH material enriched with kaolinite and crystalline Fe oxides (Reddy *et al*., 1997; Zachara *et al*., 1989).

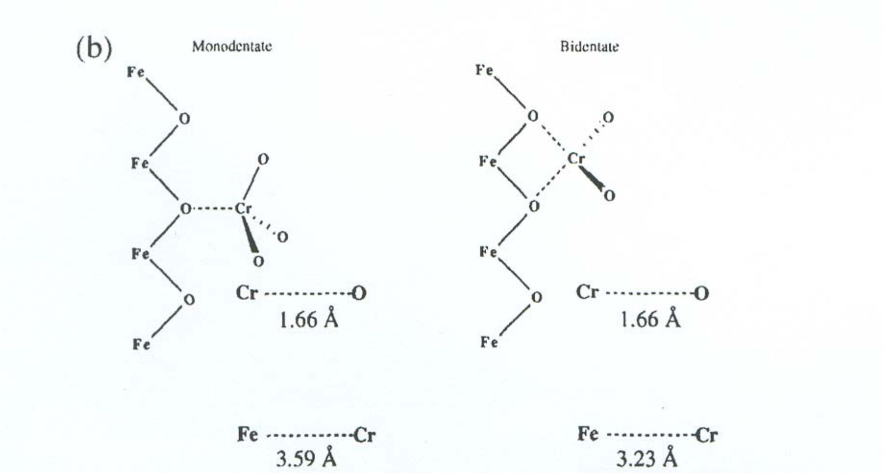

Figure 1.2 The possible surface complexes formed by Cr(VI) on goethite

Source: Fendorf, 1994

Although Cr(VI) was initially thought to form outer-sphere complexes (Zachara *et al.,* 1987; Zachara *et al.,* 1989; Benjamin and Bloom, 1981), Fendorf and Sparks (1994) found Cr(VI) formed both bidentate and monodentate inner-sphere complexes on goethite, as illustrated by figure 1.2 (Fendorf and Sparks, 1994; Deng *et al*., 1996), whereas Kendelewicz *et al* (1998) found Cr(VI) also formed inner-sphere complexes on hematite, binding to the surface as tetrahedral $Cr(VI)O_4$.

Samad and Watson (1996) revealed Cr(VI) sorption onto goethite to be maximum at a pH value of 6.5, as predicted by the second acid dissociation constant for chromate. On metal oxides, maximum sorption of anions of diprotic acids typically occurs at pH values of about the second dissociation constant of the anion. Sorption decreased significantly as pH decreased (Samad and Watson, 1996). Deng *et al.* (1996) found only 20 % of Cr(VI) sorbed onto goethite was remobilised after a 60-hour period of flushing with 0.5 molar $NaClO_4$ at a flow rate of 5.9 mL h^{-1} at 25 ºC and pH 5. In contrast, 67 % of sorbed Cr(VI) was remobilised from the goethite system under the same conditions at a pH value of 9 (Deng *et al.*, 1996).

Ferrous iron containing minerals – especially magnetite (Fe_3O_4), but also biotite, hematite and goethite – has been shown to reduce sorbed Cr(VI) effectively to Cr(III) (Eary and Rai, 1989; Kendelewicz *et al.*, 1998; Samad and Watson, 1996; Fendorf, 1994; Peterson *et al.* 1995). Under such conditions Peterson, Brown and Parks (1995) proposed that Cr(VI) can be sorbed as tridentate inner-sphere Cr(III) complexes onto the magnetite surface. Deng *et al.* (1996), however, concluded that the reduction of Cr(VI) to Cr(III) on the magnetite surface containing Fe(II) can be described by a reductive precipitation mechanism and subsequent formation of $Cr(OH)_3$ and/or (Fe, Cr)$(OH)_3$ precipitates as Cr(VI) is reduced to Cr(III) after sorption by Fe(II) sites on the mineral surface. No Cr(III) or Cr(VI) ions were remobilised when the magnetite reacted Cr(VI) surfaces were flushed with 0.5 molar $NaClO_4$ at a flow rate of 5.9 mL h^{-1} at 25 ºC at pH 5, confirming the reductive precipitation mechanism proposed (Deng *et al.*, 1996). Peterson *et al.* (1995), however, found Cr(VI) formed outer-sphere complexes on magnetite and maghemite in the absence of redox transformation; maghemite exhibited a substantially poorer sorption capacity for Cr(VI). Peterson *et al.* (1995) ascribed the reduction of Cr(VI) to Cr(III) on the magnetite surface to heterogeneous electron transfer resulting in the formation of an oxidised sorbate layer on the mineral surface. The extent to which Cr(VI) is reduced was found to be dependent on the exposure time and thickness of the sorbate layer. The sorbate layer consisted mainly of Cr(III)- and Fe(III)-oxyhydroxide phases, the former comprising the outermost portion of the layer. Cr(VI) reduction, however, may not be complete, in which case Cr(VI) will dominate the outer portion of the sorbate layer with regards to Cr(III) (Kendelewicz *et al.*, 1998). It has been hypothesised that the reduction reaction occurring on the magnetite surface oxidises magnetite to maghemite, which is a poor sequester of Cr(VI) (Peterson *et al*. 1995), thereby increasing the risk of Cr(VI) pollution in an environment where the addition of Cr(VI) surpasses the available binding sites present on the magnetite mineral surface.

Hexavalent Cr may form inner-sphere complexes not only on Fe hydrous oxides, but also on Al hydrous oxides, thereby diminishing the risk of Cr(VI) mobility and bioavailability substantially. Soils with low levels of Fe and Al hydrous oxides may exhibit a dangerously low sorption affinity for Cr(VI), however (Fendorf and Sparks, 1994).

Layered double hydroxides (LDH) have also been identified as potential sinks for anionic pollutants such as Cr(VI). Layered double hydroxides are characterised by positively charged layers exhibiting the composition $[M^{II}_{1-x}M'^{III}_{x}(OH)_2]^{x+}$; where M may comprise Mg, Ca, Ni, Co, Cu and Zn, and M' Al, V, Cr, Fe and Ga; and $0.15 < x < 0.33$. Anions are incorporated between the layers to restore charge neutrality in much the same way that alkali and alkali earth metal cations are intercalated in clays dominated by negative charge. The resulting compounds exhibit the formula $[M^{II}_{1-x}M'^{III}_{x}(OH)_2]^{x+}(A^{n-})_{x/n}.H_2O$, where A represents the anion and n the anionic charge. The chromium exchange capacity of LDHs is dependent on the positive charge of the hydroxide layer, the leaving tendency of the outgoing anion, and the thermodynamic stability of the LDH containing CrO_4^{2-}. These LDHs, especially those containing Mg^{2+}, Ca^{2+}, Al^{3+}, and Fe^{3+}, are rather soluble and would therefore not be an effective means by which Cr(VI) can be rendered less of a hazard (Prassanna, Padmanabha and Kamath, 2006).

Reactions that immobilise Cr(VI) do not alter its toxicity, but the risk imposed by this ion is diminished. The environmental risk posed by sorbed Cr(VI) is therefore determined by the sorbate’s stability (Fendorf, 1994).

1.5 Reduction of Cr(VI) to Cr(III)

Reactions that reduce Cr(VI) to Cr(III) are of major importance in decreasing the hazard this ion poses to the environment. Organic matter, sulphides and ferrous iron are mostly responsible for the reduction of Cr(VI) to Cr(III). It would seem plausible that Cr(VI) would directly be reduced to Cr(III) under reducing conditions. This, however, is not the case because kinetic limitation, based on electron symmetry constraints in the electron transfer process, stabilises the existing Cr oxidation state, either Cr(VI) or Cr(III). A suitable redox couple is therefore needed to complex with the Cr ion (Fendorf, 1994). Reduction of Cr(VI) to Cr(III) has been proved to be low at pH values above 4.5 (Eary and Rai, 1991; Becquer *et* al., 2003). It is of utmost importance to assess the potential of all soils to reduce Cr(VI) to Cr(III), as well as the re-oxidation of Cr(III) to Cr(VI) (Fendorf, 1994).

1.5.1 Cr(VI) reduction by organic matter

Cr(VI) is toxic to all living organisms owing to its strong oxidising capabilities. This property makes Cr(VI) ideal for controlling potentially hazardous microbial activity in contaminated systems such as industrial waters (Fendorf, 1994), but also makes it a dangerous effluent and a hazard to all living organisms. Hexavalent Cr may oxidise, and itself be reduced by both living tissue (Ishibashi, Cervantes and Silver, 1990) and residual organic matter (Bartlett and Kimble, 1976b; James and Bartlett, 1983b; Fendorf, 1994).

Soils high in organic matter content have proved to reduce Cr(VI) effectively, regardless of the soil pH. Less degraded organic matter, such as cow manure, has a markedly more limited effect on Cr(VI) reduction, being appreciable only when the soil pH decreased to below 3 (Fendorf, 1994; Bartlett and Kimble, 1976b). Soluble low molecular weight organic matter, such as ascorbic and gallic acid, has also proved to be highly effective reductants of Cr(VI) (Nakayama, Kuwamoto, Tsurubo, Tokoro and Fujinaga, 1981b; James and Bartlett, 1983b). Gallic acid has, in fact, proved to rapidly and completely reduce Cr(VI) to Cr(III) until either the Cr(VI) or the gallic acid has been depleted (Fendorf, 1994). Cr(VI) sorbed onto amorphous phases of Fe and Al oxides, minerals and organic matter may not be effectively reduced by gallic acid, however (James and Bartlett, 1983c). It is thought that the complexation structure of Cr(VI) on these amorphous sesquioxides and organic matter is such that electron orbital interaction with the reducing agent is limited (Fendorf, 1994; James and Bartlett, 1983c).

The reduction of Cr(VI) by organic matter results in the formation of Cr(III) and an organic product. A high probability for complex formation between the Cr(III) ion and the organic product therefore does exist. This complex may be either stable or soluble, depending on the characteristics of the chelating agent (James and Bartlett, 1983a; Fendorf, 1994). These Cr(III)-organic matter complexes may then eventually complex with manganese oxides, ultimately leading to the re-occurrence of Cr(VI) in the soil or water (Fendorf, 1994).

1.5.2 Cr(VI) reduction by Fe(II)

While the organic reductants of Cr(VI) may form soluble chelated complexes (Fendorf 1994; James and Bartlett, 1983a), thereby enhancing the potential of Cr(III) to be oxidised by manganese oxides to Cr(VI), reduction of Cr(VI) by ferrous iron eliminates this possibility (Fendorf 1994; James and Bartlett, 1983b). Owing to the low solubility of $Fe,Cr(OH)_{3(S)}$, Fe(II) will not only reduce Cr(VI) effectively, but will also remove Cr(III) from solution (Sass and Rai, 1987). The formation of this Cr(III) precipitate will diminish the risk of Cr(III) oxidation to Cr(VI) (Fendorf *et al.*, 1992).

Ferrous iron is one of the dominant reductants of Cr(VI) used on industrially generated Cr waste (Fendorf 1994; Eary and Rai, 1988). The reduction of Cr(VI) by Fe(II) can be expressed by the reaction:

$$Cr(VI)_{(aq)} + 3Fe(II)_{(aq)} = Cr(III)_{(aq)} + 3Fe(III)_{(aq)}$$

Hexavalent Cr reduction is thought to be stoichimetric at pH values below 10 in simple electrolyte systems. The reduction reaction is rapid, Cr(VI) being completely reduced within minutes. Brown precipitates were also found to form at pH values above 4. These precipitates are suspected to form from the reaction (Fendorf 1994; Eary and Rai, 1988):

$$xCr(III) + (1\text{-}x)Fe(III) + 3H_2O = (Cr_xFe_{1-x})(OH)_{3(s)} + 3H^+$$

where x can vary from 0 to 1. The brown precipitates were thought to be $Cr_{0.25}Fe_{0.75}(OH)_3$ (Fendorf 1994; Eary and Rai, 1988; Sass and Rai, 1987).

Ferrous iron should therefore impart a strong influence on Cr chemistry under reducing conditions, especially when considering that $Fe(II)_{(aq)}$ concentrations and Fe(II) bearing solids are prevalent under anoxic conditions (Fendorf, 1994). Ferrous iron was found to be the dominant reductant of Cr(VI) in a forested wetland soil system at redox levels less than +100 mV (Masscheleyn, Pardue, DeLaune and Patrick, 1992). Reduction of Cr(VI) by Fe(II) would be especially important in a low organic matter and biological activity system (Fendorf, 1994). It was also observed that Fe(II) species were the major reductant of Cr(VI) in sands and gravel of a suboxic aquifer (Anderson, Kent and Davis, 1994); therefore, in acidic soils, Fe(II) influenced Cr(VI) at least as much as organic material (Eary and Rai, 1991).

Ferrous iron would not be predicted to have a major influence on Cr(VI) in oxygenated systems, however, owing to the rapid oxidisation of Fe(II) to Fe(III) by dissolved oxygen at all but highly acidic pH values (Stumm and Morgan, 1981). Nonetheless, Eary and Rai (1989) found the oxidation of $Fe(II)_{(aq)}$ by Cr(VI) to be even more rapid than by oxygen – even under well-aerated, high pH conditions. This implies that dissolving Fe(II)-bearing minerals may have a substantial effect on Cr(VI) reduction (Fendorf, 1994). Cr(VI) was found to be reduced by Fe(II) present in hematite (Eary and Rai, 1989; Kendelewicz *et al*., 1998), goethite (Samad and Watson, 1996), magnetite (Peterson *et al*. 1995) and biotite; mineral dissolution seemed to control the rate of Cr(VI) reduction in the latter (Eary and Rai, 1989; Fendorf, 1994), but Kendelewicz *et al*. (1998), as well as Samad and Watson (1996), found Cr(VI) reduction by hematite and goethite to occur only after Cr(VI) sorption onto the mineral surface. Magnetite was found to exhibit a major capacity to reduce Cr(VI) to Cr(III) after sorption of the Cr(VI) species at pH values ranging around 5 (Deng *et* al., 1996; Kendelewicz *et al*. 1998; Peterson *et al*. 1995).

In the case of minerals such as $FeCO_3$, $Fe(OH)_2$, FeS and FeS_2, Cr(VI) reduction may occur at the mineral-water interface, or upon mineral dissolution where reduction may be enhanced because of elevated $Fe(II)_{(aq)}$ levels (Fendorf, 1994; Erdem, Gűr and Tűmen, 2004). Siderite ($FeCO_3$) was found to exhibit a maximum reduction capacity in an aqueous solution of about 17 mg Cr(VI)/g siderite at pH values less than 4. A pH increase was noted, however, owing to the consumption of H^+ ions in the Cr(VI) reduction process, as well as to Ca and Mg impurities contained as dolomite in the siderite crystal structure (Erdem, Gűr and Tűmen, 2004). Iron sulphites in particular may have a major effect on Cr(VI) reduction as these minerals can persist in oxygenated systems, although prevalent in anoxic environments. Reduction of Cr(VI) by iron sulphides is pH dependent, with reduction being greatest at lower pH values (3.0). However, at neutral pH values (7.0) significant amounts (just over 90%) of Cr(VI) species present were reduced by FeS. Iron sulphides may therefore impart an important influence on Cr toxicity, especially under anaerobic conditions (Fendorf, 1994).

1.6 Sorption of Cr(III) onto soil mineral surfaces

The retention of Cr(III) on naturally occurring mineral surfaces is an effective means of inhibiting the leaching of Cr(III) ions either deeper down the soil profile or in lower-lying areas in the landscape containing manganese oxide minerals which may oxidise Cr(III) to Cr(VI) (Dubbin, 2004; Fendorf, 1994). Cr(III) is rapidly and specifically sorbed by many constituents of the soil environment, including Fe, Al and Mn-oxides, as well as clay minerals (Bradl, 2004; Charlet and Manceau, 1992). The dangers regarding Cr(III) sorption onto manganese oxides should not be neglected when assessing Cr transformation, however. When sorbed onto soil mineral surfaces other than manganese oxides, the potential for Cr(III) oxidation by manganese oxides present in the specific soil environment would be determined purely by the stability of the bound Cr(III) phase (Fendorf, 1994).

The surface structures of Cr(III) sorbed onto smectite clays (Fendorf, 1994; Corker, Evans and Rummey, 1991), goethite (Fendorf, Li and Guther, 1996; Charlet and Manceau, 1992), and silica (Fendorf *et al.*,1996; Fendorf and Sparks, 1994) have been determined by X-ray absorption fine structure spectroscopy (XAFS). As illustrated by figure 1.3, Cr(III) forms an inner-sphere complex on both goethite and silica. As Cr(III) surface coverage increased on goethite and silica, a hydrous chromium oxide (HCO) phase occurred (Fendorf, 1994). This HCO phase also formed in the interlayers of smectite clays (Fendorf, 1994; Rengasamy and Oades, 1978; Corker *et al.*, 1991).

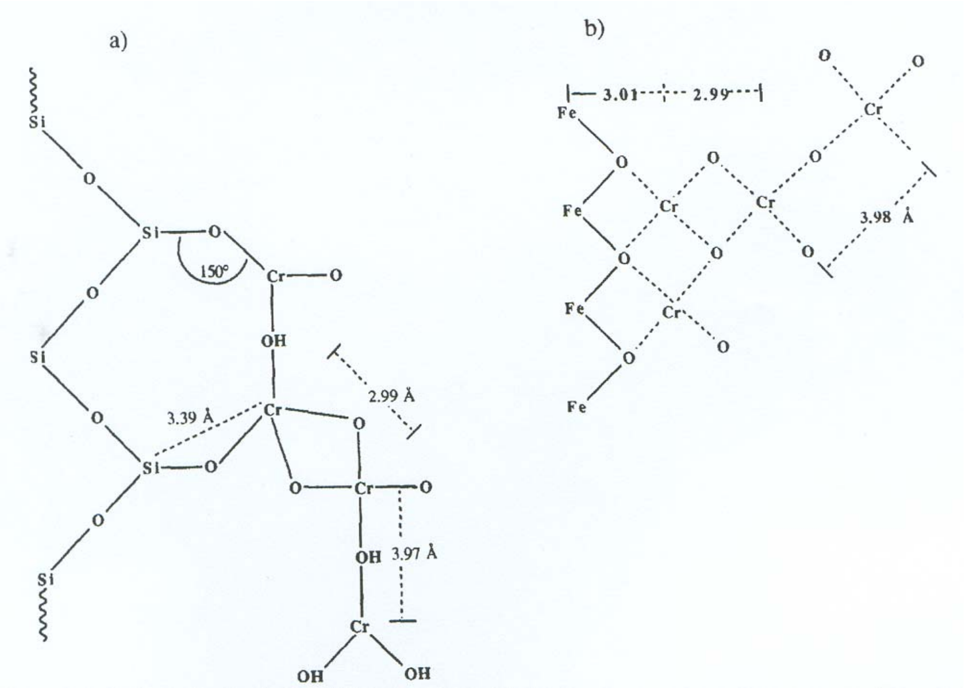

Figure 1.3 Complexation of Cr(III) on a) silica and b) goethite

Source: Charlet and Manceau, 1992

Initially a monodentate Cr(III) surface precipitate formed on silica, but as surface coverage exceeded $\varphi = 0.20$, Cr(III) formed a multinuclear metal hydroxide surface phase (HCO), $Cr(OH)_3.nH_2O$ (Fendorf, 1994; Fendorf and Sparks, 1994; Fendorf *et al.*,1996) At coverages of ten times the amount of Cr(III) needed to form a monolayer encapsulating the silica surface ($\varphi = 10$), discrete moieties or clusters formed (Fendorf and Sparks, 1994), rather than an even distribution across the silica surface. Although the primary growth appears to be an elongation away from the silica surface, these HCO clusters tend to expand in both width and height, even fusing together in some areas. This may lead to the conclusion that Cr(III) sorption on silica increases owing to precipitation mechanisms away from the silica surface. The final state properties of the reacted colloid would therefore exhibit both unreacted silica and hydrous chromium oxide (Fendorf *et al.*,1996).

Based on the crystallographic parameters of both silica and the hydrous chrome oxide precipitate, the surface features observed by the scanning force microscopy (SFM) are not unexpected. Because the Cr-O distance (1.99A) is much greater than that for Si-O (1.61A), the $Cr(OH)_3.nH_2O$ precipitate would not readily expand epitaxially across the silica surface because bond differences would retard such a process (Fendorf *et al.,* 1996).

Cr(III) was found to form predominantly inner-sphere complexes with both goethite and hydrous ferric oxide (Charlet and Manceau, 1992). Multinuclear species of hydrous chrome oxide were noted prior to monolayer coverage. Growth on these surfaces appeared to be epitaxial before distributing away from the surface (Charlet and Manceau, 1992; Fendorf *et al.,* 1996). This is in accordance with bond lengths as the Cr-O distance (1.99A) is very similar to that of the Fe-O distance (1.97A). This similarity in bond distances should provide favourable conditions for epitaxial growth (Fendorf *et al.,* 1996). The local structure of the Cr(III) precipitate was found to be similar to α-CrOOH at monolayer and lower surface coverage. This contrasts with the hydrous chrome oxide phase on silica, which resembles a γ-CrOOH type local structure (Charlet and Manceau, 1992; Fendorf *et al.,* 1994). It thus appears that Cr(III) adopts the goethite-type structure at monolayer or lower surface coverage (Fendorf *et al.,*1996).

Goethite-reacted Cr(III) showed a rolling topography after a five-day hydration period. Although no appreciable surface alteration was noted after reacting with Cr(III) at a concentration to cover half of the goethite surface ($\varphi = 0.50$), the goethite surface appeared smoothed when reacted with ten times ($\varphi = 10$) the amount of Cr(III) needed for monolayer coverage. This is hypothesised to arise from the preferential deposition of the hydrous chrome oxide in kinks, crevices or edge sites on the goethite mineral surface. Therefore, SFM does provide substantial evidence that the hydrous chrome oxide precipitate distributes epitaxially across the goethite surface, unlike the clusters formed on the silica surface (Fendorf *et al.,* 1996).

Although hydrous chrome oxide may occur on goethite, silica and smectite, its surface morphology differs markedly. These differences in surface morphologies are of utmost importance when considering the stability and reactivity of Cr(III) precipitates on mineral surfaces. The much higher surface area precipitate clusters formed on the silica surface would be much more reactive than the evenly distributed precipitate formed on goethite. The hydrous chrome oxide precipitated in the interlayers of the smectite clays would seem to be most stable, as a very limited precipitate surface is exposed (Fendorf, 1994; Fendorf *et al.,* 1996).

Multinuclear Cr(III) species were also identified on hematite (Eggleston and Stumm, 1993). Scanning tunnelling microscopy (STM) images revealed that Cr(III) may form triply coordinated surface complexes by sorbing onto vacant Fe sites on hematite. Although slower than for most transition metals, ion diffusion rates was still faster than would be expected based on Cr(III) ligand exchange in solution. The associated activation energies were found to be approximately half (45 to 56 kJ/mol) of those measured for water exchange of aqueous $Cr(H_2O)_5OH^{2+}$ species (93kJ/mol) (Fendorf, 1994; Eggleston and Stumm, 1993). These findings are in agreement with rate measurements of Cr(III) sorption onto Al_2O_3, which were much more rapid than would be expected, based on water exchange rates for Cr(III) (Wehrli, Ibric and Stumm, 1990). It would therefore seem that Cr(III) adsorption and nucleation on hydrous oxides are rapid, but the retention on such surfaces is weaker than would be expected, based on aqueous Cr(III) ligand exchange rates (Fendorf, 1994). Using XAFS, Cr(III) was found to form tridentate inner-sphere complexes or Cr(III) surface clusters on magnetite surfaces at near neutral pH values (Peterson *et al*. 1995).

Cr(III) can further be effectively sorbed by Na-montmorillonite through two mechanisms: (i) cation exchange in the interlayers, resulting from the interaction between Cr(III) ions and negative permanent charge; and (ii) the formation of inner-sphere complexes through $Si\text{-}O^-$ and $Al\text{-}O^-$ groups at the clay particle edges (Kraepiel, Keller and Morel, 1999; Abollino *et al.,* 2002). The latter is particularly pH dependent because silanol and aluminol groups are protonated at pH values below 4, leading to the mobilisation of montmorillonite bound metals (Abollino *et al.,* 2002). Na-montmorillonite exhibited a total sorption capacity of 5.20 mg/g towards Cr(III) at a pH value of 5.5. The presence of organic ligands in solution, however, was found to hinder Cr(III) sorption onto montmorillonite owing to the formation of metal-ligand complexes in solution (Abollino *et al.,* 2002). Cr(III), apart from hydroxy-Cr, may form hydroxyl Al-Cr on montmorillonite surfaces (Dubbin, 2004).

1.7 Organic ligand induced dissolution of Cr(III)

Cr(III) precipitates show markedly different morphologies, depending on the mineral surface upon which Cr(III) is sorbed. These differences exhibit a pronounced influence on the stability, solubility and reactivity of the surface precipitate. At less than monolayer surface coverage, reactivity is dominated by bond strengths of the sorbate-to-surface or, in the case of nucleation, bonds within the multinuclear species. If the bond strength of the surface structure and nucleated phase were to be the same, then a multinuclear species would be less reactive than a distributed sorbate, since some of the metal ions will be protected from exposure to the surrounding environment. Under coverage greater than monolayer, the reactivity of the surface phase is a function of surface morphology. A distributed precipitate would have a lower exposed surface area than a clustered precipitate and should be less reactive (Fendorf *et al.*, 1996; Fendorf, 1994).

The rather evenly distributed hydrous chrome oxide precipitate on goethite would therefore be stable and less reactive than its silica counterpart, exhibiting a much greater exposed surface area. When reacted with oxalate, a common plant root exudate, approximately 17 % of silica sorbed Cr(III) dissolved within one hour, whereas less than 1 % of goethite sorbed Cr(III) dissolved in the same time. Of a pure hydrous chrome oxide, prepared through titration and used as a reference, 20 % dissolved within one hour. Initial dissolution rates exhibited the same trend: 0.180 mol/ L for the pure HCO; 0.166 mol/L for Cr(III)-silica; and 0.042 mol/L for Cr(III)-goethite. After a four-hour dissolution time, concentrations were elevated to 349 and 224 μM for pure HCO and Cr(III)-silica, respectively. Only 66 μM of Cr(III)-goethite dissolved within this time. Cr(III) would therefore seem considerably more stable on goethite than on silica, the pure HCO precipitate being least stable (Fendorf *et al.*, 1996).

1.8 Oxidation of Cr(III) to Cr(VI) by Mn-oxides

The oxidation of Cr(III) to Cr(VI) poses a significant environmental risk, since a rather harmless species is transformed into an extremely toxic one. Manganese oxides have proved to be the only natural occurring oxidant of Cr(III) (Cooper, 2002; Stepniewska *et al.*, 2004; Fendorf, 1994; Eary and Rai, 1987; Saleh *et al.*, 1989).

The oxidation of Cr(III) in soils by various manganese oxide minerals has been demonstrated (Cooper, 2002; Fendorf 1994; Bartlett and James, 1979) and can be described by a two-step mechanism: (i) the hydrolysis of Cr(III) in chromite or industrial rich waste such as metallurgical slags to a Cr(III) hydroxide species; and (ii) the oxidation of the Cr(III) hydroxide species to Cr(VI) by Mn-oxides (Stepniewska *et al.*, 2004; Cooper, 2002; Fendorf 1994; Bartlett and James, 1979). The following reaction describes this (Stepniewska *et al.*, 2004; Fendorf 1994; Bartlett and James, 1979):

$$Cr(OH)^{2+} + 1.5MnO_2 = HCrO^{-}_4 + 1.5Mn^{2+}$$

where the speciation depicted is ruled by a pH of approximately 5. The speciation of Cr(III) and Cr(VI) will influence the stoichiometric proportions of H^+ consumed and released by the reaction. This reaction is strongly dependent on pH and is most effective in pH values ranging from 4 to 6 (Stepniewska *et al.*, 2004; Fendorf, 1994).

Various factors, such as the retention of reaction products or reactants or the alteration of the manganese oxide surface, may influence and limit oxidation. Reaction products, however, were eliminated as a possible cause of the decrease in oxidation rate at pH values above 4 (Fendorf *et al.*, 1993). Microscopic and spectroscopic evidence revealed the formation of a $Cr(OH)_3.nH_2O$ surface precipitate on the manganese oxide surface. This newly formed precipitate was identified by selected diffraction area patterns and energy dispersive spectroscopy (Fendorf *et al.,* 1992). The local structure of the Cr hydroxide on birnessite (δ-MnO_2) was found, through XAFS spectroscopy, to resemble γ-CrOOH (Charlet and Manceau, 1992). Additional information supporting the formation of a surface precipitate was demonstrated by modelling the rate of Cr(III) oxidation by manganite (MnOOH) at pH values above 5 (Johnson and Xyla, 1991). The chromium hydroxide surface precipitate inhibits Cr(III) oxidation by the manganese oxide surface in two ways: first, it acts as a redox stable sink for oxidisable, soluble Cr(III); second, it forms a physical barrier between the aqueous Cr(III) and Mn surface (Fendorf, 1994).

Only through electron transfer can the Cr(III) ion be oxidised to Cr(VI). For electron transfer to occur between the manganese oxide mineral and Cr(III), the formation of a inner-sphere complex is a prerequisite. Outer-sphere complexation would not allow sufficient orbital overlap, thereby inhibiting oxidation (Fendorf *et al.,* 1992). The formation of a bidentate surface complex would be the most viable means for oxidation. Retention of Cr(III) in vacancies of birnessite (δ-MnO_2), however, has also been postulated (Charlet and Manceau, 1992). The necessity of Cr(III) inner-sphere complexation on manganese oxides would seem to indicate that oxidation may be inhibited by competitive ion sorption (Fendorf, 1994). This is not the case because the stable d_3 electron configuration imparts its slow ligand exchange properties, and also makes it an excellent complexant. It is therefore unlikely that many ions present in the environment will retard the oxidation of Cr(III) through competitive sorption. Surface precipitate formation on manganese oxide surfaces may, however, inhibit Cr(III) oxidation effectively. The necessity of forming a surface precipitate to inhibit Cr(III) oxidation is well demonstrated for competitive sorption influences of Al, La, Mn(II), and Cr(VI) on Cr(III) oxidation (Fendorf *et al.,* 1993). Only Al at pH values surpassing 4 inhibited the oxidation of Cr(III), owing to the formation of an Al hydroxide surface precipitate (Fendorf, 1994).

In a stable solid-phase Cr(III) system, the oxidation of Cr(III) to Cr(VI) will be dependent on the dissolution rate of the Cr(III) solid in the presence of manganese oxides. Therefore, organic chelating agents that enhance mineral dissolution may promote Cr(III) oxidation. For oxidation to occur, however, the Cr(III) organic matter complex must form a surface complex with the manganese mineral surface (Fendorf, 1994; James and Bartlett, 1983a).

It seems likely that all manganese oxides are effective oxidants of Cr(III). Even pyrolusite (β-MnO_2), being the Mn-oxide mineral with the highest point of zero charge and most crystalline structure, has been hypothesised to oxidise Cr(III) to Cr(VI) (Eary and Rai, 1987; Saleh *et al*., 1989; Stepniewska *et al*., 2004). Cooper (2002), however, stated that both pyrolusite (β-MnO_2) and birnessite (δ-MnO_2) are incapable of oxidising Cr(III) to either $HCrO^-_4$ or CrO_4^{2-} under natural soil conditions owing to a lack of free energy resulting from negative log K values for the specific reactions. Fendorf and Zasoski (1993), reported oxidation reaction in the presence of pyrolusite (β-MnO_2) to be less extensive and slower than for other manganese oxides. Pyrolusite (β-MnO_2) is said to be uncommon in most soils (Sparks, 2003). Oxidation of Cr(III), however, has been shown to be rapid and extensive when reacted with birnessite (δ-MnO_2) (Fendorf and Zasoski, 1993), and especially manganite (MnOOH) (Cooper, 2002; Johnson and Xyla, 1991), hausmanite (Mn_3O_4) (Cooper, 2002; Rophael and Boulis, 1982), and braunite (Mn_2O_3) (Rophael and Boulis, 1982).

Cooper (2002) found the oxidation of Cr(III) to Cr(VI) in ultramafic soils from Zimbabwe to occur only in subsoils subject to wetting and drying cycles, containing easily reducible forms of Mn-oxides. The frequent occurrence of Fe and Mn concretions would indicate alternating oxidising and reducing conditions because of a seasonal water table. No oxidation of Cr(III) to Cr(VI) was observed in topsoils, mainly because a less moist environment leads to less easily reducible Mn-oxide minerals.

1.9 Inhibiting Cr(III) oxidation to Cr(VI)

Although competitive sorption of ions such as La and Mn(II) has proved rather futile in retarding Cr(III) oxidation, surface precipitate formation has shown to be highly effective in inhibiting Cr(III) oxidation by manganese oxides (Fendorf 1994; Fendorf *et al.*, 1993). The formation of metal hydrous oxide precipitates on the surface of manganese oxides diminishes the risk of Cr(III) oxidation through a mechanism similar to that through which Cr(III) oxidation is self-inhibiting (Fendorf, 1994).

Both Fe and Al have proved to successfully inhibit the oxidation of Cr(III) by forming a metal hydroxide surface precipitate at concentration and pH values sufficient to invoke precipitation. When the metal hydroxide is extensive enough to completely encapsulate the manganese oxide surface, Cr(III) oxidation was nonexistent (Fendorf *et al.*,1993). Al and Fe hydroxide precipitate formation could therefore serve as an important means to diminish the risk of Cr(III) oxidation to the more toxic Cr(VI) ion in the natural environment, as well as treated contaminated sites (Fendorf, 1994).

1.10 Conclusion

Although the chemical transformation of Cr in single mineral system environments has been thoroughly investigated, not much is known of Cr interaction with specific mineral phases in the natural soil environment. Only by understanding the transformation of Cr under natural soil conditions can the mobility and potential detrimental effect of Cr on human health and environmental quality be assessed.

Nonetheless, through logical thinking, valuable information can be deduced when studying Cr in single or dual mineral systems. The hazard of Cr(III) oxidation to Cr(VI) can be circumvented by knowledge of Cr(III) sorption onto soil constituents such as the amorphous sesquioxide and clay mineral fractions. Rather than forming surface complexes on hydrous oxides or phyllosilicate clay minerals, Cr(III) appears to adopt a hydrous chromium oxide structure in the majority of cases. The stability of these phases must be assessed when extrapolating Cr(III) mobility to soil environmental conditions. In addition, Cr(VI) is known to be reduced by Fe(II), sulphides and organic matter. Furthermore, the presence of Fe(II) on soil mineral edges, as is the case for biotite and magnetite, may reduce Cr(VI) to Cr(III) and precipitate the ion as a stable Fe(III),Cr(III) hydroxide.

Since organic chelating agents, which may not only be present in significant concentrations, but may also withstand natural weathering processes, can remobilise Cr(III), their influence on Cr mobility and oxidation needs to be researched. Although shown to oxidise Cr(III) readily to Cr(VI) under laboratory conditions, the extent to which Mn-oxide minerals can oxidise Cr(III) to Cr(VI), as well as the kinetics of such a reaction, has not been investigated in a multi-component soil system. Assessing the hazard Cr might pose in the environment has thus reached the point where knowledge gathered on single component systems should be applied and researched in multi-component systems.

1.11 References

ABOLLINO, O., ACETO, M., MALANDRINO, M., SARZANINI, C. and MENTASTI, E. 2002. Adsorption of heavy metals on na-montmorillonite. Effect of pH and organic substances. *Water research*, 37:1619–1627.

AMACHER, C.C., GIRVIN, D.C., ZACHARA, J.M. and SMITH, S.C. 1989. Chromate adsorption on goethite: Effects of aluminium substitution. *Soil Science Society of America Journal,* 53:411–418.

ANDERSON, L.D., KENT, D.B. and DAVIS, J.A. 1994. Batch experiments characterizing the reduction of Cr(VI) using suboxic material from a mildly reducing sand and aquifer. *Environmental Science and Technology*, 28:178–185.

BARTLETT, R.J. and JAMES, B. 1979. Behaviour of chromium in soils: III. Oxidation. *Journal of Environmental Quality,* 5:31–35.

BARTLETT, R.J. and JAMES, B.R. 1988. Mobility and bioavailability of chromium in soils. In: Nraigu, J.O. and Nieborer, E. (eds). *Chromium in the Natural and Human Environments*. New York: Wiley, pp 267–303.

BARTLETT, R.J. and KIMBLE, J.M. 1967b. Behaviour of chromium in soils: I. Trivalent forms. *Journal of Environmental Quality,* 5: 373–383.

BECQUER, T., QUANTIN, C., SICOT, M. and BOUDOT, J.P. 2003. Chromium availability in ultramafic soils from New Caledonia. *The Science of the Total Environment*, 301(2003):251–261.

BENJAMIN, B.B. and BLOOM, N.S. 1981. Effects of strong binding of anionic adsorbates on adsorption of trace metals on amorphous iron oxyhydroxides. In: Tewari, P.H. (ed.). *Adsorption from Aqueous Solution.*, New York: Plenum, pp 41–61.

BRADL, H.B. 2004. Adsorption of heavy metal ions on soils and soil constituents. *Journal of Colloid and Interface Science,* 277:1–18.

CHARLET, L. and MANCEAU, A.A. 1992. X-ray adsorption spectroscopy study of the sorption of Cr(III) at the oxide-water interface: I. Molecular mechanisms of Cr(III) oxidation by Mn oxides. *Journal of Colloidal Interface Science,* 148:425–442.

COOPER, G.R.C. 2002. Oxidation and toxicity of chromium in ultramafic soils of Zimbabwe. *Applied Geochemistry,* 17:981–986.

CORKER, J.M., EVANS, J. and RUMMEY, J.M. 1991. EXAFS studies of pillared clay catalysts. *Mater. Chem. Phys*., 29:201–209.

DENG, Y., STJERNSTROM, M. and BANWART, S. 1996. Accumulation and remobilization of aqueous chromium(VI) at iron oxide surfaces: Application of thin-film continuous flow-through reactor. *Journal of Contaminant Hydrology,* 141–151.

DUBBIN, W.E. 2004. Influence of organic ligands on Cr desorption from hydroxyl-Cr intercalated montmorillonite. *Chemosphere* 54*:*1071–1077.

EARY, L.E. and RAI, D. 1987. Kinetics of chromium(III) oxidation to chromium(VI) by reaction with manganese dioxide. *Environmental Science and Technology,* 21:1186–1193.

EARY, L.E. and RAI, D. 1988. Chromate removal from aqueous waste by reduction with ferrous iron. *Environmental Science and Technology*, 22: 972–977.

EARY, L.E. and RAI, D. 1989. Kinetics of chromate reduction by ferrous ions derived from hematite and biotite at 25°C. *American Journal of Science,* 289:180–213.

EARY, L.E. and RAI, R. 1991. Chromate reduction by subsurface soils under acidic conditions. *Soil Science Society of America Journal*, 55:676–683.

EGGLESTON, C.M. and STUMM, W. 1993. Scanning tunneling microscopy of Cr(III) chemisorbed on α-Fe_2O_3 (001) surface from aqueous solution: Direct observation of surface mobility and clustering. *Geochimica et Cosmochimica Acta,* 57:4843–4850.

ERDEM, M., GűR, F. and TűMEN, F. 2004. Cr(VI) reduction in aqueous solution by siderite. *Journal of Hazardous Materials,* B113:217–222.

FENDORF, S.E. 1994. Surface reactions of chromium in soils and waters. *Geoderma,* 67:55–71.

FENDORF, S.E., FENDORF, M., SPARKS, D.L. and GROSKY, R. 1992. Inhibition mechanisms of Cr(III) oxidation by δ-MnO_2 .1: Characterization. *Environmental Science and Technology,* 26:79–85.

FENDORF, S.E., LI, G. and GUNTER, M.E. 1996. Micromorphologies and stabilities of chromium(III) surface precipitates elucidated by scanning force microscopy. *Soil Science Society of America Journal,* 60:99–106.

FENDORF, S.E. and SPARKS, D.L. 1994. Mechanisms of chromium(III) sorption onto silica. II: Effect of reaction conditions. *Environmental Science and Technology,* 28: 290–297.

FENDORF, S.E. and ZASOSKI, R.J. 1992. Inhibition mechanisms of Cr(III) oxidation by manganese oxides. *Journal of Colloid and Interface Science,* 148:37–54.

FENDORF, S.E., ZASOSKI, R,J. and BURAU, R.G. 1993. Competing metal ion influences on Cr(III) oxidation by δ-MnO_2. *Soil Science Society of America Journal,* 57:1508–1515.

FENDORF, S.E., STAPLETON, M.G., LAMBLE, G.M., KELLY, M.J. and SPARKS, D.L. 1994. Mechanism of Cr(III) sorption onto silica. 1: An X-ray adsorption fine structure spectroscopic analysis. *Journal of Environmental Science and Technology*, 28:284–289.

HU, G. and DEMING, R.L. 2005. Speciation of bio-available chromium in soils by solid-phase extraction and graphite furnace atomic absorption spectrometry. *Analytica Chimica Acta,* 535:237–242.

ISHIBASHI, Y., CERVANTES, C. and SILVER, S. 1990. Chromium reduction in *Pseudomonas putida*. *Applied Environmental Microbiology,* 56:2268–2270.

JAMES, B.R. 1994. Hexavalent chromium solubility and reduction in soils enriched with chromite ore processing residue. *Journal of Environmental Quality,* 23:227–233.

JAMES, B.R. and BARTLETT, R.J. 1983b. Behaviour of chromium in soils. VI. Interaction between oxidation-reduction and organic complexation. *Journal of Environmental Quality,* 12:173–176.

JAMES, B.R. and BARTLETT, R.J. 1983c. Behavior of chromium in soils. VII. Adsorption and reduction of hexavalent forms. *Journal of Environmental Quality,* 12:177–181.

JOHNSON, C.A. and XYLA, A.G. 1991. The oxidation of Cr(III) to Cr(VI) on the surface of manganate. *Geocimica et Cosmochima Acta,* 55:2861–2866.

KENDELEWICZ, T., LIU, P., DOYLE, C.S., BROWN, G.E., NELSON, E.J. and CHAMBERS, S.A. 1998. X-ray adsorption and photoemission study of the adsorption of aqueous Cr(VI) on single crystal hematite and magnetite surfaces. *Surface Science*, 424:219–231.

KRAEPIEL, A.M.L., KELLER, K. and MOREL, F.M.M. 1999. A model for metal adsorption on montmorillonite. *Journal of Colloidal Interface Science,* 210(1):43–54.

MASSCHELEYN, P.H., PARDUE, J.H., DELAUNE, R.D. and PATRICK, W.H. 1992. Chromium redox chemistry in a Lower Mississippi Valley bottomland hardwood wetland. *Environmental Science and Technology,* 26:1217–1226.

NAKAYAMA, E., KUWAMOTO, T., TSURUBO, S., TOKORO, H. and FUJINAGA, T. 1981b. Chemical speciation of chromium in sea water. Part 2. Effects of manganese oxides on reducible organic materials on the redox processes of chromium. *Analitica Chimica Acta,* 130:401–404.

PETERSON, M.L., BROWN, G.E. and PARKS, G.A. 1995. Direct XAFS evidence for heterogenous redox reaction at the aqueous chromium/magnetite interface. *Colloids and Surfaces,* 107:77–88.

PRASSANNA, S.V., PADMANABHA, P.R. and KAMATH, P.V. 2006. Layered double hydroxides as potential chromate scavengers. *Journal of Colloid and Interface Science*, 304:292–299.

RAI, D., SASS, B.M. and MOORE, D.A. 1987. Chromium(III) hydrolysis constants and solubility of chromium(III) hydroxide. *Inorganic Chemistry,* 26:345–349.

REDDY, K.R., PARUPUDI, U.S., DEVULAPALLI, S.N. and XU, C.Y. 1997. Effects of soil composition on the removal of chromium by electrokinetics. *Journal of Hazardous Materials,* 55:135–158.

RENGASAMY, P. and OADES, J.M. 1978. Interactions of monomeric and polymeric species of metal ions with clay surfaces. Aluminum (III) and chromium(III). *Australian Journal of Soil Resources,* 16:53–66.

ROPHAEL, M.W. and BOULIS, S.N. 1982. Kinetics and oxidation of chromium(III) ions by trimanganese tetraoxide and manganese(III) oxide. *Surface Technology,* 16:243–248.

SALEH, F.Y., PARKENTON, T.F., LEWIS, R.V., HUANG, J.H. and DICKSON, K.L. 1989. Kinetics of chromium transformation in the environment. *Science of the Total Environment,* 86:25–41.

SAMAD, H.A. and WATSON, P.R. 1996. An XPS study of the adsorption of chromate on goethite (α – FEOOH*). Applied Surface Science*, 108:371–377.

SASS, B.M. and RAI, D. 1987. Solubility of amorphous chromium(III)-iron(III) hydroxide solid solution. *Inorganic Chemistry,* 25:2228–2232.

SCHINDLER, P.W. and STUMM, W. 1987. The surface chemistry of oxides, hydroxides and oxide minerals. In: Stumm, W. and Morgan, J.J. (eds). *Aquatic Surface Chemistry*. New York: Wiley, pp 83–110.

STEPNIEWSKA, Z., BUCIOR, K. and BENNICELLI, R.P. 2004. The effect of MnO_2 on sorption and oxidation of Cr(III) by soils. *Geoderma,* 122:291–296.

STUMM, W. and MORGAN, J.J. 1996. *Aquatic Chemistry*. *Chemical Equilibria and Rates in Natural Waters. Third Edition*. New York: John Wiley & Sons.

TURNER, M.A. and RUST, R.H. 1971. Effects of chromium on growth and mineral nutrition of soyabeans. *Soil Science Society of America Journal,* 35:2145–2150.

WEHRLI, B., IBRIC, S. and STUMM, W. 1990. Adsorption kinetics of vanadyl(VI) and chromium(III) to aluminium oxide: Evidence for two-step mechanism. *Colloidal Surfaces,* 51:77–88.

ZACHARA, J.M., GIRVIN, D.C, COWAN, C.E. and RESCH, C.T. 1989. Chromate adsorption on amorphous iron oxyhydroxide in the presence of major groundwater ions. *Environmental Science and Technology,* 21:589–594.

ZACHARA, J.M., AINSWORTH, C.C., COWAN, C.E. and RESCH, C.T. 1989. Adsorption of chromate by subsurface soil horizons. *Soil Science Society of America Journal,* 53:418–428.

Chapter 2 Nickel transformation on soil mineral surfaces: a review

2.1 Abstract

Although regarded as an essential plant nutrient, nickel can reach toxic levels, endangering environmental quality and human health. Ni is known to cause cancer and numerous skin disorders. A comprehensive knowledge of the interactions of Ni with soil constituents and the potential mobility of the element is of utmost importance. This paper summarises the reactions of Ni with, as far as possible, all of the major soil mineral phases, specifically emphasising the formation of Ni hydroxide and mixed Ni hydroxide precipitates. In addition, the ageing and subsequent immobilisation of Ni precipitates, as influenced by mineral dissolving silicon, are investigated.

Key words: Ni, sesquioxide minerals, pyrophyllite, gibbsite, silica, kaolinite, metal hydroxides, layered double hydroxides, precipitate ageing, Si

2.2 Introduction

Nickel is used extensively in electroplating processes, nickel-cadmium (NiCd) battery production, arc welding, pigmentations of numerous paints, ceramics, surgical and dental prostheses, magnetic tapes, and computer components (Baytak and Tűrker, 2005). Furthermore, industrial processes, especially mining activities, may lead to atmospheric fallout (Ekosse *et al.*, 2004), whereas the production of steel and the subsequent slag formation and discarding may also contribute to elevated environmental nickel levels. Nickel is thought to be one of the most mobile heavy metals found in the natural soil environment (Christensen *et al.*, 1996). Although considered an essential plant nutrient, elevated levels of Ni can be toxic to all living organisms, causing, among other illnesses, cancer of the respiratory tract and throat in humans, as well as numerous skin disorders (Baytak and Tűrker, 2005; Staunton, 2004). The maximum Ni levels permitted by the Code of Practice for Agricultural Use of Sewage Sludge are constituted at a total content of 75 mg/kg in topsoils (DoE, 1996). Sorption of Ni, like most cationic heavy metals, depends, among others, on the nature of the mineral and organic constituents, ionic strength, the soil solution composition, soil pH, rhizosphere conditions, competing ions, microbial activity and an array of pedological processes, such as preferential water flow and element mobility through redox conditions (Echeverria *et al*., 1998; Staunton, 2004).

2.3 Sorption of nickel onto iron oxide minerals

Heavy metals were found to be sorbed by hematite and goethite in the order Cu > Pd > Zn > Cd > Co > Ni > Mn > Ca > Mg, except for an interchange in position for Cu and Pb on hematite (Trivedi, Axe and Dyer, 2001; Schwertmann and Taylor, 1989). This trend has been found to be in agreement with electronegativity and the inverse of the hydrated ionic radii multiplied by the number of waters in the primary solvation shell (Trivedi *et al.,* 2001). Heavy metal sorption onto iron oxides seemed to be strongly pH dependent, showing a steep rise of adsorption within a narrow pH-range (figure 2.1) (Jeon *et al.,* 2003; Trivedi *et al.,* 2001; Dixon and Weed, 1989). The adsorption edge or pH range was shown to be metal specific, and followed the order given above (Schwertmann and Taylor, 1989).

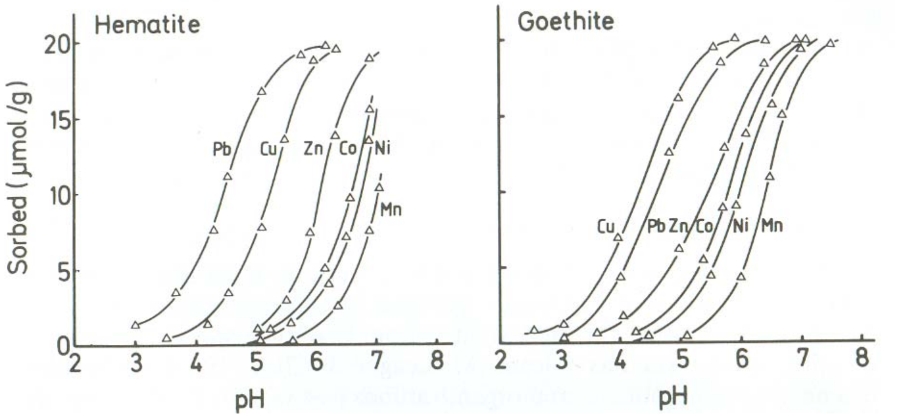

Figure 2.1 The effect of pH on the sorption of various heavy metals on hematite and goethite

Source: Schwertmann and Taylor, 1989

The pH of maximum rise in sorption can be correlated to the first hydrolysis constant of the metal ion, $K = (MOH^+)/(M^{2+})(OH^-)$. The hydrolysed species seemed therefore to be preferentially sorbed over the unhydrolysed one. Although not fully understood, several mechanisms predicting the complexes formed between the metal ion and iron oxide surface have been proposed. The metal ion may form a mono- (1) or binuclear (2) complex (Schwertmann and Taylor, 1989):

$$\text{Fe-OH} + \text{M}^{2+} = \text{Fe-O-M}^{+} + \text{H}^{+} \qquad (1)$$

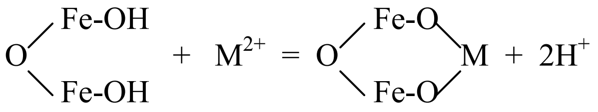

(2)

As the pH increases, the hydrolysed species, rather than the unhydrolysed ion, will be sorbed:

$$\text{Fe-OH} + \text{M}^{2+} + \text{H}_2\text{O} = \text{Fe-O-MOH} + 2\text{H}^{+}$$

Heavy metal sorption onto iron oxides such as goethite and hematite has been found not to be ionic strength dependent, thereby indicating the formation of inner-sphere complexes (Jeon *et al.,* 2003; Trivedi *et al.,* 2001). Goethite seemed to have a rather high affinity for Ni, as demonstrated by figure 2.1. Isotherms revealed a linear relationship between Ni in bulk solution and Ni sorbed (Trivedi *et al.,* 2001).

Competitive sorption onto goethite, however, has been observed. Both Ni and Zn bind onto a high affinity site on goethite, whereas alkaline earth metals such as Ca bind to a lower affinity site. No competitive sorption was therefore observed for a Ni-Ca or Zn-Ca binary system at pH values 5, 6 and 7 at 25 °C. Because Ni and Zn are of the same group in the periodic table and show similar affinities for goethite, competition between these ions is plausible. At lower metal concentrations, when sorption sites are not limited, no inhibiting effect of Ni and Zn sorption has been observed, but as site saturation increased, added Ni displaced some sorbed Zn and vice versa. This phenomenon has been observed at pH values 5, 6 and 7. These results indicate sorption reversibility and ion competitions (Trivedi *et al.,* 2001).

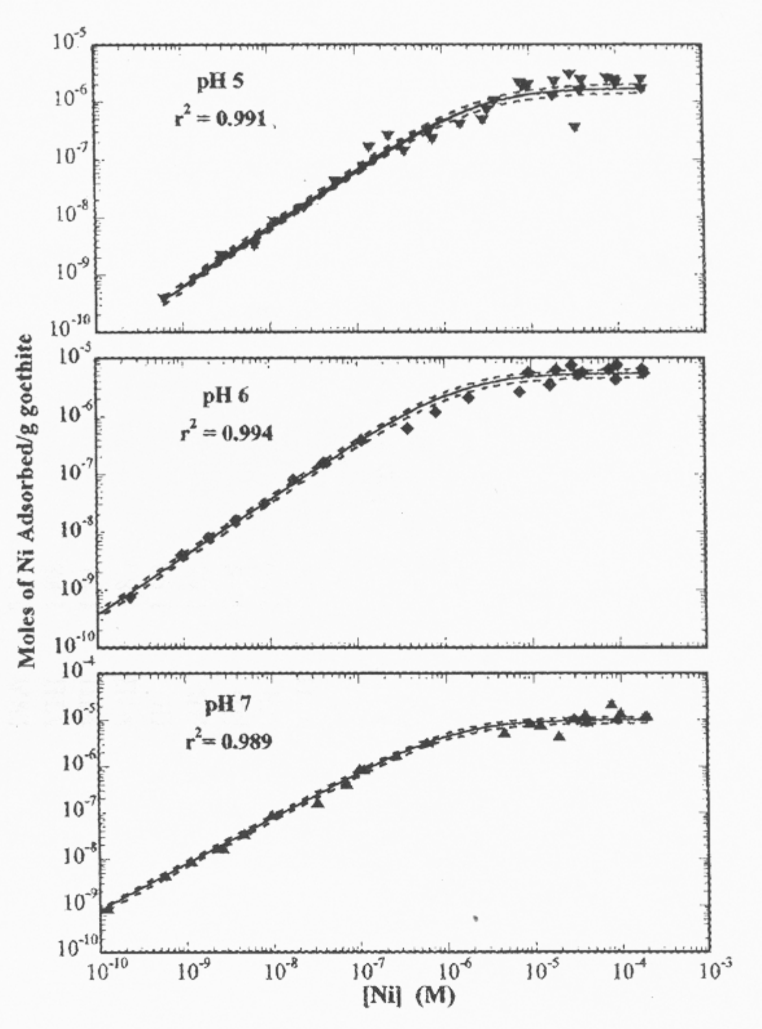

Figure 2.2 Isotherms of Ni sorbed onto 1 g/L goethite at 25°C and an ionic strength of 10^{-3}

Source: Trivedi *et al.*, 2001

Ni sorption onto goethite-coated silica was greater than that found in a pure silica system; the goethite coating also showed a greater affinity for Ni than the discrete goethite system. Xu and Axe (2004) found the pH_{PZC} of the goethite-coated silica to be between that of pure silica and goethite. In a system where silica is only partially coated by goethite, both silica and goethite surfaces contribute to sorption processes. Studies show that nanometre iron oxide coatings greatly increased sorption capacity (Xu and Axe, 2004).

For a synthesised amorphous iron oxyhydroxide, $Fe(OH)_3$, the solubility of sorbed heavy metals was found to increase with decreasing pH values, following a desorption edge. The desorption of Ni from $Fe(OH)_3$ increased sharply over a pH range of 1 to 2 units (Kedziorek and Bourg, 1996).

Desorption of Ni from the amorphous $Fe(OH)_3$ surface at $pH < 3$ is thought to be due to two simultaneous processes: the partial dissolution of the amorphous $Fe(OH)_3$ mineral; and desorption of the Ni ions from the mineral surface. The latter contributed 60 % to the solubilisation of sorbed Ni, which may be macroscopically described by the equation:

$$SOM + xH = SOH_x + M$$

where SOM represents a metal-surface site complex, SOH a site unassociated with any species of M, and x the apparent ratio of moles of protons released or consumed per mole of adsorbate removed or released from/to the solution (Kedziorek and Bourg, 1996).

In a $Fe(OH)_3$–humic acid mixture, sorbed Ni is solubilised when $pH < pH_{PZC}$ of the $Fe(OH)_3$. The PZC of $Fe(OH)_3$ is said to be approximately 8.5 (Sparks, 2003). Ni desorption seemed to be significant at neutral pH values, but low at moderately low pH values. In the pH range between the pH_{PZC} of the two mineral phases, little Ni was found to be desorbed (Kedziorek and Bourg, 1996). This may be owing to the sorption of humic acid at these pH values onto the $Fe(OH)_3$ surface, thereby trapping the metal ions (Kedziorek and Bourg, 1996). The solubility of humic acid increased as the pH increased (Kedziorek and Bourg, 1996).

Kedziorek and Bourg (1996) found the solubilisation of Ni at low pH values in the presence of the $Fe(OH)_3$-humic acid mixture to be partially linked to the dissolution of the amorphous $Fe(OH)_3$ phase. For $pH > pH_{PZC}$ of amorphous $Fe(OH)_3$, the solubilisation of Ni was linked to the dissolution of the humic acid; the quantity of desorbed Ni, however, was found to be smaller than that of a pure humic acid system. At low pH values, the humic acid was strongly bound to the $Fe(OH)_3$ surface. A fraction of the Ni is thought to be solubilised owing to competition with protons for binding to the humic acid functional groups. The humic acid dissolved when pH surpassed a value of 5.0. When the pH_{PZC} (humic aid) < pH < pH_{PZC} (inorganic phase), no solubilisation of heavy metals was observed. In the presence of amorphous $Fe(OH)_3$, humic acid dissolved only at pH 5.0, compared with dissolution at pH 3.0 in a pure system. In the $Fe(OH)_3$-humic acid system Ni solubilisation is greatest at low and neutral pH values, but decreases between the PZC of the two solids (Kedziorek and Bourg, 1996).

Time and temperature also contribute to the sorption of heavy metals onto Fe-oxides. A linear relationship between Ni sorption onto goethite and the square root of time has been found, indicating diffusion processes. Diffusion may be rate- determining when metal ions migrate into micropores of the crystal. An increase in temperature, especially between 5 and 35 °C, will accelerate this process. Ion diffusion may explain why a fraction of sorbed heavy metals are not easily extracted, even with strong acids (Schwertmann and Taylor, 1989).

2.4 Sorption of Ni onto manganese oxides

Weakly hydrolysed cations, such as Ni, are strongly sorbed onto oxide surfaces, even in the presence of a large excess of indifferent electrolytes. Ni is thought to be specifically sorbed. Owing to the large surface area, low PZC, and high negative charge of Mn-oxides, specific sorption is strongly expressed. The total charge associated with the Mn-oxide mineral is dependent on the PZC, pH, and any residual permanent charge owing to the substitution of Mn^{2+} and Mn^{3+} for Mn^{4+}. Differences in PZC among specific minerals seem not to affect specific adsorption significantly. Specific adsorption occurs strongly in all of the cryptocrystalline oxides of manganese. Sorbed ions may even be incorporated into the crystal structure of manganese oxide minerals (McKenzie, 1989).

Metal ions are thought to be sorbed onto manganese oxides in the order Pd > Cu > Mn > Co > Zn > Ni (MacKenzie, 1980). One mole of H^+ is released per mole of Ni sorbed. These sorption phenomena lead to the accumulation of heavy metals in soils rich in manganese oxides. Hydrogen peroxide extracts of manganese oxide nodules contained up to 0.14% Ni. Manganese oxides showed high affinity for Pd and Co in particular, and to a lesser extent Ni (McKenzie, 1989).

2.5 Sorption of Ni onto aluminium oxides

Many polyvalent cations can be specifically sorbed by Al-oxides, sorption changing from little sorption to complete sorption within a narrow pH range. Different cations are adsorbed at different pH ranges. Ni was found to be most effectively sorbed between pH 5.8 and 6.5 by an Al-gel that exhibited a point of zero charge of 9.4. The strength of cation sorption by Al-gel can be expressed by the pH at which half of the cation sorption occurred. The following sequence was observed:

Cu (4.8) > Pb (5.2) > Zn (5.6) >Ni (6.3) > Co (6.5) > Cd (6.6) > Mg (8.1) >Ca (9.1) > Sr (9.2) > Ba (10.5)

The numbers in parenthesis indicate the pH values at which half of the cations in solution were sorbed (Ho Hsu, 1989).

Sorption of heavy metals onto Al-oxides may be seen as a competition between the metal ion and H^+ for the deprotonated surface hydroxide. Most divalent cations have an affinity for oxygen and can therefore compete effectively with H^+ for the surface Al-OH or Al-H_2O. Specific adsorption takes place when the affinity of the metal ion is strong enough to liberate H^+ from the OH^- or H_2O at the reactive sites. Cations exhibiting a relatively low affinity for oxygen can release H^+ from H_2O at higher pH levels, forming an Al-OH-metal bond, whereas cations of high affinity for oxygen may release H^+ from OH^- at very low pH values, resulting in the formation of an Al-O-Metal bond. Below a certain pH value, H^+ may be strongly held and not be displaced. This may explain why certain cations are sorbed at certain pH values and why different cations release different amount H^+ ions from the mineral surface (Ho Hsu, 1989).

The strength of sorption can be effectively correlated with the electronegativity of metal ions. The larger the portion of covalent bonding, the more strongly the specific ion will be held by the Al-oxide surface. The percentage ionic bonding can be calculated by the formula:

$$p = 16|X_A - X_B| + 3.5|X_A - X_B|^2$$

where p represents the percentage ionic bonding, X_A and X_B the electronegativity of atoms A and B (Ho Hsu, 1989).

The sorption capacity is related rather to reactive surface than total surface area. Noncrystalline aluminium is therefore much more effective in sorbing heavy metals than crystalline minerals such as gibbsite and pseudoboehmite. Furthermore, it should be remembered that H^+ is much more easily displaced from the surface Al-OH at higher pH values, whereas the edge Al on a mineral surface is coordinated with more H_2O molecules. It should require less energy to replace a H^+ from Al-H_2O than from Al–OH (Ho Hsu, 1989).

2.6 Sorption of Ni onto clay minerals

Scheidegger, Fendorf and Sparks (1996) found Ni sorption onto pyrophyllite, a full cell 2:1 type dioctahedral clay, to be highly dependent on ionic strength at pH values less than 7, but not at all dependent on ionic strength at pH values above 7. Initial metal concentration had no effect on the sorption of Ni onto pyrophyllite. Sorption at pH 6 was found to be fast and reversible, whereas sorption at pH 7.5 was much slower, being attributed to nucleation processes. Traditionally, it has been thought that metal ion sorption processes dependent on ionic strength are indicative of the formation of outer-sphere complexes (Sparks, 2003; Ford *et al.*, 2001).

Heavy metals are easily and rapidly sorbed by kaolinite in the following sequence: Cu(II) > Ni > Co(II) > Mn(II). This sequence is probably due to hydrolysis constants, ionic radii, and solubility of these ions. Cu(II) is the most sorbed ion, owing to its smaller ionic radii and low solubility. This order of sorption may also be dependent on the substitution of hydrogen in hydroxyl groups of kaolinite. Metal-OH^+ is formed and sorption processes are rapidly completed by interaction with the negative charge on kaolinite. Kaolinite also sorbs metal ions by their outer sheet of hydroxyl groups:

$$M^{2+} + H_2O = MOH^+ + H^+$$

$$SiO^- + MOH^+ = SiMOH$$

$\mathrm{nSi\text{-}OH + M^{n+} = (Si\text{-}O)_n\text{-}M + nH^+}$

The clay surface may also be negatively charged, providing sorption sites for metal ions (Yavuz, Altunkaynak and Gzel, 2003):

$\mathrm{nSiO^- + M^{n+} = (Si\text{-}O)_n\text{-}M}$

Sorption onto kaolinite mainly takes place at the proton-bearing surface functional groups such as silinol and aluminol exposed at the edges of the clay sheets, as permanent structural charge is minor (Sparks, 2004; Dixon and Weed, 1989; Yavuz, Altunkaynak and Gűzel, 2003). Complexes formed between heavy metals and kaolinite surface functional groups seem to be rather stable (Yavuz, Altunkaynak and Gűzel, 2003).

Desorption of Ni from kaolinite takes place at pH values about two units higher than observed for amorphous $Fe(OH)_3$. Figure 2.3 shows the solubilisation of Ni from the kaolinite surface (Kedziorek and Bourg, 1996).

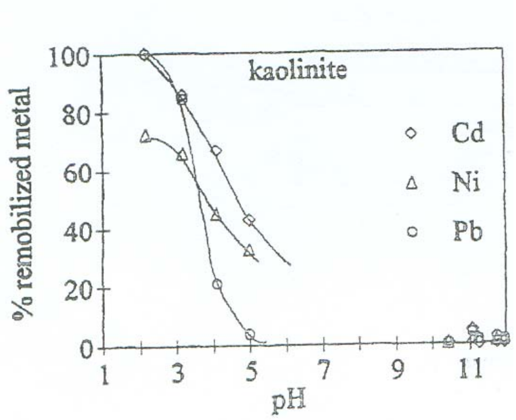

Figure 2.3 Solubility of heavy metals from a kaolinite system
Kedziorek and Bourg, 1996

For a kaolinite-amorphous $Fe(OH)_3$ mixture, Ni solubilised at acid pH values. For a kaolinite-humic acid mixture no metals were solubilised below a pH of 3.0, the PZC of the system. Below pH 5.0, very small quantities of heavy metals were remobilised, but as the pH reached 6.0, all heavy metal ions sorbed were solubilised. This corresponds to the solubility of humic acid in the presence of the kaolinite (figure 2.4) (Kedziorek and Bourg, 1996).

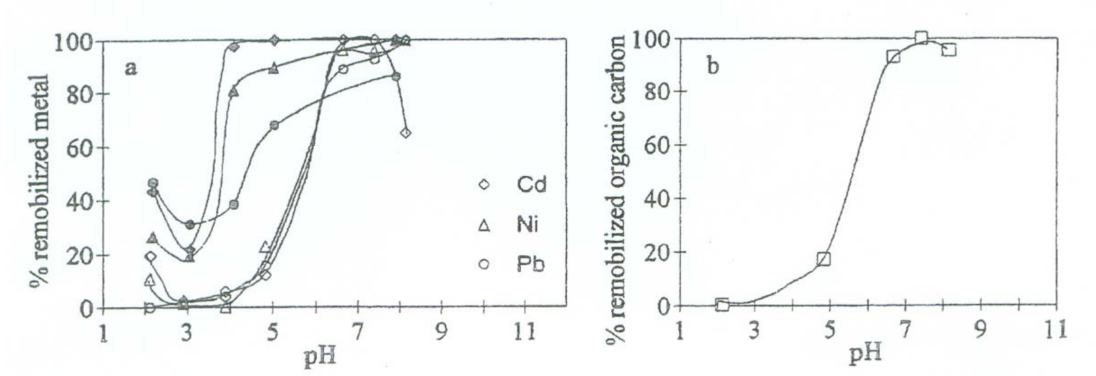

Figure 2.4 Solubilisation of heavy metals from a mixed kaolinite-humic acid system (open symbols) and their theoretical solubilisation (filled symbols); (b) solubilisation of humic acid from the mixed kaolinite-humic acid system

Source: Kedziorek and Bourg, 1996

Humic acid tends to form soluble complexes with heavy metals at basic pH values and insoluble complexes at acid pH values. The humic acid binds to the kaolinite surface through the formation of complexes with the structural Si and Al atoms of kaolinite (Inoue, Zhao and Huang, 1990), as well as with the surface metals sorbed onto the kaolinite surface. At low pH values the desorption of Ni seems to be controlled by partial complexation with solid humic acid. Ni is thus retained at moderately low pH values in the kaolinite-humic acid mixture. At higher pH values the dissolved concentration of humic acid is controlled by the solubility of the humic acid. Weak interactions, involving solubilisation, take place between the humic acid and kaolinite, thereby remobilising sorbed heavy metals (Kedziorek and Bourg, 1996).

Montmorillonite can sorb heavy metals either through cation exchange in the interlayers resulting from the interactions between ions and negative permanent charge or through the formation of inner-sphere complexes with Si-O$^-$ and Al-O$^-$ functional groups at the clay particle edges. Both mechanisms are pH dependent. In acid conditions most silanol and aluminol functional groups are protonated, leading to weaker heavy metal bonding and increased mobility (Dixon and Weed, 1989; Sparks, 2004; Abollino *et al.*, 2002).

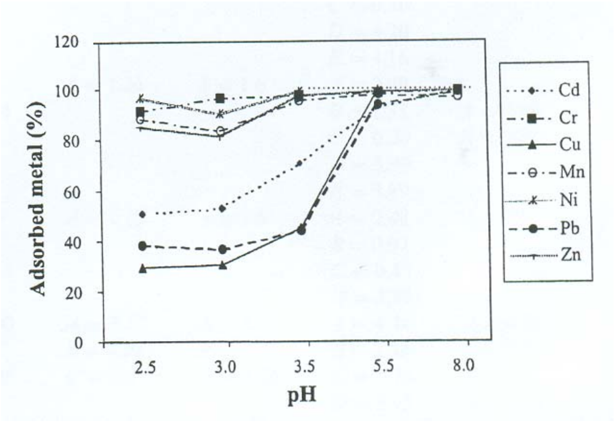

Figure 2.5 Sorption of eight heavy metals onto Na-montmorillonite as a function of pH (initial metal concentration = 1 × 10^{-4}M)

Source: Abollino *et al.*, 2003

Figure 2.5 illustrates the sorption of eight heavy metal ions, including Ni and Cr(III), onto montmorrilonite as a function of pH. As expected, the amount of heavy metals sorbed decreased as pH decreased owing to the protonation of silanol and aluminol functional groups. This is especially evident for Cu, Pd and Cd. Surface complexation reactions are also influenced by electrostatic attraction. Owing to a larger ionic radius, Cd and Pb have lower charge densities and are therefore more affected by the protonation and deprotonation of surface functional groups. The behaviour of Cu(II) may be because of the structure of its aquion. $[Cu(H_2O)_6]^{2+}$ exhibits a tetragonal distortion owing to the Jahn-Teller effect in which the octahedral structure has been contracted along the x^- and y^- axis. The binding of ligands along the x^- and y^- axis is therefore supported, whereas binding along the z^- axis is inhibited owing to the shielding of ligands from Cu^{2+} ion by an extra electron. This results in a structure with two longer and four shorter bonds, thereby hindering the binding of the Cu aquion to the clay functional groups. This effect is more pronounced when the clay functional groups are protonated as binding is supported only along the x^- and y^- axis. The sorption of Cu, Cd and Pb is therefore hindered by cation exchange mechanisms, whereas the sorption of Ni and Cr(III) is dominated by cation exchange. These factors contribute to a different pH effect on each ion. At pH equal to or less than 3, these metals are increasingly sorbed in the order: Cu < Pb < Cd < Zn < Mn ≅ Cr(III) ≅ Ni.

The total sorption capacity of montmorrilonite is said to be remarkable (table 2.1) and increases in the order: Pb = Cd < Cu < Zn < Mn < Ni < Cr (Abollino *et al.*, 2002).

Table 2.1 Total sorption capacity of Na-montmorillonite towards certain heavy metals

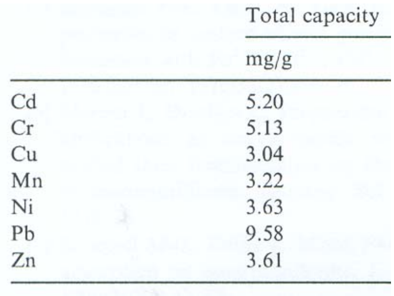

	Total capacity mg/g
Cd	5.20
Cr	5.13
Cu	3.04
Mn	3.22
Ni	3.63
Pb	9.58
Zn	3.61

Source: Albollino *et al.,* 2002

2.7 Formation of Ni surface precipitates

The formation of surface precipitates plays an important role in the retention of Ni on a variety of mineral phases (Charlet and Manceau, 1994; Peltier *et al.*, 2006). It is crucial, however, to assess the composition and structure of these precipitates, as their solubility and, consequently, risk to the environment are dependent on it (Scheinost, Ford and Sparks, 1999).

In a study conducted by Scheinost *et al,* (1999) 95 % of Ni was removed from solution within 3 days by pyrophyllite, and within 4 weeks by talc; talc being a 2:1 trioctahedral clay. Gibbsite removed 50 % of Ni in solution within 4 months. The removal of Ni by silica showed the same trend as that for gibbsite (figure 2.6). These experiments were conducted at pH 7.5 and 22 °C in a background electrolyte solution of 0.1 M $NaNO_3$, and a solid concentration of 5 g/L. Scheidegger, *et al.* (1998), however, found pyrophyllite to remove 95 % of all Ni in solution in less than a day and gibbsite to remove 90 % of the solution Ni within 24 days. The slower reaction kinetic of the Scheinost experiment can be attributed to the lower initial Ni concentration; 1.5 mM instead of 3.0 mM, as used by Scheidegger *et al,* (1998), thereby reducing the degree of super-saturation with respect to the forming precipitates. All other experimental conditions were in accordance (Scheinost, *et al.*, 1999).

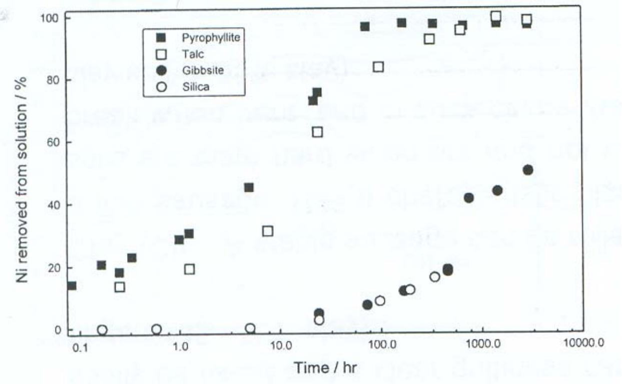

Figure 2.6 The sorption of Ni by pyrophillite, talc, gibbsite and silica as a function of time

Source: Scheinost *et al.,* 1999

As the reactions of talc and pyrophyllite are similar and the kinetics much higher than for silica and gibbsite, the presence or absence of Al in the mineral phases does not seem to influence the kinetics of precipitation (Scheinost, *et al.,* 1999). It does, however, influence the stability and solubility of the formed precipitates (Scheckel, Scheinost and Sparks, 2000). Other factors contributing to Ni precipitation may include the mineral surface area and selectivity for Ni. Si (pyrophyllite, talc and silica) and Mg (talc) were released during the reaction with Ni, indicating mineral dissolution (Scheinost *et al.,* 1999).

The release of Si from the pyrophyllite system continued almost log-linear over a 4-month period and did not decrease even after the Ni concentration reached a steady state after 3 days. This indicates that Ni may not, at least over the long term, enhance mineral dissolution as previously thought (Scheinost *et al.,* 1999; Scheidegger, Fendorf and Sparks, 1998).

Through spectroscopic analysis Scheinost *et al.* (1999) found a Ni-Al layered double hydroxide (LDH) precipitate to form in the presence of the Al-containing minerals pyrophyllite and gibbsite. A α-Ni(OH)$_2$ precipitate formed in the presence of talc and silica (Scheckel *et al.*, 2000; Scheinost, *et al.,* 1999). Figure 2.7 illustrates, to a degree, the differences between Ni-Al LDH and α-Ni(OH)$_2$ (Scheinost *et al.* 1999). Similar experiments conducted on montmorillonite and vermiculite, however, resulted in the formation of non-LDH type precipitates such as Ni phyllosilicates and α-Ni(OH)$_2$ (Dahn *et al.*, 2002; Scheinost and Sparks, 2000).

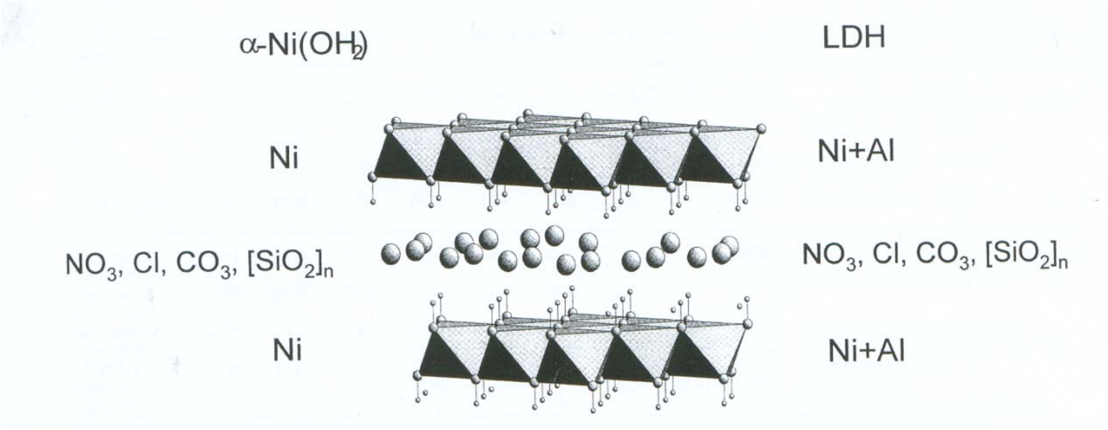

Figure 2.7 The structure and composition of α-Ni(OH)$_2$ in comparison to a Al-Ni LDH. The R$_{Ni-Ni}$ of α-Ni(OH)$_2$ is 3.07 A, whereas that of Al-NI LDH is 3.05 – 3.08 A

Source: Scheinost *et al.*, 1999

The formation of the Ni-Al LDH phase indicates the dissolution of the mineral surface, and either a higher thermodynamic stability or faster precipitation of Ni-Al LDH than α-Ni(OH)$_2$. The initial formation of a α-Ni(OH)$_2$ within the first 24 hours on the gibbsite surface can be attributed to the slower dissolution and Al release rate compared with pyrophyllite. This may be because of the higher stability of gibbsite in contrast to that of pyrophyllite in a system where the silicic acid concentration exceeds $10^{-4,3}$ M (Scheinost, *et al.*, 1999; Hemingway and Sposito, 1996); a condition always fulfilled in the pyrophillite system. Within the first three days the α-Ni(OH)$_2$ phase on gibbsite completely transformed to a Ni–Al LDH phase, supporting the hypothesis that the layered double hydroxide precipitate is thermodynamically more stable (Scheckel *et al.*, 2000; Scheinost, *et al.*, 1999; Scheidegger *et al.*,1996).

Immediate transfer of Al from the Al-bearing minerals pyrophyllite and gibbsite to the layered double hydroxide phase is favoured above an alternative scenario explaining the incorporation of Al into the LDH (Scheckel *et al.*, 2000; Scheinost *et al.*, 1999; Scheidegger *et al.*, 1996). The alternative explanation suggests the intermediate formation of an Al hydroxide phase. Depending on the stability of the Ni-Al LDH, and considering the Ostwald step rule, two scenarios can be proposed: first, if Ni-Al LDH is less stable than diaspore (α-AlOOH), it could act as an immediate sink for Al; and second, if Ni-Al LDH is more stable, diaspore would form first, only to later transform into a LDH phase, possibly involving other Al-intermediates (Scheinost *et al*., 1999). Allada, Navrotsky and Boerio-Goates (2005) suggested that solution pH (greater than 7.0 being favourable) and the ratio of Al to divalent metal ion (Ni) activity, rather than thermodynamic preference, most probably control the extent to which Al substitutes into the LDH structure.

Depending on the availability of Al, both Ni-Al LDH and α-$Ni(OH)_2$ may act as important sinks for Ni. In soils and sediments, adsorption onto variable or permanent charged sites, as well as precipitation of Ni onto mineral surfaces, may be active simultaneously and of utmost importance in rendering Ni immobile (Scheinost *et al*., 1999; Peltier *et al.*, 2005).

2.8 Ageing of Ni surface precipitates

Although much work has been done in recent years on the ability of naturally occurring minerals to sequester heavy metals and render them immobile, not much is known about the long-term stability and potential release into the environment of these sorbed heavy metals (Scheckel, Scheinost, Ford and Sparks, 2000). Research, however, has been done on the long-term stability of nickel precipitates on clay minerals in particular.

Nickel sorbed onto pyrophyllite at a pH of 7.5 to form a precipitate consistent with an Al-Ni layered double hydroxide. Soluble Al was not introduced into the system, meaning that the Al in the surface precipitate was derived from the mineral surface. Dissolution of the mineral surface was confirmed by measuring the release of Si. The uptake of Ni onto the pyrophyllite mineral surface was complete within one month. However, a considerable reduction in desorption of Ni was observed beyond one month. In fact, over a period of one year the Ni-precipitate seemed only to become more stable and less soluble (Scheckel *et al*., 2000; Ford, Scheinost, Sheckel and Sparks, 1999; Scheidegger, Lamble and Sparks, 1996).

Characterisation of the short-range structure confirmed the formation of an Al-Ni LDH. It was also found that the Si released due to the dissolution of the pyrophillite mineral was incorporated into the crystal structure of the Al-Ni LDH. It seemed plausible that the Si exchanged for nitrate and other anions in the layers between the Al-Ni LDH, thereby cementing the precipitate to form an Al-Ni phyllosilicate precursor (Scheckel *et al.,* 2000). A hypothetical scheme illustrating the transition of the Al-Ni LDH to an Al-Ni phyllosilicate precursor is shown in figure 2.8 (Ford *et al.*, 2001).

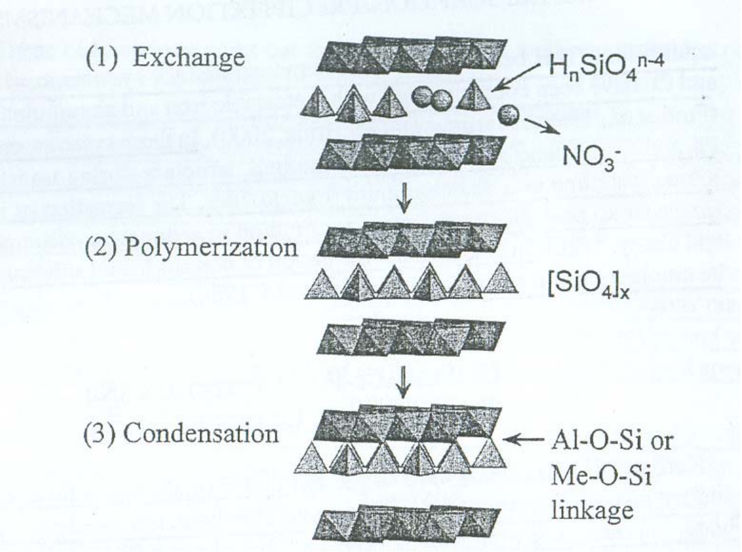

Figure 2.8 Schematic illustration of a possible mechanism for the stabilization of an Al-Ni LDH precipitate over time

Source: Ford *et al.,* 2001

Ni also precipitated onto gibbsite as a Ni-Al LDH, but formed $Ni(OH)_2$ on a talc surface (Scheckel *et al.,* 2000). Through spectroscopic evidence, the formation of a crystalline phyllosilicate within the first few months can be excluded. A phyllosilicate precursor, as in the case of pyrophyllite, may, however, form on silica and talc; consisting of α-$Ni(OH)_2$ with Si polymers in the interlayer (Scheinost *et al.,* 1999). It would therefore seem that the presence of both Al and Si in a system will inevitably lead to a more stable Ni-precipitate (Scheckel *et al.,* 2000). The formation of an Al-Ni phyllosilicate precursor or α-$Ni(OH)_2$ phyllosilicate precursor may be common in soils and sediment (Ford *et al.,* 2001), although this still needs to be proved.

2.8 Ni surface precipitate stability

Scheckel *et al.* (2000) conducted experiments to determine the stability of Ni-surface precipitates on pyrophyllite, talc and gibbsite. Experimental conditions included a pH of 7.5, initial Ni concentration of 3 mM, a background electrolyte concentration of 0.01 M $NaNO_3$, and a solid:solution mineral mass ratio of 10 g/L. Dissolution of the surface precipitates was conducted by HNO_3, to induce proton-promoted dissolution, at pH 4.0 and 1.0 mM EDTA, to induce ligand promoted dissolution, at pH 7.5. The precipitates were left to age for up to one year.

In accordance with other studies (Scheidegger, Fendorf and Sparks, 1996; Scheidegger *et al.,*1996; Scheckel *et al.,* 1999) a Ni-Al LDH phase formed on pyrophyllite and a α-$Ni(OH)_2$ phase formed in the presence of talc. For gibbsite, the initial surface precipitate phase after 24 hours was α-$Ni(OH)_2$, but then transformed to Ni-Al LDH. In all systems, some Ni may have been present as adsorbed Ni (Scheckel *et al.,* 2000). Adsorbed Ni, however, under such experimental conditions, constitutes only a small fraction of the overall Ni in the system after one day (Scheidegger *et al.,* 1997). Removal of Ni from the minerals aged at least one day is therefore due to the dissolution of the surface precipitates (Scheckel *et al.,* 2000).

Ligand promoted dissolution by EDTA was found to be more effective than protolysis by HNO_3 at pH 4.0. As indicated by figure 2.9, the stability of the phases decreased from Ni-Al LDH on pyrophyllite to α-$Ni(OH)_2$ on talc to Ni-Al LDH on gibbsite when extracted with EDTA after one month. However, extraction at pH 4.0 with HNO_3 after one month showed a decrease in precipitate stability in the order, pyrophyllite, talc and gibbsite. This trend seem to be primarily dependent on the extractant, since the order of stability after one year was consistent with results obtained using EDTA at one month ageing (Scheckel *et al.,* 2000). This sequence can be explained by the greater stability of Al-for-Ni substituted hydroxide layers compared with a pure Ni-hydroxide, as well as the silicate for nitrate or carbonate exchanged interlayers (Ford *et al.,* 2001; Scheckel *et al.,* 2000; Scheinost *et al.,* 1999; Peltier *et al.,* 2006). All precipitate phases stabilised drastically with time, as shown by figure 2.11 (Scheckel *et al.,* 2000).

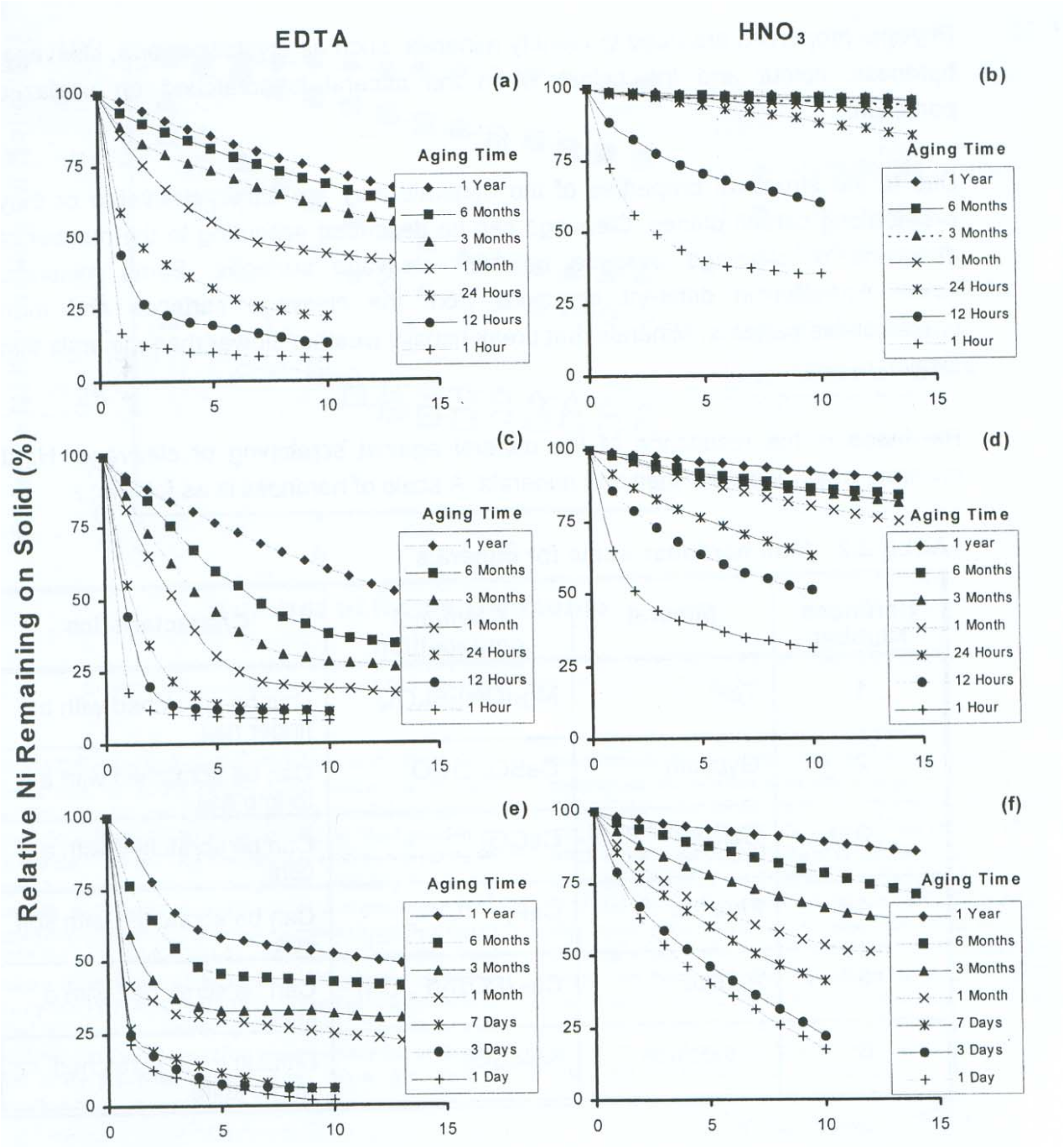

Figure 2.9 The rate of Ni desorption from Ni reacted minerals as a function of aging of surface precipitates. Replenishment steps with EDTA at pH 7.5 are shown on the left hand side, and replenishment steps with HNO_3 at pH 4.0 on the right hand side. Ni reacted minerals are from top pyrophillite (a & b), talc (c & d), and gibbsite (e & f)

Source: Scheckel *et al.*, 2000

The higher stability of the pyrophyllite Ni-Al LDH precipitate and the talc α-$Ni(OH)_2$ precipitate are therefore attributed to the formation of phyllosilicate precursors, whereas the gibbsite Ni-Al LDH is less stable owing to a lack of structural Si. Nonetheless, the Ni-Al LDH precipitate found on gibbsite also stabilised with time, indicating another factor, besides silication, must be responsible for the ageing effect

(Scheckel *et al.,* 2000). This factor may be crystal growth owing to Ostwald ripening (Sutheimer, Maurice and Zhou, 1999; Scheckel *et al.,* 2000). Crystal growth may also have a substantial effect on the ageing of precipitates on pyrophyllite and talc (Scheckel *et al.,* 2000).

Peltier *et al.* (2006) determined the enthalpies of formation for Ni LDH phases with different inorganic anion interlayer species. Enthalpy and free energies of formation for Ni LDH phases increased in the order CO_3^{2-}, SO_4^{2-}, NO_3^-, suggesting that carbonate is the most stable of the common inorganic anion interlayer species. CNS analysis confirmed up to 30 % substitution on a charge equivalent basis of carbonate for nitrate and a 10 % substitution of carbonate for sulphate in the interlayers. Results also seem to indicate that carbonate substitution will occur even at very low CO_3^{2-} concentrations. Therefore carbonate, if present, will probably dominate the interlayers of newly formed Ni LDH precipitates. Furthermore, Ni LDH phases were found to be thermodynamically favoured over pure Ni hydroxide phases on soil minerals containing soluble Al, and became increasingly more likely to form at pH values surpassing 6.5. The substitution of silica for carbonate in the interlayers has also been found to be thermodynamically favoured. After reacting with the newly formed Ni LDH phase for two weeks, 40 % of carbonate ions were replaced with $H_3SiO_4^-$. Aside from the anion exchange, the resulting phase showed no significant changes in structure of either the octahedral Ni-Al sheets or the Ni:Al ratio. The water content of the interlayer, however, decreased dramatically after silication.

The enthalpies of formation (ΔH_f°) of all Ni-Al LDH phases have also been found to be significantly more negative than those for either $Ni(OH)_2$ or $NiCO_3$. The samples containing higher levels of nitrate in the interlayers were found to have less negative enthalpies of formation values than the equivalent sulphate or carbonate interlayers; the carbonate substituted phase being thermodynamically the most favoured (Peltier *et al.* 2006).

It would therefore seem that the formation of Ni LDH phases and their subsequent silication may reduce the mobility and bioavailability of Ni in soils rich in minerals such as pyrophyllite, kaolinite and gibbsite (Peltier *et al.,* 2006; Scheckel *et al.,* 2000; Scheinost *et al.,* 1999).

2.9 Conclusion

Detailed studies on Ni precipitation and the stabilising effect of dissolving Si thereupon have been conducted, and can be used to postulate the stability of Ni precipitates on certain mineral surfaces. Whereas Ni tends to precipitate as a metal hydroxide on mineral surfaces not containing Al, an Al-Ni layered double hydroxide (LDH) phase forms in the presence of Al. Ni LDH phases have also been shown to precipitate in the presence of Fe(III), and possible numerous trivalent cations such as Cr(III). Although LDH phases exhibit lower enthalpy of formation values, these precipitates are not necessarily less soluble than the Ni hydroxide phases. LDH phases do tend to be more stable than Ni hydroxide phases when both have been subject to Si cementation.

As yet, not much is known of Ni sorption and precipitation onto the amorphous sesquioxide minerals, especially Al and Mn oxides. Furthermore, few studies have attempted to correlate the mechanisms derived from single and dual mineral phase systems to multi-component soil systems. The next logical step in Ni research should therefore be the elucidation of mechanisms by which this notoriously mobile element is sequestered by soil constituents under natural conditions. Only by understanding the basic concepts of Ni chemistry, especially in multi-component soil systems, can the potential hazard this element poses in the environment not only be assessed, but also managed.

2.10 References

ALLADA, R.K., NAVROTSKY, A. and BOERIO-GOATES, J. 2005. Thermochemistry of hydrotalcite-like phases in the $MgO-Al_2O_3-CO_2-H_2O$ system: A determination of enthalpy, entropy, and free energy of hydrotalcite-like solids. *American Mineralogist*, 90: 329 – 355.

BATCHELOR B. Leach models for contaminations immobilized by pH-dependent mechanisms. *Environmental Science and Technology,* 29(11):1721–1726.

BAYTAK, S. and TűRKER, R.A. 2005. Determination of lead and nickel in environmental samples by flame atomic absorption spectrometry after column solid-phase extraction on Ambersorb-572 with EDTA. *Journal of Hazardous Material,* 129:130–136.

CHRISTENSEN, T.H., LEHMANN, N., JACKSON, T. and HOLM, P.E. 1996. Cadmium and nickel distribution coefficients for sandy aquifer materials. *Journal of Contaminant Hydrology,* 24:75–84.

DAHN, R., SCHEIDEGGER, A.M., MANCEAU, A., SCHLEGEL, M.L., BAEYENS B., BRADBURY, M.H. and MORALES, M. 2002. Neoformation of Ni phyllosilicates upon Ni uptake on montmorillonite: A kinetic study by powder and polarized extended x-ray adsorption fine structure spectroscopy. *Geochimica et Cosmochimica Acta,* 66:2335–2347.

DoE, 1996. *Code of Practice for the Agricultural Use of Sewage Sludge*. Second edition., UK: Department of Environment.

ECHEVERRIA, J.C., MORERA, M.T., MAZKIARAN, C. and GARRIDO, J.J. 1998. Competitive sorption of heavy metals by soils. isotherms and fractional factorial experiments. *Environmental Pollution,* 101:275–284.

EKOSSE, G., VAN DEN HEEVER, D.J., DE JAGER, L. and TOTOLO, O. 2004. Environmental chemistry and mineralogy of particulate air around Selebi-Pikwe nickel-copper plant, Botswana. *Minerals Engineering*, 17:49–535.

FORD, R.G., SCHEINOST, A.C., SCHECKEL, K.G. and SPARKS. 1999. The link between clay mineral weathering and structural transformation in Ni surface precipitates. *Journal of Environmental Science and Technology*, 18:3140–3144.

FORD, R.G., SCHEINOST, A.C. and SPARKS, D.L. 2001. Frontiers in metal sorption. *Advances in Agronomy,* 74:41–61.

HO HSU, P.A. 1989. Aluminium hydroxides and oxydroxides. In: *Minerals in the Soil Environment.* Second edition. Edited by Dixon, J.B., and Weed, S.B. SSSA Book Series: 1. Madison, Wisconsin: Soil Science Society of America, 366–369.

JEON, B.H., DEMPSEY, B.A., BURGOS, W.D. and ROYER, R.A. 2003. Sorption kinetics of Fe(II), Zn(II), Co(II), Ni, Cd(II) and Fe(II)/Me(II) onto hematite. *Water Research,* 37: 4135–4142.

KEDZIOREK, M. A. M. and BOURG, A.C.M. 1996. Acidification and solubilisation of heavy metals from single and dual-component model solids. *Applied Geochemistry,* 11:299–304.

McKENZIE, R.M. 1989. Manganese oxides and hydroxides. In: *Minerals in the Soil Environment.* Second edition. Edited by Dixon, J.B., and Weed, S.B. SSSA Book Series: 1. Madison, Wisconsin: Soil Science Society of America, 457 – 461.

NATIONAL RESEARCH COUNCIL, Committee on Biological Effects of Atmospheric Pollutants, 1974. *Chromium.* National Academy of Science, Washington, D.C.

PELTIER, E., ALLADA, R., NAVROTSKY, A. and SPARKS, D.L. 2006. Nickel solubility and precipitation in soils: A thermodynamic study. *Clay and Clay Minerals,* 54:153–164.

SCHEIDEGGER, A. M., FENDORF, M. and SPARKS, D.L. 1997. Mechanisms of nickel sorption on pyrophillite; Macroscopic and microscopic approaches. *Soil Science Society of America Journal,* 60:1763–1772.

SCHEIDEGGER, A. M., LAMBLE, G. M. and SPARKS, D.L. 1996. Spectroscopic analysis for the formation of mixed cation hydroxide phases upon metal sorption on clay and aluminum oxides. *Journal of Colloid and Interface Science,* 186:118–128.

SCHECKEL, K.G., SCHEINOST, A.C., FORD, R.G. and SPARKS, D. 2000. Stability of layered Ni hydroxide surface precipitates – A dissolution kinetic study. *Geochimica et Cosmochimica Acta,* 64:2727–2735.

SCHEINOST, A.C., FORD, R.G. and SPARKS, D. L. 1999. The role of Al in the formation of secondary precipitates on pyrophyllite, gibbsite, talc, and amorphous silica: A DRS study. *Geochimica et Cosmochimica Acta,* 63:3193–3203.

SCHEINOST, A.C. and SPARKS, D. L. 2000. Formation of layered single and double metal hydroxide precipitates at the mineral/water interface: A multiple scattering XAFS analysis. *Journal of Colloid and Interface Science,* 223:167–178.

SWERTMANN, U, and TAYLOR, R.M. 1989. Iron oxides. In: *Minerals in the Soil Environment.* Second edition. Edited by Dixon, J.B., and Weed, S.B. SSSA Book Series: 1. Madison, Wisconsin: Soil Science Society of America, 409–415.

SPOSITO, G. 1989. *Chemical Equilibria and Kinetics in Soils.* New York: Oxford University Press, 138–176.

SPARKS, D.L., 2004. *Environmental Soil Chemistry*. Second edition. Academic Press, 60 – 61, 352.

STAUNTON, S. 2004. Sensitivity analysis of the distribution coefficients, Kd, of nickel with changing soil chemical properties. *Geoderma*, 122:281–290.

TRIVEDI, P., AXE, L. and DYER, J. 2001. Adsorption of metal ions onto goethite: single-adsorbate and competitive systems. *Journal of Colloid and Surface Chemistry,* 191:107–121.

WHO 1996. Guidelines for Drinking Water Quality. Second edition. Volume 2. *Health Criteria and Other Supporting Information*. Geneva: World Health Organization, 940–949.

XU, Y. and AXE, L. 2004. Synthesis and characterization of iron oxide-coated silica and its effect on metal sorption. *Journal of Colloid and Interface Science*, 282: 11 – 19.

YAVUZ, O., ALTUNKAYNAK, Y. and GűZEL, F. 2003. Removal of copper, nickel, cobalt and manganese from aqueous solution by kaolinite. *Water Research*, 37:948–952.

Chapter 3 Environmental extractability of chromium(III) and nickel correlated with soil water potential and the mineralogy of three South African Highveld soils

3.1 Abstract

The growing use in agriculture of chromium(III)- and nickel-containing industrial by-products, such as steel plant slag, necessitates an investigation into the environmental extractability of these elements. This study aims to determine the effect of soil water potential on Cr(III) and Ni extractability, as well as the association of Cr(III) and Ni with certain soil mineral phases. Furthermore, the study attempts to determine soil characteristics which might be used to predict Cr(III) and Ni mobility. The extractability of Cr(III) and Ni under soil water potential values ranging from -1 to -3100 $J.kg^{-1}$ was investigated, using $Mg(NO_3)_2$ and diammonium EDTA. Three mineralogically contrasting soils were used, and the association of Cr(III) and Ni with certain soil mineral phases, after reaching air dried conditions, was determined using 0.1 M $Mg(NO_3)_2$, 0.02 M diammonium EDTA, pH 2.0, 0.1 M $NH_2OH.HCl$, and pH 3.0, 0.175 M $(NH_4)_2C_2O_4$ + 0.1 M $H_2C_2O_2$ (Tamm's reagent). Three main conclusions could be reached: (i) whereas Cr(III) is effectively sorbed and precipitation initially ascribed to bulk-solution saturation, Ni is substantially more mobile and precipitation more pronouncedly influenced by mineral surfaces; (ii) both elements seem to associate mainly with the amorphous Fe fraction of the soils investigated; and (iii) even though neither Cr(III) nor Ni mobility could be linked to field classifiable soil characteristics, laboratory scale parameters (soil mineralogy, CEC and AEC) and soil water potential estimations have shown promise in predicting Cr(III) and Ni mobility.

Key words: Cr(III), Ni, soil water potential, environmental extractability, sorption, mineralogy

3.2 Introduction

Since the advent of the Industrial Revolution, ever-more-heavy metal-rich waste is being produced annually. On a planet with a still-expanding population and diminishing living space, the discerning and beneficial utilisation of these industrial by-products may be a viable option. Steel plant slag, for example, is being used as an agricultural liming agent on the Eastern Highveld of South Africa. Since steel plant slag contains potentially detrimental levels of heavy metals such as Cr and Ni, it is of utmost importance to comprehend the risk these elements may pose to environmental quality and human health by assessing their interactions with soil constituents. The study focused on Cr(III) and Ni.

Although rather harmless in itself, Cr(III), especially in concretionary subsoils, can be oxidised to the hazardous Cr(VI) ion by an array of Mn oxide minerals (Stepniewska, Bucior and Bennicelli, 2004; Cooper, 2002; Fendorf, 1994; Charlet and Manceau, 1992; Saleh *et al.*, 1989; Eary and Rai, 1987; Bartlett and James, 1979, etc), thus warranting an investigation into the trivalent ion's mobility. Cr(III) is rapidly and specifically sorbed by many soil constituents (Bradl, 2004; Charlet and Manceau, 1992) and at slightly acidic to neutral pH conditions its mobility is governed by the stability of the bound Cr(III) phase (Fendorf, 1994).

Cr(III) has been shown to form inner-sphere complexes and precipitate as a hydrous chrome oxide phase (HCO) on goethite (Fendorf, Li and Gunter, 1996; Charlet and Manceau, 1992), quartz (Fendorf *et al.*, 1996; Fendorf and Sparks, 1994; Charlet and Manceau, 1992) and smectite clays (Fendorf, 1994; Rengasamy and Oades, 1978). Whereas the HCO phase, $Cr(OH)_3.nH_2O$, distributed uniformly across the goethite phase, adopting its mineral structure, it precipitated as clusters and moieties onto quartz, rendering the latter less stable and more mobile. The HCO phase found in the smectite clay interlayers was shown to be more stable than the HCO phase precipitated onto goethite (Fendorf, 1994). Cr(III) is sorbed onto montmorillonite, a dioctahedral smectite clay (Sparks, 2003), either through cation exchange in the interlayers or inner-sphere complexation through $Si-O^-$ and $Al-O^-$ groups at the clay particle edges (Abollino *et al.,* 2002; Kraepiel, Keller and Morel, 1999;). Cr(III), apart from hydroxy-Cr, may form hydroxyl Al-Cr on montmorillonite surfaces (Dubbin, 2004). Multinuclear Cr(III) species were also identified on hydrous ferric oxide (Charlet and Manceau, 1992), hematite (Eggleston and Stumm, 1993) and Al_2O_3 (Wehrli, Ibric and Stumm, 1990).

Ni, being one of the most mobile heavy elements (Christensen *et al.*, 1996), has been postulated to be specifically sorbed at near-neutral pH values onto goethite, hematite

(Jeon *et al*., 2003; Trivedi, Axe and Dyer, 2001) and all of the cryptocrystalline oxides of Mn. Sorption onto Al oxide minerals was found to be significant at pH values between 5.8 and 6.5 (Ho Hsu, 1989). Studies further show that nanometre iron oxide coatings greatly enhance Ni sorption (Xu and Axe, 2004). Solubility of synthesised amorphous $Fe(OH)_3$ sorbed Ni increased sharply with decreasing pH, culminating at pH 3.0 (Kedziorek and Bourg, 1996). Scheidegger, Fendorf and Sparks (1996), found Ni sorption onto pyrophyllite to be highly dependent on ionic strength and reversible at pH values less than 7, but not dependent on ionic strength at pH values above 7, indicating nucleation processes at higher pH values. Ni sorption onto montmorillonite is dominated by cation exchange and hindered at low pH values owing to protonated functional groups on the clay sheet edges (Abollino *et al.,* 2002). Owing to kaolinite exhibiting minor permanent charge, sorption of Ni takes place mainly at the exposed $Si\text{-}O^-$ and $Al\text{-}O^-$ functional groups (Yavuz, Altunkaynak and Gűzel, 2003). Ni desorption from kaolinite was found to be most pronounced at pH 5.0 (Kedziorek and Bourg, 1996).

Through spectroscopic analysis, Scheinost *et al*., (1999) found that a Ni-Al layered double hydroxide (LDH) precipitates formed in the presence of the Al-containing minerals pyrophyllite and gibbsite. A $\alpha\text{-}Ni(OH)_2$ precipitate formed in the presence of talc and silica (Scheckel *et al*., 2000; Scheinost *et al.,* 1999). Similar experiments conducted on montmorillonite and vermiculite, however, resulted in the formation of non-LDH type precipitates such as Ni phyllosilicates and $\alpha\text{-}Ni(OH)_2$ (Dahn *et al*., 2002; Scheinost and Sparks, 2000). The stability of precipitates at pH 7.5 was found to decrease in this order: Ni-Al LDH on pyrophyllite to $\alpha\text{-}Ni(OH)_2$ on talc to Ni-Al LDH on gibbsite (Scheckel *et al*., 2000).

Although progress has been made regarding the elucidation of heavy metal sorption and precipitation mechanisms in single or dual component mineral systems, not much is known about the interaction of heavy metals with multi-component mineral systems such as soils and sediments. The next logical step would therefore be the correlation of element mobility with field and/or laboratory classifiable soil characteristics. This study thus aims to investigate the environmental extractability, using an array of extractants, and the mechanisms by which Cr(III) and Ni are sequestered in multi-component soil systems, and to identify easily determinable soil characteristics as a means of assessing Cr(III) and Ni mobility under natural soil conditions. ‘Environmental extractability’ refers to an assessment of the distribution of elements between certain soil phases, including adsorption and sorption through amorphous Al, Fe and Mn oxides, as well as an indication of the maximum levels that may be dissolved under natural soil conditions. The easily determinable field classifiable characteristics would entail soil colour, as an indication of soil mineralogy, and texture, as an indication of cation exchange capacity. According to Brady and Weill (1999), soil colour is derived mainly from sesquioxide and organic matter coatings, and can be viewed as an indication of dominating mineralogy, while soil texture may be used to indicate the cation exchange capacity of soils. Subsoils exhibiting low organic content clearly display the colours of sesquioxide minerals, such as the red of hematite, the yellow of goethite and the brown of maghemite. Mn oxide minerals often colour the soil black (Brady and Weill, 1999). Higher clay content soils displaying red and yellow colouration – as opposed to leached, white coloured and low clay content soils – are therefore thought to sequester Cr(III) and Ni more effectively.

3.3 Materials and methods

Three Eastern Highveld soils, differing on the bases of drainage and relief, were collected from profile pits and passed through a 2 mm sieve. Each soil was characterised using field and laboratory determinable characteristics and contaminated with Cr(III) and Ni, as discussed under section 3.3.2.

3.3.1 Soil characterisation

The soils were classified according to the South African Soil Classification System (1991) and the soil colour was determined by means of the Munsell soil colour chart. The “feel method”, as described by Brady and Weill (1999), was used to determine soil texture in the field. Table 3.1 summarises these field determinable characteristics.

Table 3.1 Soil form, colour and texture as determined under field conditions

Soil form (horizon)	Colour	Texture
E-horizon	7.5YR 8/1 (**White**)	Sand
Yellow brown apedal B	7.5 YR 5/8 (**Yellow**)	Sand clay loam
Red apedal B	2.5 YR 3/6 (**Red**)	Sand loam

These soils comprised a bleached E-horizon (White), formed through lateral removal of sesquioxides and colloidal clay minerals, a yellow brown apedal B-horizon (Yellow) and red apedal B-horizon (Red). The latter two soils are indicative of well-drained, oxidising conditions and dominated by sesquioxide minerals. The three soil horizons were collected from Longlands, Avalon and Bainsvlei soil forms, respectively.

The following laboratory parameters were determined:

(i) To determine clay content and mineralogy, the clay fraction from each soil was separated through sedimentation and pre-treated using peroxide, CDB treatment and Mg-saturation. Peroxide was used to facilitate the removal of organic matter, while the latter two treatments removed amorphous iron oxide mineral phases. To determine the clay mineralogy, x-ray diffraction (XRD) analysis was performed on random, oriented, glycolated, and heated clay samples (Singer, Kirsten and Buhmann, 1994). The clay content and mineralogy as determined are presented in table 3.2.

Table 3.2 Soil clay content and mineralogy expressed as a percentage of the bulk soil composition

Soil Clay content (%)		Clay mineralogy (%)				
		Smectite (Montmorrilonite)	Kaolinite	Mica	Goethite	Quartz
White	4.7	-	1.8	0.9	-	2.0
Yellow	23.2	1.9	4.6	1.4	1.2	14.2
Red	16.3	-	9.3	0.6	1.0	5.4

(ii) To determine the amorphous Al and Fe oxide content, a pH 3.0 solution of 0.175 M $(NH_4)_2C_2O_4$ and 0.1 M $H_2C_2O_2$, known as Tamm's reagent, was used. pH 2.0, 0.1 M $HH_2OH.HCl$ was used to determine the amorphous Mn oxide content (Bertsch and Bloom, 1996; Loeppert and Inskeep, 1996; Gambrell, 1996). The methodology is discussed under section 3.3.2, and the results are summarised in table 3.8.

(iii) Determining the cation and anion exchange capacities for each soil involved the addition of 25 ml of 1.0 M KCl to 2.5 g soil weighed off in 45 ml polyethylene centrifuge tubes. After shaking for one hour on a reciprocal shaker at 100 oscillations per minute, the suspensions were centrifuged for 15 minutes at 3 500 rpm and the supernatant discarded. The samples were then washed five times, using 0.01 M KCl. At the final washing, the suspension pH values were adjusted to span the expected point of zero nett charge (PZNC) range for each soil, using 0.01 M KOH and 0.01 M HCl (Zelazny, He and Vanwormhoudt, 1996). Attempts to adjust the pH values to 4.0, 5.0, 6.0, 7.0 and 8.0 for the yellow brown apedal B-horizon (Yellow) and to 3.0, 4.0, 5.0, 6.0 and 7.0 for the E-horizon (White) and red apedal B-horizon (Red) failed. After shaking the suspension for four hours at 100 oscillations per minute, centrifuging for 15 minutes at 3 500 rpm, and recording the suspension pH values, it was noted that the soils still expressed a certain degree of buffering. Final pH values were found not to differ as hoped for. It is hypothesised that a degree of mineral dissolution occurred during the final washing, as the red apedal B-horizon (Red) in particular yielded a turbid supernatant, even after 0.2 μm membrane filtering. The supernatant centrifuged from each sample was nonetheless decanted, membrane filtered, and stored for K^+ and Cl^- determination (C_1). To obtain the entrained solution (V_1), each centrifuge tube was weighed and it was assumed that the K^+ and Cl^- concentrations equalled that of the final washing. The samples were then washed four times with 10 ml of 0.5 $NaNO_3$ and centrifuged as before. The supernatant after each washing was decanted into 50 ml volumetric flasks (V_2), brought to volume and analysed for K^+ and Cl^- (C_2) (Zelazny *et al*., 1996). Although the point of zero nett charge, where the cation exchange capacity (CEC) equals the anion exchange capacity (AEC), could not be determined, the final solution pH values and calculated CEC and AEC values (summarised in table 3.1) can still be used as an indication of surface charge characteristics. The experiment was conducted in triplicate and the K^+ concentrations read on a Jobin Yvon Horiba, model: Ultima inductive couple plasma-atomic emission spectroscopy (ICP-AES) fitted with a sequential, radial torch at 766.490 nm. Cl^- concentrations were determined using a Dionex DX 120 ion chromatograph (chemically suppressed IC detector).

The following formulas were used to calculate CEC and AEC:

$$\text{CEC } (\text{cmol}_c\text{kg}^{-1}) = 0.1\ (C_2V_2 - C_1V_1) / 39\ W$$

$$\text{AEC } (\text{cmol}_c\text{kg}^{-1}) = 0.1\ (C_2V_2 - C_1V_1) / 35.5\ W$$

where

C_1 = concentration (mg.L^{-1}) of K^+ and Cl^- in the final washing solution of 0.01 M KCl,
C_2 = concentration (mg.L^{-1}) of K^+ and Cl^- in the displacing solution of 0.5 M $NaNO_3$,
V_1 = volume (ml) of the solution entrained in the soil after the final washing with 0.01 M KCl,
V_2 = total volume (ml) of the displacing solution of 0.5 M $NaNO_3$,
39 = atomic weight of K^+,
35.5 = atomic weight of Cl^- and,
W = oven dried soil sample weight (g).

Table 3.3 Cation exchange and anion exchange capacity determined at three pH values for each of the soils investigated

Soil	**pH**	**CEC ($cmol_c.kg^{-1}$)**	**AEC ($cmol_c.kg^{-1}$)**
White	4.74	12.1	-0.06
	5.6	12.2	-0.02
	5.9	13.6	-0.18
Yellow	3.95	22.4	3.19
	4.75	25.4	2.04
	6.9	29.7	1.67
Red	4.78	12.1	6.23
	5.57	13.7	5.05
	5.93	15.4	4.96

Negative AEC values, as found for the E-horizon (White) in table 3.3, have also been reported by numerous authors, including Anderson and Sposito (1992), and Laverdiere and Weaver (1977). These errors are attributed by Zelazny *et al*, (1996) to disregarding negative adsorption and its influence on ion concentrations in the entrained solution. The surface potential requirements of electroneutrality are satisfied by positive adsorption of counterions (opposite charge) and negative adsorption (exclusion) of coions (same charge). The electric double layer therefore exhibits both counterions and coions, the latter increasing in concentration with distance from the charged mineral surface. The values contained in table 3.3 may thus be regarded as an underestimation of CEC and AEC, but serve nonetheless as an indication of surface charge characteristics.

3.3.2 Batch equilibration study

After collection and sieving, the pH of each soil was adjusted to 6.5, using 0.02 M $Ca(OH)_2$. To adjust each soil's pH, buffer curves were compiled and the volume of the analytical grade $Ca(OH)_2$ needed to obtain the desired pH value was calculated (Thomas, 1989). The $Ca(OH)_2$ concentration was determined through titration with 0.01 M HCl.

Soil water retention curves for each soil were compiled in order to correlate Cr(III) and Ni extractability with soil water content. The compilation of these curves entailed the subjection of three water saturated samples of each soil to pressure conditions of 10, 100, and 1000 J.kg^{-1} for 24 hours using pressure pots. After this, each sample was weighed, oven dried at 105 ºC for 54 hours, and weighed again. The mean gravimetric water content value, in percentage, for each soil was determined and plotted against the above pressure potential values. The gravimetric soil water content was calculated using the formula $\Theta = M_{water}/M_{solids}$, as proposed by Hillel (1982). A graph (using Microsoft Excel's power function) was fitted satisfactorily through each soil's data set, enabling the calculation of various gravimetric soil water content values at corresponding soil water potential levels. Table 3.4 summarises the gravimetric soil water content and the soil water potential of the soils.

Table 3.4 Gravimetric soil water content (%) of the investigated three Highveld soils linked to soil water potential (J.kg^{-1})

Soil water potential (J.kg^{-1})	Gravimetric soil water content (%)		
	White	**Yellow**	**Red**
-1	18.2	25.7	24.1
-3	10.7	23.7	18.1
-10	7.78	19.4	15.8
-25	5.89	16.4	12
-100	2.59	5.3	6.94
-1500	1.23	5.3	3.8
-3100	0.42	0.81	0.67

3.3.2.1 Experimental setup

A 100 g sample of each soil was weighed off into a 10 cm diameter polyethylene bucket and treated with 15 mg.kg^{-1} Cr(III) and 15 mg.kg^{-1} Ni using chromium(III) nitrate nonahydrate and nickel nitrate hexahydrate. Water was added to saturate the samples. Each treatment, except the air dried treatment, was replicated three times. The air dried treatment was replicated four times. Control samples were always included.

The samples were left to dry in a constant temperature room at 35 ºC and weighed regularly (initially every 10 min, then, as the soils neared air dried conditions, approximately every few hours,) to determine the gravimetric soil water content and removed for analyses at what were calculated to be the following water potential levels: -1, -3, -10, -25, -1500 and -3100 $J.kg^{-1}$. After removal from the constant temperature room and prior to analysis, the samples were kept in airtight buckets to prevent further evaporation. All of the samples were therefore subject to a reaction time of 36 hours.

After being weighed off for analyses, an additional sample from each bucket was collected and oven dried at 105 ºC to verify whether the estimated soil water content had been reached. In most cases, the soil water content deviated from what was hoped for. This deviation, however, was never more than 20 % and is regarded as not substantial. The soil water content determined through oven drying was used when calculating the concentration of Cr(III) and Ni extracted from the wet soil samples. Cr(III) and Ni concentrations, although extracted from the wet soil samples, are therefore expressed in terms of the oven dried soil sample weights.

Determining the extractability of Cr(III) and Ni in the partially dried samples (- 1 to -1500 $J.kg^{-1}$) involved extraction by 0.1 M $Mg(NO_3)_2$ and 0.02 M diammonium EDTA. All of the extractants listed below were used to determine the Cr(III) and Ni levels associated with certain soil mineral phases once the soil samples reached air dried (-3100 $J.kg^{-1}$) conditions. Al, Fe and Mn concentrations were also determined for the latter.

(i) *0.1 M* $Mg(NO_3)_2$: To 5 g soil weighed off in a 45 ml polyethylene centrifuge tube, 10 ml of the $Mg(NO_3)_2$ solution was added. The solution was placed on a reciprocal shaker for two hours at 180 revolutions per minute (rpm), and centrifuged for 10 minutes at 1 500 rpm. The supernatant was passed through an ashless Whatman no 42 filter paper (Amacher, 1996).

(ii) *0.02 M diammonium EDTA*: The extraction procedure entailed the addition of 30 ml of the EDTA solution to 10 g of soil weighed off in a 45 ml polyethylene centrifuge tube. The soil suspension was then placed on a reciprocal shaker for two hours at 180 rpm and centrifuged for 20 minutes at 2 500 rpm. The supernatant was passed through an ashless Whatman no 42 filter paper (Jean, Bordas and Bollinger, 2006).

(iii) *pH 2.0, 0.1 M $NH_2OH.HCl$*: To 5 g soil, 25 ml of the $NH_2OH.HCl$ solution was added, and the mixture was placed on the reciprocal shaker for 30 minutes at 180 rpm. The solution was centrifuged at 1 500 rpm for 20 minutes, and the suspension passed through ashless Whatman no 42 filter paper (Jean, Bordas and Bollinger, 2006; Balasoiu, Zagury and Deschênes, 2000; Gambrell, 1996).

(iv) *pH 3.0, 0.175 M $(NH_4)_2C_2O_4$ + 0.1 M $H_2C_2O_2$* (known as Tamm's reagent): 30 ml of Tamm's reagent was added to 1 g soil that had previously been weighed off in a 45 ml polyethylene centrifuge tube. The suspension was then placed on a reciprocal shaker for two hours at 180 rpm and centrifuged at 25 rpm for 15 minutes. This procedure was conducted in the dark to prevent photoreduction and retard the crystalline Fe oxide dissolution rate (Loeppert and Inskeep, 1996; Bertsch and Bloom, 1996).

(v) *EPA 3051A digestion*: The method entailed the dissolution of 0.5 g of soil in 10 ml of concentrated HNO_3. The soil:acid suspension was digested in a microwave digestion unit for 10 minutes, using fluorocarbon polymer microwave vessels. Each vessel was sealed prior to heating. After digestion, the solution was left to cool, filtered, and centrifuged and the concentrations were read on a Jobin Yvon Horiba, model: Ultima ICP-AES, fitted with a sequential, radial torch.

Calculating the residual Cr(III) and Ni fraction was done by subtracting the highest extracted Cr(III) and Ni values from the total concentrations added to the soils. To determine the residual Cr(III) fraction, Tamm's reagent values were used. The Ni fraction not extracted from the yellow brown apedal B-horizon was also determined using the Tamm's reagent value, whereas the $NH_2OH.HCl$ values were employed in calculating the residual Ni fraction for the E-horizon (White) and red apedal B-horizon (Red).

All of the extractants were read on a Spectro Genesis axially viewed ICP-AES, except where noted otherwise. Blank and reference samples were included. Prior to extraction all glassware and equipment used were suspended in a 1:10 HNO_3 solution for 24 hours and washed with ultra-pure water to limit contamination. Throughout the study, only ultra-pure water and reagents of analytical grade were used.

Statistical analysis entailed the use of SAS 9.1. To investigate significant differences between Cr(III) and Ni extracted levels, soil type sequestration capacities, and the influence of soil water content on Cr(III) and Ni mobility, analysis of variance (ANOVA) tables were compiled and the Tukey t-test conducted. The respective least squares difference (LSD) values were derived at 5 % confidence interval levels.

3.3.2.2 Experimental approach

To elucidate the choice of water potential levels, this line of logic was followed: Whereas a soil water potential of 0 $J.kg^{-1}$ would indicate water saturation, field capacity is stated to be between -15 and -30 $J.kg^{-1}$ and wilting point at -1500 $J.kg^{-1}$. Once soil has reached a water potential level of -3100 $J.kg^{-1}$, water molecules are held so rigidly by colloidal soil surfaces that much of it is considered nonliquid and can move only in the vapour phase (Brady and Weill, 1999). Correlating Cr(III) and Ni extractability to soil water potential therefore serves as a means to investigate the potential leachability of these elements under field conditions, especially since an E-horizon is seldom completely dry, and copious amounts of water can be stored for quite some time by apedal B-horizons after irrigation or rain.

The logic behind the choice of extractants entailed the following:

(i) 0.1 M $Mg(NO_3)_2$ was used as an indication of ions adsorbed and bound through electrostatic forces onto the exchange complex of the soil (Amacher, 1996), as well as neutral salt soluble precipitates. Although little consistency in the adsorption selectivity order can be found when dealing with divalent or trivalent ions, the hydrated ionic radius, ion charge density, solution pH and specific soil mineral (adsorbent) do seem to be significant factors (Sparks, 2003). Although probably out-competed by the Cr^{3+} ion owing to the latter's higher charge density, the Mg^{2+} ion would seem to compete quite effectively with the Ni^{2+} ion for sites on the exchange complex. Cr(III) and Ni ions extracted using 0.1 M $Mg(NO_3)_2$ may therefore be regarded as bound through physical forces such as

Van der Waal's forces and electrostatic outer-sphere complexation and regarded as in constant equilibrium with soil solution (Sparks, 2003; Brady and Weill, 1999).

(ii) 0.02 M diammonium EDTA induces ligand-promoted dissolution by binding onto the mineral surfaces or sorbed metal cations. Binding is facilitated through exchanging one or more uncoordinated carboxylate groups with surface groups such as HO^-. The formation of such a surface complex may polarise the metal-oxygen bond in sesquioxides, as well as the bond between a sorbed metal and a silanol or aluminol functional group on clay surfaces. Subsequently, the dissolution of the metal from the mineral surface will be enhanced (Nowack and Sigg, 1997). EDTA extractable Cr(III) and Ni can therefore be seen as the dissolution of Cr(III) and Ni from inner-sphere and surface precipitate complexes bound through the O^{2-} and HO^- groups surrounding the sesquioxide structural units, as well as binding through clay silanol and aluminol groups. Naturally, Cr(III) and Ni held by electrostatic forces will also be extracted using 0.02 M diammonium EDTA. It should be noted, however, that EDTA has been shown to dissolve metal oxide minerals. The following simplified two-step reaction serves as an example of the mechanism by which EDTA dislodges ions from mineral surfaces. M denotes a specific metal ion (Nowack and Sigg, 1997):

- Mineral surface=M-OH + $EDTA^{4-}$ → Mineral surface=M-$EDTA^{3-}$ + H_2O (1)

Several intermediate species may form owing to the partial dissociation of the EDTA complex. In the subsequent steps, the M-$EDTA^{3-}$ is detached from the surface.

- Mineral surface= M-$EDTA^{3-}$ → mineral surface=MOH (new) + $MEDTA^-$ (2)

(iii) pH 2.0, 0.1 M $NH_2OH.HCl$, is a mild reducing reagent that is commonly used to mobilise Mn from its amorphous oxides, thus also extracting trace metals sorbed onto or occluded in these oxides (Luo and Christie, 1997; Amacher, 1996; Gambrell, 1996), and is reported to minimally attack coexisting Fe oxides

(Krasnodebska-Ostrega, Emons and Golimowski, 2001; Luo and Christie, 1997; Gambrell, 1996).

(iv) Tamm's reagent, consisting of a pH 3.0, 0.175 M $(NH_4)_2C_2O_4$ and 0.1 M $H_2C_2O_2$ solution, has been correlated with a quantitative estimate of the amorphous Fe (Loeppert and Inskeep, 1996) and Al (Bertsch and Bloom, 1996) oxide mineral component in soil. Although crystalline Fe oxide minerals will also react with ammonium oxalate, the reaction is rate dependent and the preferential dissolution of poorly crystalline Fe oxides phases (including ferrihydrate) confirmed (Schwertmann, 1991). The acid ammonium oxalate solution has little effect on kaolinite, montmorillonite, vermiculite and illite (Hodges and Zelansky, 1980), but does dissolve trioctahedral layered silicates such as biotite and chlorite (Loeppert and Inskeep, 1996).

(v) The EPA 3051A digestion method was used to determine the pseudo-total levels of Cr, Ni, Al, Fe and Mn.

3.4 Results and discussion

3.4.1 Cr(III) and Ni mobility correlated with soil water potential

Using $Mg(NO_3)_2$ as an extractant yielded Cr(III) values below the method detection limit, despite reading against a standard range reaching into parts per billion. As indicated by figure 3.1 and table 3.5, the $Mg(NO_3)_2$ extractable Ni fraction is steadily immobilised as the soils dry out. The immobilisation of Ni as the soil dries out is exemplified by the low clay content E-horizon (White). Apart from the Ni concentrations extracted at -10 and -25 $J.kg^{-1}$, all other treatments summarised by figure 3.1 were found to differ significantly ($P<0.001$). A major fraction of Ni therefore seems to be bound through electrostatic forces and outer-sphere complexation. Adsorption might lead to a local saturation at the mineral water interface and subsequent precipitation. As the soil further dries out, the soil solution will become more and more oversaturated, necessitating Ni to precipitate onto mineral surfaces.

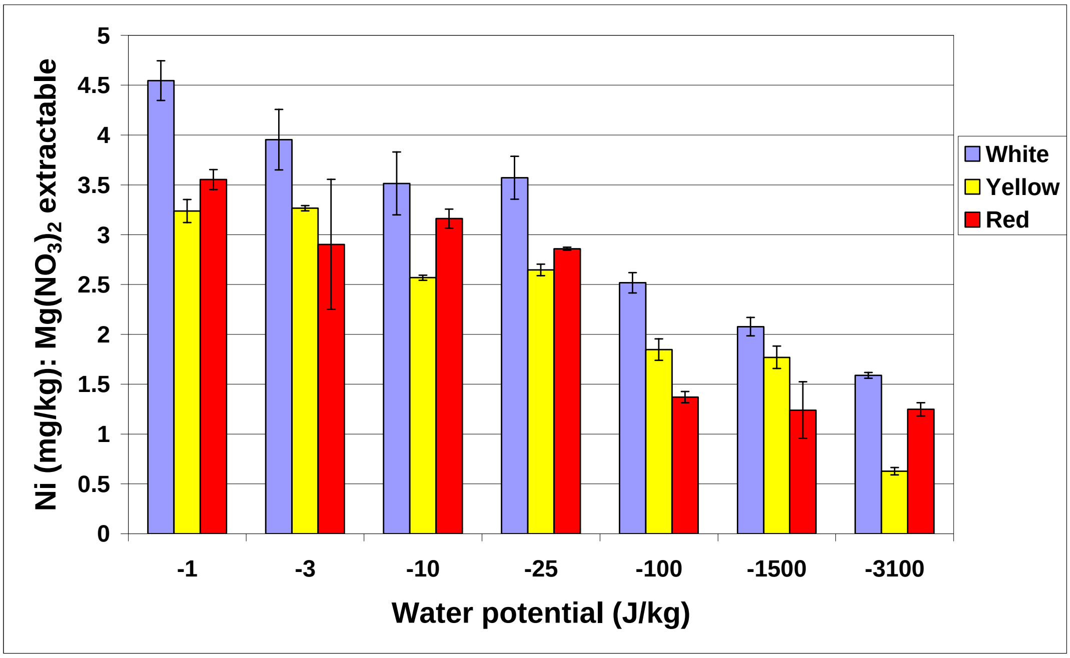

Figure 3.1 The 0.1 M $Mg(NO_3)_2$ extractable Ni fraction correlated with soil water potential

Error bars indicate the standard deviation from the mean values displayed

Owing to the E-horizon (White) being dominated by quartz surfaces, as opposed to the sesquioxide surfaces and higher clay fractions of both the red apedal (Red) and yellow brown apedal B-horizon (Yellow), it is expected that the E-horizon (White) would yield the highest $Mg(NO_3)_2$ extractable Ni fraction. The higher montmorillonite clay content and consequently higher cation exchange capacity (CEC) of the yellow brown apedal B-horizon (Yellow) would explain the less mobile Ni fraction when compared with the Red apedal B-horizon (Red), the latter's clay fraction being dominated by kaolinite, which leads to a lower CEC. According to Sparks (2003), smectite (montmorillonite) exhibits a CEC of between 80 and 150 cmol.kg^{-1}, whereas kaolinite exhibits a CEC of between 5 and 15 cmol.kg^{-1}. The more densely positively charged sites of the montmorillonite clay would lead to a more pronounced lowering of the activation energy needed for the precipitation of Ni, therefore contributing as a factor in rendering the yellow brown apedal B-horizon (Yellow) a more effective sequester of Ni.

Table 3.5 0.1 M Mg(NO$_3$)$_2$ extractable Ni at certain soil water potential levels

	White		Yellow		Red	
Water potential (J.kg^{-1})	***Ni Extracted (mg.kg^{-1})**	**Percentage (%)**	***Ni Extracted (mg.kg^{-1})**	**Percentage (%)**	***Ni Extracted (mg.kg^{-1})**	**Percentage (%)**
-1	4.55a	30.3	3.24d	21.6	3.55c	23.7
-3	3.95b	26.3	3.27d	21.8	2.9e	19.3
-10	3.54c	23.4	2.57g	17.1	3.16d	21.1
-25	3.71c	25	2.65fg	17.7	2.86ef	19.1
-100	2.52g	16.8	1.85i	12.3	1.37kl	9.13
-1500	2.08h	13.9	1.77i	11.8	1.24l	8.27
-3100	1.59jk	10.6	0.63m	4.2	1.25l	8.33
LSD(.05)	0.223		0.223		0.223	

***15 mg.kg^{-1} Ni were added to each treatment**

In contrast to the immobilisation of Ni owing mainly to electrostatic interaction and outer-sphere complexation, the values derived for Mg(NO$_3$)$_2$ extractable Cr(III) (below the method detection limit regardless of soil water content) would indicate specific sorption of Cr(III) in the soil environment. This tendency is further substantiated by the EDTA extractable Cr(III) fraction, exemplified by figure 3.2 and table 3.6.

The effective sequestration of Cr(III), even at near water saturated conditions, would indicate the formation of inner-sphere surface complexes and surface precipitates in particular. The low EDTA extractable Cr(III) fraction, as reflected in table 3.6, may be ascribed to mineral-induced surface precipitation, but is probably because of the soil solution being oversaturated with regards to Cr(III). A substantial fraction of the added Cr(III) is sequestered, even at near saturated conditions. No clear correlation between Cr(III) extractability and soil type could be made, however. This would indicate precipitation because soil solution saturation dominated. Cr(III) extractability at water potential levels of -1500 and -3100 J.kg^{-1} , however, do correlate with hypotheses regarding Cr(III) mobility and soil type. Mineral-induced precipitation therefore also contributes to Cr(III) immobilisation.

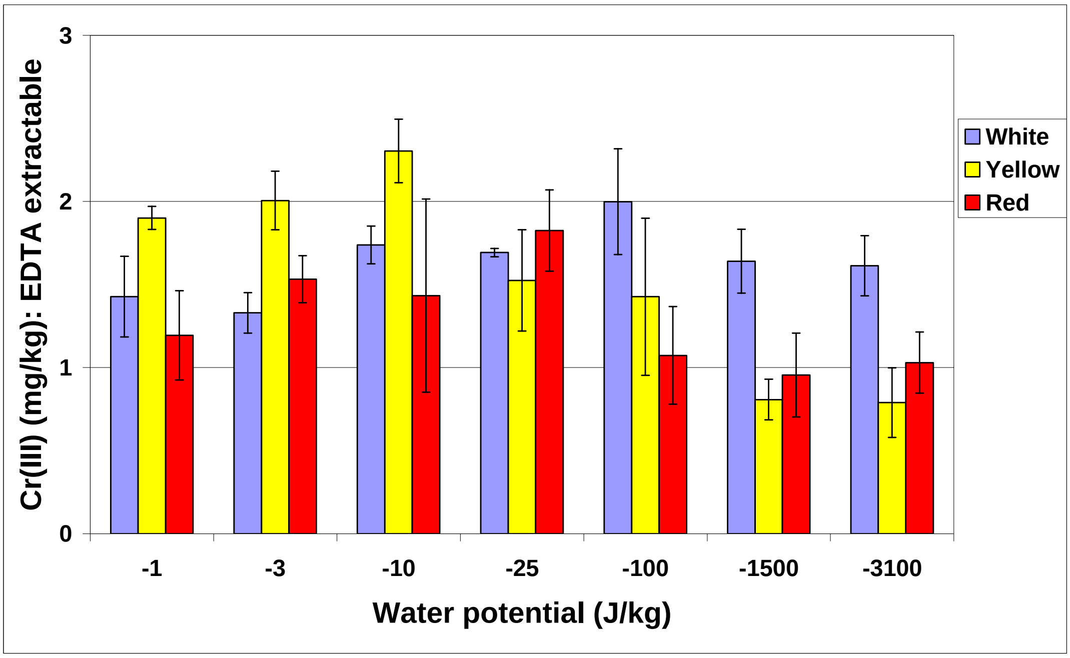

Figure 3.2 The 0.02 M diammonium EDTA extractable Cr(III) fraction correlated with soil water potential

Table 3.6 0.02 M diammonium EDTA extractable Cr(III) at certain soil water potential levels

	White		**Yellow**		**Red**	
Water potential ($J.kg^{-1}$)	***Cr(III) Extracted ($mg.kg^{-1}$)**	**Percentage (%)**	***Cr(III) Extracted ($mg.kg^{-1}$)**	**Percentage (%)**	***Cr(III) Extracted ($mg.kg^{-1}$)**	**Percentage (%)**
-1	1.43ghi	9.53	1.9bc	12.7	1.19ijk	7.9
-3	1.33hij	8.87	2bc	13.3	1.53fgh	10.2
-10	1.74cdef	11.6	2.26a	15.3	1.43ghi	9.5
-25	1.69cdef	11.27	1.63ghi	10.8	1.83bcde	12.2
-100	1.99ab	13.27	1.43efgh	9.5	1.07jk	7.1
-1500	1.64defg	10.93	0.81l	5.4	0.95kl	6.3
-3100	1.61efgh	10.73	0.79l	5.3	1.03kl	6.9
LSD(.05)	0.283		0.283		0.283	

***15 $mg.kg^{-1}$ Cr(III) were added to each treatment**

A combination of mineral-induced and bulk saturation precipitation will explain the lower EDTA extractable Cr(III) fraction from the yellow brown apedal B-horizon

(Yellow) at -1500 and -3100 J.kg^{-1}. Because the yellow brown apedal B-horizon (Yellow) contains a higher montmorillonite clay content than either of the other two soils investigated, it can be hypothesised that Cr(III) would more readily form polymeric inner-sphere complexes in this soil. Clearly indicated by figure 3.2 and table 3.6, the EDTA extractable Cr(III) fraction from the yellow brown apedal B-horizon (Yellow) is significantly higher ($P<0.001$) at near saturated conditions (-1 to -10 J.kg^{-1}) than found for either the E-horizon (White) or red apedal B-horizon (Red). This would indicate the formation of complexes between Cr(III) and silanol and/or aluminol functional groups, not disregarding the influence of sesquioxides, being more pronounced in the yellow brown apedal B-horizon (Yellow) and precipitation to occur more readily in the E-horizon (White) and red apedal B-horizon (Red) at near saturated conditions. Consequently, the Cr(III) phase precipitated in the yellow brown apedal B-horizon (Yellow) as the soil nears air dried conditions will tend to be through polymeric metal complexes (dimers and trimers), rather than the more soluble homogenous precipitation, as in the E-horizon (White) and, to some extent, in the red apedal B-horizon (Red). Furthermore, the higher degree of adsorbed water (table 3.4), as found in the yellow brown apedal B-horizon (Yellow), would also hinder inner-sphere complexation. As the soil nears a water potential of -3100 J.kg^{-1}, the interaction between cations in solution and the soil mineral phases would be more pronounced and complexation more polymerised. Mineral-induced precipitation can be ascribed to one, or all of the following mechanisms:

(i) the lowering of the energy of nucleation by the soil mineral surface
(ii) the dielectric constant near the soil mineral surfaces being lower than that of the solution due to ion adsorption (Sparks, 2003) and/or
(iii) the precipitation of sorbed polymers and polynuclear species owing to local bulk saturation (Ford *et al*., 2001).

Precipitation in the red apedal B-horizon (Red) seems to be a more even combination of homogenous precipitation and precipitation of polymerised species. Like the yellow brown apedal B-horizon (Yellow) – only more subtle – the EDTA extractable Cr(III) fraction (indicated by figure 3.2 and table 3.6) from the red apedal B-horizon (Red) shows a significant decrease ($P<0.0001$) in mobility once the soil has dried to -100 J.kg^{-1}. This would substantiate the hypothesis regarding the formation of inner-sphere Cr(III) and surface complexes leading to a more stable precipitate, but rendering the element more mobile at water content levels that do not induce bulk precipitation. Also, the higher adsorbed water content (indicated by table 3.4) as opposed to the E-horizon (White) would contribute to Cr(III) mobility and sequestration at soil water potential levels nearing -3100 J.kg^{-1}.

In contrast, no substantial difference in EDTA extractable Cr(III) fraction could be noted for the E-horizon, regardless of soil water potential. The latter would therefore be dominated by the formation of a less polymerised and more homogenous precipitate. These findings are in accordance with spectroscopic analyses that show Cr(III) to precipitate as more soluble nodules and clusters on quartz (Fendorf *et al.*, 1996; Fendorf and Sparks, 1994; Charlet and Manceau, 1992), while forming polynuclear species and more evenly distributed precipitates on sesquioxides (Fendorf, Li and Gunter, 1996; Eggleston and Stumm, 1993; Charlet and Manceau, 1992; Wehrli *et al.* , 1990) and clay minerals (Fendorf, 1994; Rengasamy and Oades, 1978). The lower cation exchange capacity (table 3.3) of the E-horizon (White), when compared with the other two soils, would entail a higher activation energy needed for surface precipitation to occur, thus contributing to the observed phenomena.

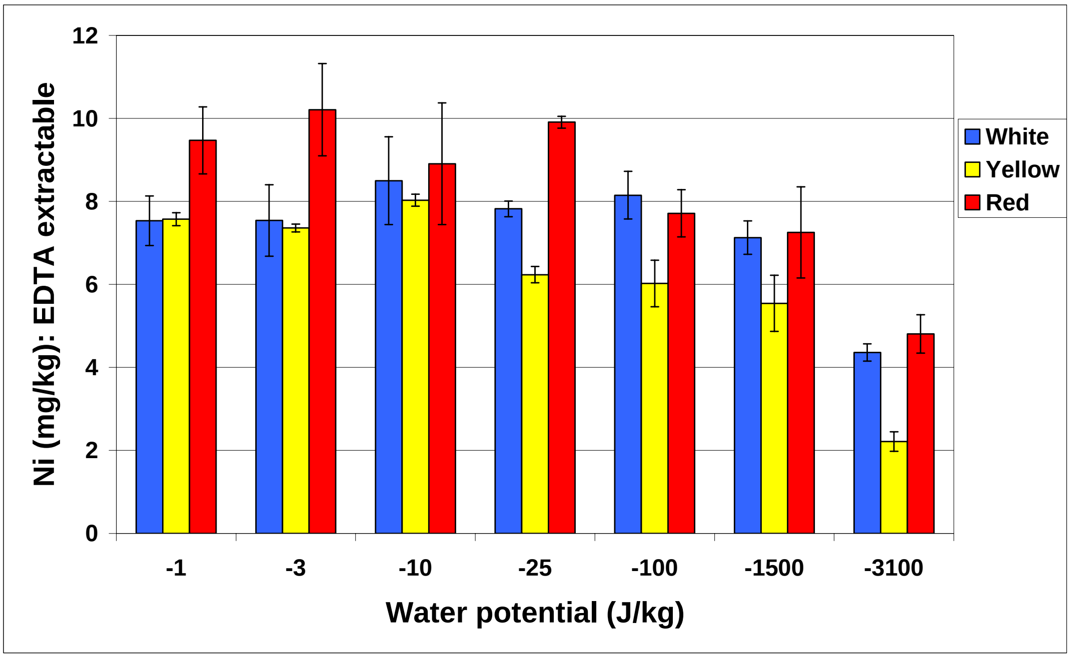

Figure 3.3 The 0.02 M diammonium EDTA extractable Ni fraction correlated with soil water potential

Whereas Cr(III) precipitation can be classified as precipitation influenced directly or indirectly by soil mineral surfaces, but dominated by bulk-solution precipitation, the precipitation of Ni (as indicated by figure 3.1, figure 3.3 and table 3.5), would seem to be influenced more pronouncedly by soil mineralogy. Nonetheless, precipitation owing to bulk-solution precipitation is evident when comparing the extractability of Ni near water saturation to that nearing -3100 $J.kg^{-1}$. The high Ni values extracted using 0.02 M diammonium EDTA for all three soil types investigated and summarised in table 3.7, coupled with the 0.1 M $Mg(NO_3)_2$ extractable fraction, highlight the assumption. Only once the soils had reached a water potential of -3100 $J.kg^{-1}$ was a substantial decrease in Ni extractability noted. Ni is thought to be sorbed mainly through electrostatic forces, outer-sphere complexes and weakly held inner-sphere complexes. Not being able to extract all of the Ni added to the soils using 0.02 M diammonium EDTA would entail that nucleation and precipitation do occur, even at near saturated conditions (-1 to -10 $J.kg^{-1}$), although this is overshadowed by the mobile nature of Ni.

Table 3.7 0.02 M diammonium EDTA extractable Ni at certain soil water potential levels

	White		**Yellow**		**Red**	
Water potential ($J.kg^{-1}$)	***Ni Extracted ($mg.kg^{-1}$)**	**Percentage (%)**	***Ni Extracted ($mg.kg^{-1}$)**	**Percentage (%)**	***Ni Extracted ($mg.kg^{-1}$)**	**Percentage (%)**
-1	7.53e	50.2	7.57e	50.5	9.47ab	63.1
-3	7.54e	50.3	7.36ef	49.1	10.21a	68
-10	8.5cd	56.7	8.03de	53.5	8.91bc	59.4
-25	7.82de	52.1	6.23g	41.5	9.91a	66.1
-100	8.14bc	54.3	6.02fg	40.1	7.71cd	51.4
-1500	7.12de	47.5	5.54i	36.9	7.25de	48.3
-3100	4.36hi	29.1	2.21j	14.7	4.81gh	32.1
LSD(.05)	0.738		0.738		0.738	

***15 $mg.kg^{-1}$ Ni was added to each treatment**

Only after drying to a water potential of -25 $J.kg^{-1}$ could a substantial difference in Ni mobility be noted between the E-horizon (White) and yellow brown apedal B-horizon (Yellow), beyond which Ni is significantly less ($P<0.001$) mobile in the latter. This trend would entail the formation of polymeric complexes – albeit soluble – on the mineral surfaces of the yellow brown apedal B-horizon (yellow), while Ni ions can mostly be found in the diffusion double layer surrounding the mineral surfaces of the E-horizon (White). No significant difference could be found between the extractable Ni of these two soils up to a water potential of -25 $J.kg^{-1.}$ This is attributed to either bulk-solution precipitation and the formation of similar phases or the complexation capabilities of EDTA. To substantiate this hypothesis, Ni precipitates as a significantly ($P<0.001$) more stable precipitate in the yellow brown apedal B-horizon (yellow) as the soil nears air dried conditions, denoting a more polymerised precipitate, than for the E-horizon (White).

What was not expected, though, is the significantly higher ($P<0.001$) EDTA extractable Ni fraction yielded by the red apedal B-horizon (Red) at water potential levels of -1, -3 and -25 $J.kg^{-1}$, the latter being compared with the extractable Ni fraction from the E-horizon (White). Even when considering that Ni might be out-competed for binding sites on the exchange complex by the higher charge density Cr(III) ion, it is expected that the extractable Ni fraction will be in the range found for the E-horizon (White).

The red apedal B-horizon (Red) exhibits a higher clay fraction, higher sesquioxide content and subsequently more binding sites. These sites (as indicated by table 3.3) do not necessarily contribute to the cation exchange capacity of the soil. Table 3.3 further indicates that the red apedal B-horizon (Red) exhibits a substantially higher anion exchange capacity, whereas the soil's cation exchange capacity does not differ substantially from that of the E-horizon (White). It can therefore be argued that the red apedal B-horizon (Red), exhibiting a CEC of 15.4 $cmol_c.kg^{-1}$ and AEC of 4.96 $cmol_c.kg^{-1}$, would in fact sequester Ni less effectively than the E-horizon (White) exhibiting a CEC of 13.6 $cmol_c.kg^{-1}$ and a AEC low enough as not to be determined by the method used. Because Ni is known to be rather mobile (Christensen *et al.*, 1996) and predominantly bound through electrostatic forces – as opposed to Cr(III), which is specifically sorbed – the higher AEC exhibited by the red apedal B-horizon

(Red) would denote a less effective sequestration of Ni than found in the E-horizon (White) at approximately pH 6.5. Subsequently, the formation of surface precipitates as the soil solution becomes oversaturated would be less polymerised and more soluble owing to the less effective adsorption of Ni, than would be the case for the E-horizon (White) and the yellow brown apedal B-horizon (Yellow) in particular. The even distribution of a Cr(III) precipitate onto Fe oxide minerals (as described by Fendorf, Li and Gunter, 1996, Eggleston and Stumm, 1993, Charlet and Manceau, 1992, and Wehrli, Ibric and Stumm, 1990) may also contribute to the mobility of Ni in the red apedal B-horizon (Red). Cr(III) may occupy the negatively charged soil mineral surfaces, and the Cr(III) precipitated phase may even render the surfaces more positively charged. On the contrary, Cr(III) precipitates as nodules onto quartz surfaces (Fendorf *et al.*, 1996, Fendorf and Sparks, 1994, and Charlet and Manceau, 1992) and may not influence the charge characteristics of such surfaces as pronouncedly. The influence of Cr(III) on soil mineral charge characteristics and Ni sequestration, therefore, needs to be investigated further.

The theories presented should, however, be seen as a simplification of a complex process. Because crevices, kinks and other anomalies may be found on naturally occurring mineral surfaces, it cannot be expected that negative and positive charged sites will be distributed homogenously. The higher EDTA Ni fraction extracted from the red apedal B-horizon (Red), therefore, cannot be attributed to charge characteristics alone.

Because no significant difference could be noted between Ni mobility in the E-horizon (White) and the red apedal B-horizon (Red) at -100, -1500 and -3100 J.kg^{-1}, it is deduced that precipitation in these soils is not only attributed to bulk-solution saturation, but that these phases may constitute the same morphology. The significantly less ($P<0.001$) dissolvable Ni precipitate found in the yellow brown apedal B-horizon (Yellow) can be attributed to a more extensive mineral-induced polynucleation process and subsequent more stable precipitate.

It should be stressed, however, that no single mechanism can be seen as solely responsible for the sequestration of an element in the soil environment, albeit that one or a number of mechanisms can dominate the behaviour of a certain element.

3.4.2 Cr(III) and Ni mobility correlated with soil mineralogy

At -3100 $J.kg^{-1}$ the soil has reached a point where the water molecules surrounding the soil particles are perhaps only four or five molecules thick (Brady and Weill, 1999) and the Cr(III) and Ni initially added in liquid form are found to be essentially precipitated. Cr(III) would probably precipitate as a hydrous chrome oxide, $Cr(OH)_3.nH_2O$ (Fendorf *et al.*, 1996; Fendorf and Sparks, 1994; Charlet and Manceau, 1992), and Ni as a $Ni(OH)_2$ (Dahn *et al.*, 2002; Scheinost and Sparks, 2000; Scheckel *et al.*, 2000; Scheinost, *et al.,* 1999), although both elements might also form layered double hydroxide (LDH) phases (Peltier *et al.*, 2006; Prassanna, Padmanabha and Kamath, 2006; Scheckel *et al.*, 2000; Scheinost, *et al.,* 1999). If formed, layered double hydroxides will exhibit the formula $[M^{II}_{1-x}M'^{III}_{x}(OH)_2]^{x+,}$ where M denotes Mg, Ca, Ni, Co, Cu or Zn, and M' may comprise Al, V, Cr(III), Fe(III) and Ga, and $0.15 < x < 0.33$ (Peltier *et al.*, 2006). Although the mechanism for the formation of metal hydroxides and LDH precipitates is not well understood, these phases may occur in conjunction (Sparks, 2003). Research has shown, however, that the type of ion that is sorbed determines whether metal hydroxide surface forms, whereas the mineral surface determines the type of metal hydroxide, that is, metal hydroxide precipitates or LDH phases (Scheckel *et al.*, 2000; Scheinost, *et al.,* 1999). It is thought that bulk-solution precipitation would lead to the formation of morphologically homogenous precipitates, whereas mineral-induced precipitation would constitute a more complex morphology.

The relatively high concentrations of Al and Fe extracted from the soils investigated using EDTA (as indicated by table 3.8) render plausible the hypothesis that Ni might form a Ni-Al LDH or Ni-Fe(III) LDH phase. When considering the close correlation, (exhibited by figure 3.4) between EDTA extractable Ni and Fe, the latter especially would seem a viable option when hypothesising about Ni precipitated forms. Both the Ni-Al LDH and Ni-Fe(III) LDH precipitates are known to be soluble (Prassanna *et al.*, 2006). Although no thermodynamic data could be obtained for the formation of Cr(III)-LDH precipitates, Peltier *et al.* (2006) showed that the Ni-LDH phases, regardless of anion interlayers, exhibited substantially more negative enthalpy of formation ($\Delta H_f°$) values than was found for $Ni(OH)_2$. Evidently Ni and Cr(III) can also co-precipitate to form a Ni-Cr(III) LDH phase. Cr(III) showed no correlation with Al, Fe or Mn extracted using EDTA.

Figures 3.5 and 3.8 denote the extractable Cr(III) and Ni fractions using (apart from 0.1 M $Mg(NO_3)_2$ and 0.02 M diammonium EDTA), pH 2.0, 0.1 M $NH_2OH.HCl$ and Tamm's reagent. EPA 3051A values denote a pseudo total. The $Mg(NO_3)_2$ and EDTA extractable Cr(III) and Ni fractions have already been discussed. Of importance, however, is that EDTA does seem to dissolve a rather high fraction of Mn when compared with both the $NH_2OH.HCl$ and the Tamm's reagent extracted Mn fractions. Table 3.8 indicates that 49.4 % of the $NH_2OH.HCl$ dissolvable Mn is extracted from the E-horizon (White) using EDTA. From the yellow brown apedal B-horizon (Yellow) and the red apedal B-horizon (Red) respectively, 49.9 % and 51.7 % are extracted. This can either be because sorbed and precipitated Mn is complexed by diammonium EDTA or because EDTA dissolves a fraction of the amorphic Mn oxide phase. The latter is substantiated by Hlavay *et al.* (2004), who also state that EDTA may dissolve a certain fraction of the amorphous Al and Fe oxide phase, although not as pronouncedly as the amorphous Mn oxide phase over relatively short exposure periods (approximately 90 minutes).

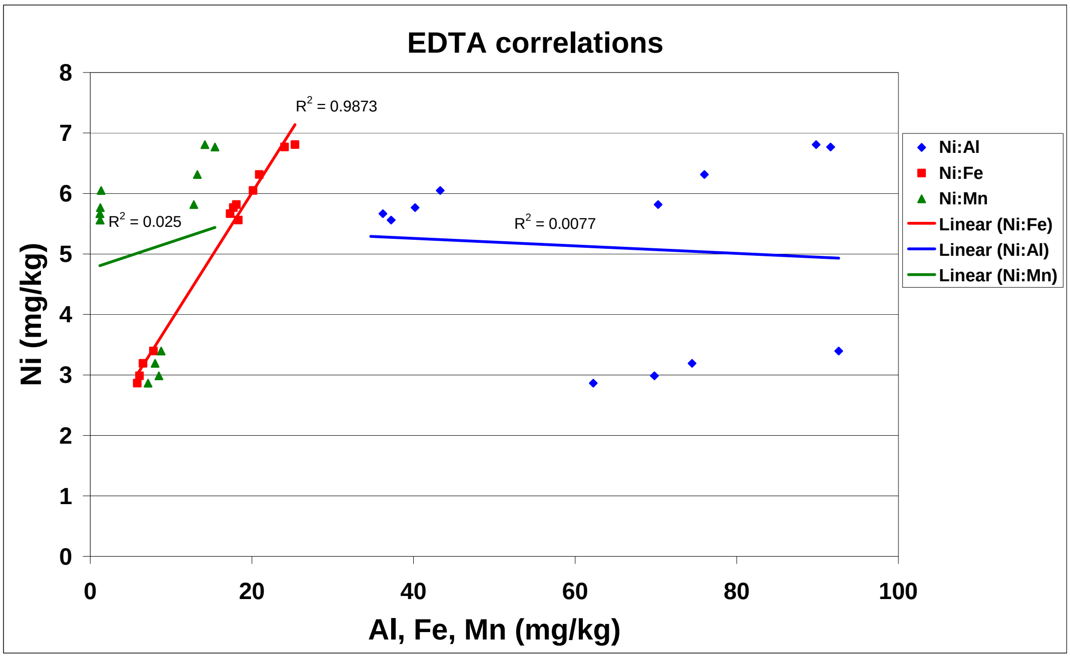

Figure 3.4 The EDTA extractable Ni fraction correlated with Al, Fe and Mn concentrations

Table 3.8 The concentrations of Cr(III), Ni, Al, Fe, and Mn extracted from three Eastern Highveld soils at a soil water potential level of -3100 J.kg^{-1} using various extractants

	^{1}Cr(III) (mg.kg^{-1})	^{1}Ni (mg.kg^{-1})	^{2}Al (mg.kg^{-1})	^{2}Fe (mg.kg^{-1})	^{2}Mn (mg.kg^{-1})
White					
$Mg(NO_3)_2$	- i	2.08g	0.185(0.05)	0.03(0.02)	0.60(0.02)
EDTA	1.61f	4.35f	51.2(13.0)	21.4(3.34)	1.33(0.1)
$NH_2OH.HCl$	2.22e	9.64c	44.1(3.77)	15.6(0.94)	2.69(0.11)
Tamm's reagent	10.1c	8.3d	230(12.1)	130(9.26)	1.51(0.22)
EPA 3051A	14.9a	14.9a	8674 (607)	4741 (102)	61.6 (6.45)
Yellow					
$Mg(NO_3)_2$	- i	0.63h	0.115(0.03)	0.02(0.01)	2.99(0.07)
EDTA	0.79gh	2.21g	83(14.1)	6.96(0.86)	8.29(0.8)
$NH_2OH.HCl$	0.67h	4.69f	80.8(3.67)	5.11(0.2)	16.6(0.45)
Tamm's reagent	9.44d	6.07e	705(19.8)	198(10.6)	13(0.82)
EPA 3051A	14b	14.6b	32787 (1018)	19428 (852)	91.5 (10.4)
Red					
$Mg(NO_3)_2$	- i	1.25h	0.18(0.04)	0.06(0.02)	3.97(0.47)
EDTA	1.03gh	4.80f	90.8(13.4)	25.1(4.22)	14.3(1.13)
$NH_2OH.HCl$	1.25fg	7.99d	75.2(1.83)	12.4(0.53)	27.6(1.1)
Tamm's reagent	9.87cd	7.67d	552(25)	347(24.6)	24.2(1.03)
EPA 3051A	14.7a	14.8ab	21607 (1067)	16204 (2208)	124 (39.6)
LSD(.05)	0.532	0.696			

[1] Values derived by subtracting control sample concentrations from treatment sample concentrations. LSD(0.5) values calculated separately for Cr(III) and Ni

[2] Values between brackets denotes the STdev for each extraction method

Nonetheless, the $NH_2OH.HCl$ solution extracted less Al and Fe from each of the soils than the EDTA solution. Therefore, the Al and Fe extracted using a $NH_2OH.HCl$ solution is thought not to comprise a major fraction of the amorphous Al and Fe oxide content. A certain fraction of the extracted Al and Fe may be derived from the dissolution of outer- and inner-sphere complexes and surface precipitated complexes bound through O^{2-} and HO^- and/or silanol and aluminol functional groups. However, the E-horizon (White) yielded the highest $NH_2OH.HCl$ extractable Fe fraction. Owing to pedogenic processes, the E-horizon (White) may contain a higher Fe(II) fraction as opposed to the apedal horizons being dominated by the Fe(III) ion. Redox chemistry dictates a high degree of stability regarding the Fe(III) fraction in the E-horizon (White), especially when considering Al substituted Fe (oxy) hydroxide minerals. The latter will render Fe(III) less reducible and $NH_2OH.HCl$ less effective in extracting Fe(III) from the soil.

Although it has been stated that most of the Mn oxide minerals found in soil are amorphous (Sparks, 2003; McKenzie, 1989), table 3.8 shows that none of the soils investigated contain high levels of $NH_2OH.HCl$ extractable Mn. Using the EPA 3051A values as a pseudo total would denote that the amorphic Mn oxide content comprises 4.4 % of the total Mn oxide content in the E-horizon (White), 18.2 % in the yellow brown apedal B-horizon (Yellow), and 19.5 % in the red apedal B-horizon (Red). The extractant, however, also dissolved some of the Al and Fe present in the soils.

Figure 3.5 and table 3.8 indicate that the $NH_2OH.HCl$ extractable Cr(III) fraction does not differ considerably from that found when using EDTA as an extractant. Although found to sorb Cr(III) effectively in single component systems (Bradl, 2004; Charlet and Manceau, 1992), it would seem that amorphous Mn oxides do not contribute substantially to the sequestration of Cr(III) in the natural soil environment. This can be attributed to a combination of the low amorphic Mn oxide content of the investigated soils and the (seemingly) higher affinity of Fe oxide minerals for Cr(III), as illustrated by figure 3.6. Nonetheless, the capability of Mn oxide minerals to oxidise Cr(III) to Cr(VI) should not be underestimated, as shown by Cooper (2002). Cooper (2002) found the oxidation of Cr(III) to Cr(VI) to occur in poorly aerated ultramafic subsoils of Zimbabwe, containing easily reducible forms of Mn oxide minerals. It should also be remembered that a low R^2 (figure 3.6) does not indicate that none of the Cr(III) associated with the Mn oxide mineral phase, only that no clear correlation can be drawn between Cr(III) extractability and Mn extractability in three differing soils.

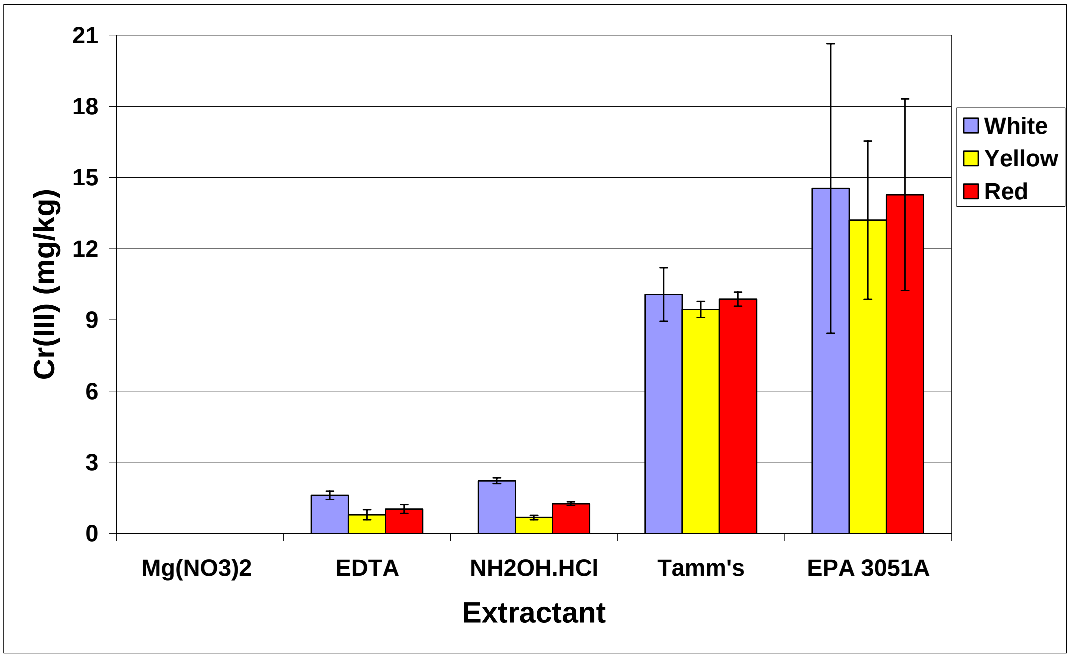

Figure 3.5 Cr(III) extractability correlated with extractants

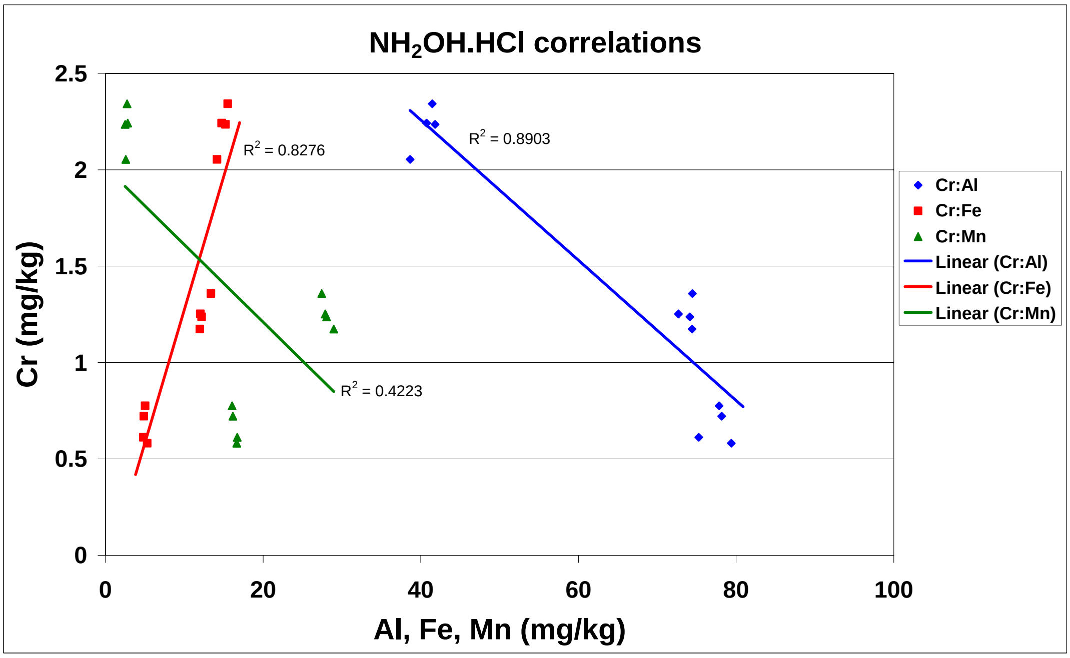

Figure 3.6 The pH 2.0, 0.1 M $NH_2OH.HCl$ extractable Cr(III) fraction correlated with Al, Fe and Mn concentrations

In contrast to the findings regarding Cr(III) extractability, $NH_2OH.HCl$ extracted high Ni concentrations. Figure 3.8, substantiated by table 3.8, shows the E-horizon (White) to yield 64.3 % Ni, and the yellow brown apedal B-horizon (Yellow) and the red apedal B-horizon (Red) to yield 31.3 % and 53.3 % Ni, respectively. Although Childs (1975), as well as Taylor and McKenzie (1966), found Mn nodules to contain higher levels of Ni than the soils from which these nodules were sieved, the $NH_2OH.HCl$ extractable Ni fraction should not be associated with amorphous Mn oxide minerals automatically. As noted previously and indicated by table 3.8, $NH_2OH.HCl$ also extracted a certain fraction of the Fe and Al content of the soils. A clear correlation between Ni and Fe extractability was found, as exemplified by figure 3.7.

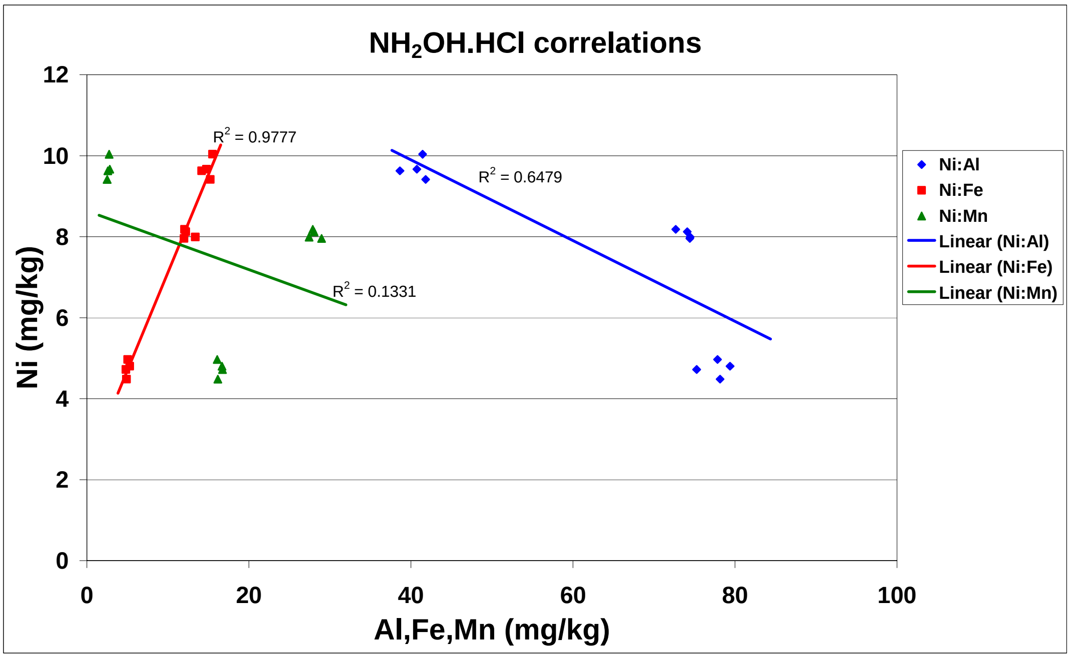

Figure 3.7 The pH 2.0, 0.1 M $NH_2OH.HCl$ extractable Ni fraction correlated with Al, Fe and Mn concentrations

From the E-horizon (White), $NH_2OH.HCl$ extractable Fe constituted 0.32 % of the EPA 3051A derived value. Fe extracted from the yellow brown apedal B-horizon (Yellow) and the red apedal B-horizon (Red) constituted 0.03 % and 0.08 % of the EPA 3051A values, respectively. Ni extractability decreased in the same sequence. The associating of Ni with the $NH_2OH.HCl$ extractable Fe fraction may indicate a higher affinity of amorphous Fe oxide minerals for Ni, but can also indicate the co-precipitation of Ni with adsorbed and inner-sphere complexed Fe. Nonetheless, the fact that $NH_2OH.HCl$ has been shown to minimally dissolve amorphous Al and Fe oxide phases (Krasnodebska-Ostrega *et al*., 2001; Luo and Christie, 1997; and Gambrell, 1996), coupled with the low Al and Fe levels extracted, when compared to Tamm's reagent, would indicate that at least a certain fraction of Ni associates with amorphous Mn oxide minerals.

Although stated by numerous authors (Loeppert and Inskeep, 1996; Bertsch and Bloom, 1996; Schwertmann, 1991; Hodges and Zelansky, 1980) to dissolve only amorphous Al and Fe oxide minerals, as well as biotite and chlorite, table 3.8 clearly indicates that a large fraction of the amorphous Mn oxide content can be extracted using Tamm's reagent. Tamm's reagent extracted 56.1 % of the Mn extracted by the $NH_2OH.HCl$ solution from the E-horizon (White), 78.5 % from the yellow brown apedal B-horizon (Yellow) and 87.9 % from the red apedal B-horizon (Red). Since Tamm's reagent acts as a reducing agent to mobilise the amorphous sesquioxide phase, the higher occurrence of Mn^{3+} and Mn^{4+} in soil mineral phases will lead to a higher Tamm's reagent extractable Mn fraction, whereas Mn^{2+} will be less extractable. Deduced from the assumption, the amorphous Mn oxide content of the yellow brown apedal B-horizon (Yellow) and red apedal B-horizon (Red) is dominated by higher valence, easily reducible Mn, whereas the E-horizon (White) contains a substantially higher Mn^{2+} fraction. Therefore, the Cr(III) and Ni fraction associated with amorphous Mn oxide minerals also contributes to the Tamm's reagent dissolvable Cr(III) and Ni values.

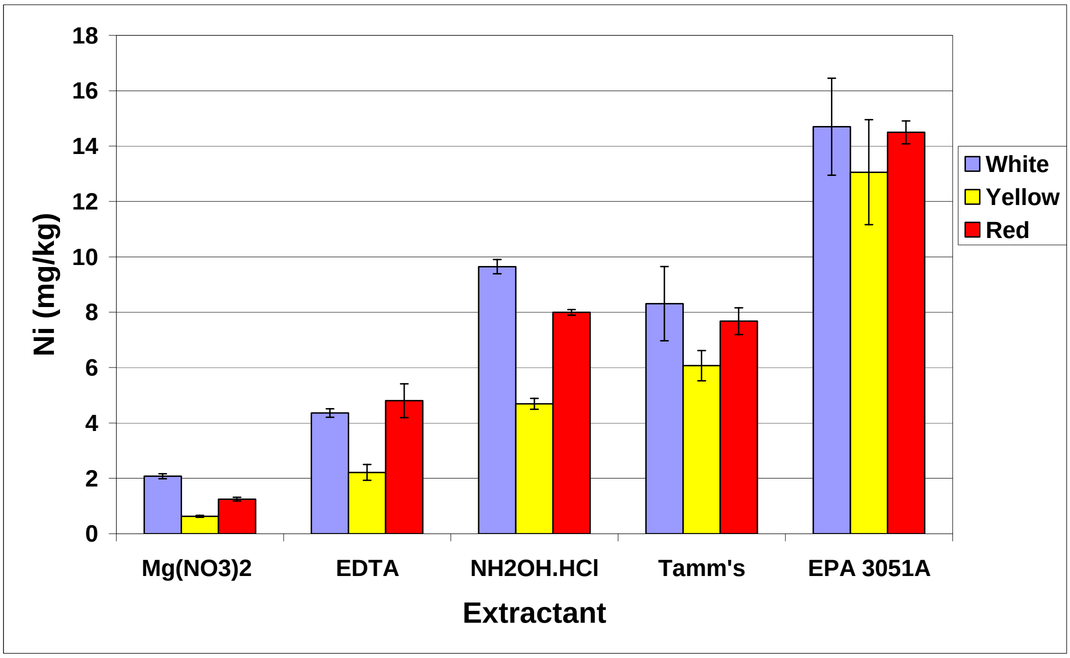

Figure 3.8 Ni extractability correlated with extractants

Expressing the Tamm’s reagent extractable Al and Fe fractions as a percentage of the EPA 3051A derived values for the same elements yielded an amorphous Al oxide content of 2.66 % for the E-horizon (white), 2.15 % for the yellow brown apedal B-horizon (Yellow), and 2.55 % for the red apedal B-horizon. The amorphous Fe oxide content comprises 2.75 % for the E-horizon (white), 1.02 % for the yellow brown apedal B-horizon (Yellow), and 2.14 % for the red apedal B-horizon of the pseudo total Fe content. These values were derived from table 3.8.

Although the amorphous Al and Fe oxide contents are relatively low, these phases still seem to sequester the majority of the Cr(III) added to the three soils. Figure 3.8 (substantiated by table 3.9) shows Tamm’s reagent to dissolve 67.1 % of the added Cr(III) in the E-horizon (White), 62.9 % in the yellow brown apedal B-horizon (Yellow), and 65.8 % in the red apedal B-horizon. The efficiency with which Tamm’s reagent extracted Cr(III), however, may be owing to a strong association and complexation of Cr(III) with oxalate and not necessarily the dissolution of amorphous Al and Fe oxide phases, although the latter have been shown to occur (Loeppert and Inskeep, 1996; Bertsch and Bloom, 1996; Schwertmann, 1991; Hodges and Zelansky, 1980). The affinity shown by Tamm’s reagent for Cr(III) is illustrated by figure 3.9.

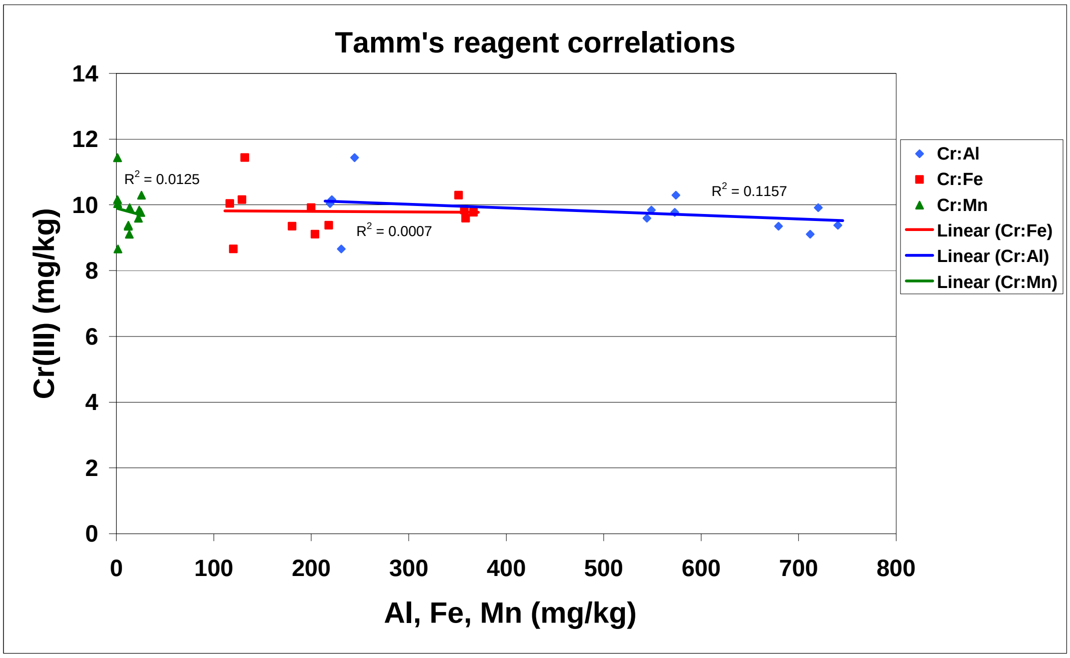

Figure 3.9 The Tamm's reagent extractable Cr(III) fraction correlated with Al, Fe and Mn concentrations

From figure 3.9 it is clear that no correlation between Cr(III) extractability and Al, Fe and Mn extractability could be observed using Tamm's reagent. The fraction of Cr(III) mobilised using Tamm's reagent is therefore attributed to the affinity shown for Cr(III) by the extractant.

Tamm's reagent also extracted high levels of Ni from each of the three soils. These concentrations (indicated by figure 3.8 and table 3.8) may also encompass the $NH_2OH.HCl$ extractable fraction and should not be regarded as indicating a sole association with amorphous Al and Fe oxide minerals.

Both the E-horizon (White) and red apedal B-horizon (illustrated by tables 3.8 and 3.9) show slightly lower Ni values when Tamm's reagent is used as an extractant, as opposed to the $NH_2OH.HCl$ solution. On the contrary, the yellow brown apedal B-horizon (Yellow) yielded significantly higher ($P<0.001$) Ni values. The latter phenomena would indicate that amorphous Al and Fe oxide minerals do sequester Ni, but that the amorphous Mn oxide mineral phase also contributes substantially. This statement is more clearly presented in the red apedal B-horizon (Red), which also contains the highest amorphous Mn oxide phase. However, correlations drawn between Ni and Al, Fe and Mn extracted with Tamm's reagent showed no trend.

Adding the Tamm's reagent Al and Fe extractable fractions showed the yellow brown apedal B-horizon (Yellow) to contain the highest amorphous Al and Fe oxide mineral phase, followed by the red apedal B-horizon (Red) and E-horizon (White). The yellow brown apedal B-horizon's (Yellow) higher cation exchange capacity and lower anion exchange capacity denote the amorphous Al and Fe oxide phase to exhibit more negatively charged binding sites than would be the case for the red apedal B-horizon (Red). This, coupled with the fact that amorphous Mn oxide minerals exhibit a lower point of nett charge than the amorphous Al and Fe oxide minerals (Sparks, 2003) – as well as Cr(III) being predominantly sequestered by the latter phase – would explain the observation that Ni is more effectively sequestered by the amorphous Mn oxide phase in the red apedal B-horizon (Red).

Table 3. 9 Cr(III) and Ni extracted as a percentage of the total concentrations added and correlated with extractants used at a soil water potential of -3100 J.kg^{-1}

	*Cr(III)		*Ni	
	Extracted (mg.kg^{-1})	**Percentage (%)**	**Extracted (mg.kg^{-1})**	**Percentage %**
White				
Mg(NO$_3$)$_2$	-	-	2.08	13.9
EDTA	1.61	10.7	4.35	29
NH$_2$OH.HCl	2.22	14.8	9.64	64.3
Tamm's reagent	10.1	67.1	8.3	53.7
EPA 3051A	14.9	99	14.9	99.2
Yellow				
Mg(NO$_3$)$_2$	-	-	0.63	4.2
EDTA	0.79	5.27	2.21	14.7
NH$_2$OH.HCl	0.67	4.47	4.69	31.3
Tamm's reagent	9.44	62.93	6.07	40.5
EPA 3051A	14	93.1	14.6	97.5
Red				
Mg(NO$_3$)$_2$	-	-	1.25	8.33
EDTA	1.03	6.87	4.80	32.1
NH$_2$OH.HCl	1.25	8.33	7.99	53.3
Tamm's reagent	9.87	65.8	7.67	51.1
EPA 3051A	14.7	98.3	14.8	98.9

***15 mg.kg^{-1} Cr(III) and Ni were added to each treatment**

Using the Tamm's reagent values to calculate the residual Cr(III) fraction and the NH$_2$OH.HCl values to calculate the residual Ni fraction contained by the E-horizon (White) and red apedal B-horizon (Red) illustrates that the soils investigated sequester a certain fraction of Cr(III) and Ni quite effectively. To calculate the residual Ni fraction in the yellow brown apedal B-horizon, Tamm's reagent values were used because this extractant yielded the highest extractable Ni concentrations. Table 3.10 summarises the fraction of Cr(III) and Ni that was not extracted by any of the extractants listed, the EPA 3051A extraction being the exception.

Table 3.10 The Cr(III) and Ni fraction not extracted from the three investigated soils

	[1]Cr(III)		**[1]Ni**	
	Not extracted ($mg.kg^{-1}$)	**Percentage (%)**	**Not extracted ($mg.kg^{-1}$)**	**Percentage (%)**
White	4.93	32.9	5.36	[2]35.7
Yellow	5.56	37.1	8.93	59.6
Red	5.13	34.2	7.01	[2]46.7

[1]15 $mg.kg^{-1}$ Cr(III) and Ni were added to each treatment

[2]Values calculated by subtracting the pH 2.0, 0.1 M $NH_2OH.HCl$ Ni values from the total concentration added. Tamm's reagent values were used to calculate the value for the Yellow soil

An evaluation of table 3.10 can falsely lead to regarding Ni as less mobile and more effectively sequestered than would be the case for Cr(III). Ni has been shown to be substantially more mobile when using weaker extractants such as $Mg(NO_3)_2$ and EDTA. Nonetheless, both these elements seem to be subject to the formation of non-soluble surface polymerised complexes and precipitates, as well as a certain degree of lattice diffusion and isomorphic substitution. Crystal growth through Ostwald ripening and/or sorbate ageing may also render ions less mobile (Sparks, 2003). The immobilisation of ions through crystal growth, however, is not considered a viable explanation in this case, as the 36-hour incubation time frame may not allow it.

3.4.3 Predicting Cr(III) and Ni mobility

Although care should be taken when attempting to compile criteria by which the mobility of heavy metals in the natural soil environment can be predicted, some soil characteristics that influence Cr(III) and Ni mobility can be identified. Using field classifiable soil characteristics to predict Cr(III) and Ni mobility in particular seems suspect. Neither soil form, soil colour nor soil texture could be used to predict metal mobility because Ni was found to be significantly ($P<0.001$) more mobile, using EDTA as an extractant, in the red apedal B-horizon (Red) than either of the other two soils. The latter, comprising a higher clay content and deduced from colouration to exhibit a higher sesquioxide content than the E-horizon, would have been expected to sequester Ni more effectively.

Nonetheless, an investigation into soil mineralogy and soil surface charge did yield some answers. Clearly, the higher clay content of the yellow brown apedal B-horizon (Yellow) alone does not explain the soil's Cr(III) and Ni sequestration capacity. Rather, combining them with a high smectite clay content and subsequent higher cation exchange capacity shed light on it. As 2:1 clay minerals are not as dependent on pH for exhibiting a nett negative charge, the contribution of such minerals to cation sorption is significant. Furthermore, a higher amorphous Fe oxide content would seem to contribute substantially to the sequestration of Cr(III) in particular, but also Ni.

Soils exhibiting a high Mn oxide mineral content should, nonetheless, raise concern. Not only are Mn oxide minerals capable of oxidising Cr(III) to Cr(VI), but they will also lead to mobilisation of sorbed Cr(III) and Ni under waterlogged conditions. As Mn is the first of the elements to be reduced and rendered mobile under reducing conditions (Sparks, 2003), any of the toxic elements associated with it will pose a higher risk to environmental and human health (Hlavay *et al*., 2004).

An understanding of the soil water regime governing the water potential levels of soils amended with heavy metal containing waste, such as steel plant slag, would be just as important. The Ni fraction extracted from the yellow brown apedal B-horizon (Yellow) linked to soil water potential (figure 3.3) serves as an example. At near water saturated conditions (-1 to -10 $J.kg^{-1}$) Ni extracted from the yellow brown apedal B-horizon (Yellow) did not differ significantly from that extracted from the E-horizon (White) using EDTA. Nearing air dried conditions (-3100 $J.kg^{-1}$), the yellow brown apedal B-horizon (Yellow) did sequester Ni significantly more effectively. It would therefore seem that not only certain chemical characteristics, but also climate, position in the landscape and soil depth could influence Ni mobility. At a certain soil depth, lower topographically situated soils may not dry out completely, especially in higher rainfall areas, and sequester Ni less effectively than the same soil form situated climatologically or topographically in a drier area. The soil water regime, therefore, constitutes as major a factor as any of the chemical parameters identified.

3.5 Conclusion

The environmental extractability of Cr(III) and Ni from three South African Eastern Highveld soils was assessed using five extractants. While Cr(III) was found to be sequestered rather effectively, Ni was not. Even at near water saturated conditions, the major fraction of added Cr(III) was found not to be easily mobilisable. Precipitation of Cr(III) is thought to be initially through bulk-solution precipitation, although mineral-induced precipitation contributes, as is evident from the extractability of Cr(III) at water potential levels of -1500 $J.kg^{-1}$ and - 3100 $K.kg^{-1}$. The prediction, based on soil colour and soil texture, that the yellow brown apedal B-horizon (Yellow) would sorb Cr(III) effectively, followed by the red apedal B-horizon (Red) and E-horizon (White), respectively, was upheld at water potential levels of -1500 $J.kg^{-1}$ and -3100 $J.kg^{-1}$. This was not the case, however, at higher water content conditions. Cr(III) seems to associate with the Fe fraction in soil, although the data derived cannot be used to denounce an association with any of the other soil fractions. An association with clay mineralogy was not investigated intensely.

Ni was found to be alarmingly mobile at water potential levels of -1 to -1500 $J.kg^{-1}$, regardless of soil type. Even at -3100 $J.kg^{-1}$, Ni extractability was more pronounced than found for C(III). Ni precipitation is thought to be dominated by mineral-induced precipitation at wetter conditions, although the drying out of soil will lead to bulk-solution precipitation. The inability of soil to sequester Ni effectively at soil water conditions wetter than -1500 $J.kg^{-1}$ should disqualify the use of Ni containing slag as liming material under irrigation or in areas where soil seldom dries to beyond -1500 $J.kg^{-1}$. Soil colour and soil texture could not be used as a means to predict Ni mobility. A strong correlation between Ni and the Fe fraction in soil was found. The latter was especially evident from the extraction using $NH_2OH.HCl$. Such an association may not be ascribed solely to the sorption of Ni by amorphous Fe oxide mineral phases, but also be due to the co-precipitation of Ni and Fe. As is the case for Cr(III), it cannot be concluded that Ni will associate only with Fe and with none of the other soil fractions.

In attempting to predict heavy metal mobility, the soil water regime, clay mineralogy and surface charge characterisation, rather than soil field classifiable characteristics (soil colour and texture) should be considered. Coupled with soil pH, redox conditions and the amorphous Al, Fe and Mn oxide mineral phases, these factors can be used in an attempt to predict Cr(III) and Ni mobility. It should be emphasised, however, that at best such a prediction can be regarded merely as an educated guess. Care should be taken when assessing soils for amendment with heavy metal containing substances such as steel plant slag.

3.6 References

ABOLLINO, O., ACETO, M., MALANDRINO, M., SARZANINI, C. and MENTASTI, E. 2002. Adsorption of heavy metals on na-montmorillonite. Effect of pH and organic substances. *Water Research*, 37:1619–1627.

AMACHER, M.C. 1996. Nickel, cadmiun and lead. In: *Methods of Soil Analysis. Part 3 – Chemical Methods*. Editor: D.L Sparks. SSSA Book Series no 5. Soil Science Society of America, American Society of Agronomy, Madison, Wisconsin, USA, pp 749–750.

ANDERSON, S.J. and SPOSITO, G. 1992. Proton surface charge density in soils with structural and pH-dependent charge. *Soil Science Society of America Journal* 56:1437–1443.

BALASOIU, C.F., ZAGURY, G.J. and DESHêNES, L. 2000. Partitioning and speciation of chromium, copper and arsenic in CCA-contaminated soils: Influence of soil composition. *The Science of the Total Environment*, 280:239–255.

BARTLETT, R.J. and JAMES, B. 1979. Behaviour of chromium in soils: III. Oxidation. *Journal of Environmental Quality*, 5:31–35.

BERTSCH, P.M. and BLOOM, P.R. 1996. Aluminium. *Methods of Soil Analysis*. Part 3 – Chemical Methods. Editor: D.L Sparks. SSSA Book Series no 5. Soil Science Society of America, American Society of Agronomy, Madison, Wisconsin, USA, p 530.

BRADL, H.B. 2004. Adsorption of heavy metal ions on soils and soil constituents. *Journal of Colloid and Interface Science,* 277:1–18.

BRADY, N.C. and WEILL, R.P. 1999. *The Nature and Properties of Soils*. Twelfth edition. Prentice Hall, Upper Saddle River, New Jersey, pp119, 126, 202–204, 311.

CHARLET, L. and MANCEAU, A.A. 1992. X-ray adsorption spectroscopy study of the sorption of C(III) at the oxide-water interface: I. Molecular mechanisms of Cr(III) oxidation by Mn oxides. *Journal of Colloidal Interface Science,* 148:425–442.

CHILDS, C.W. 1975. Composition of iron–manganese concretions from some New Zealand Soils. *Geoderma* 13:141–152.

CHRISTENSEN, T.H., LEHMANN, N., JACKSON, T. and HOLM, P.E. 1996. Cadmium and nickel distribution coefficients for sandy aquifer materials. *Journal of Contaminant Hydrology,* 24:75–84.

COOPER, G.R.C. 2002. Oxidation and toxicity of chromium in ultramafic soils of Zimbabwe. *Applied Geochemistry,* 17:981–986.

DAHN, R., SCHEIDEGGER, A.M., MANCEAU, A., SCHLEGEL, M.L., BAEYENS B., BRADBURY, M.H. and MORALES, M. 2002. Neoformation of Ni phyllosilicates upon Ni uptake on montmorillonite: A kinetic study by powder and polarized extended x-ray adsorption fine structure spectroscopy. *Geochimica et Cosmochimica Acta,* 66:2335–2347.

DUBBIN, W.E. 2004. Influence of organic ligands on Cr desorption from hydroxyl-Cr intercalated montmorillonite. *Chemosphere* 54:1071–1077.

EARY, L.E. and RAI, D. 1989. Kinetics of chromate reduction by ferrous ions derived from hematite and biotite at 25°C. *American Journal of Science,* 289:180–213.

EGGLESTON, C.M. and STUMM, W. 1993. Scanning tunneling microscopy of Cr(III) chemisorbed on α-Fe_2O_3 (001) surface from aqueous solution: Direct observation of surface mobility and clustering. *Geochimica et Cosmochimica Acta,* 57:4843–4850.

FENDORF, S.E. 1994. Surface reactions of chromium in soils and waters. *Geoderma,* 67:55–71.

FENDORF, S.E., LI, G. and GUNTER, M.E. 1996. Micromorphologies and Stabilities of chromium(III) surface precipitates elucidated by scanning force microscopy. *Soil Science Society of America Journal,* 60:99–106.

FENDORF, S.E. and SPARKS, D.L. 1994. Mechanisms of chromium(III) sorption onto silica. II: Effect of reaction conditions. *Environmental Science and Technology,* 28:290–297.

FORD, R.G., SCHEINOST, C.S. and SPARKS, D.L. 2001. Frontiers in metal sorption/precipitation on soil mineral surfaces. *Advances in Agronomy*, 74:41–61.

GAMBRELL, R.P. 1996. Manganese. In: *Methods of Soil Analysis. Part 3 – Chemical Methods.* Editor: D.L Sparks. SSSA Book Series no 5. Soil Science Society of America, American Society of Agronomy, Madison, Wisconsin, USA, pp 678, 750.

HILLEL, D. 1982. *Introduction to Soil Physics.* Second edition. Academic Press, Harcourt Brace Jovanovich, p 58.

HLAVAY, J., PROHASKA, T., WEISZ, M., WENZEL, W.W. and STINGEDER, J.G. 2004. Determination of trace elements bound to soil and sediment fractions. IUPAC Technical Report. *International Union of Pure and Applied Chemistry*, 76(2):425–442.

HO HSY, PO. 1989. Aluminium hydroxides and oxyhydroxides. In: *Minerals in the Soil Environment.* SSSA Book Series 1. Edited: J.B. Dixon, and S.B. Weed. Soil Science Society of America, pp 331 – 371.

HODGES, S.C. and ZELANSKY, 1980. Determination of noncrystalline soil components by weight difference after selective dissolution. *Clays and Clay Mineralogy*, 28:35–42.

JEAN, L., BORDAS, F. and BOLLINGER, J.C. 2006. Chromium and nickel mobilization from a contaminated soil. *Environmental Pollution*, 147:729–739.

JEON, B.H., DEMPSEY, B.A., BURGOS, W.D. and ROYER, R.A. 2003. Sorption kinetics of Fe(II), Zn(II), Co(II), Ni, Cd(II) and Fe(II)/Me(II) onto hematite. *Water Research,* 37:4135–4142.

KEDZIOREK, M.A.M. and BOURG, A.C.M. 1996. Acidification and solubilisation of heavy metals from single and dual-component model solids. *Applied Geochemistry,* 11:299–304.

KRAEPIEL, A.M.L., KELLER, K. and MOREL, F.M.M. 1999. A model for metal adsorption on montmorillonite. *Journal of Colloidal Interface Science,* 210(1):43–54.

KRASNODEBSKA-OSTREGA, B., EMONS, H. and GOLIMOWSKI, J. 2001. Selective leaching of elements associated with Mn–Fe oxides in forest soil, and comparison of two sequential extraction methods. *International Journal of Environmental Analytical Chemistry,* 371:385–390.

LAVERDIERE, M.R. and WEAVER, R.M. 1977. Charge characteristics of spodic horizons. *Soil Science Society of America Journal* 41:505–510.

LOEPPERT, R.H. and INSKEEP, W.P. 1996. Iron. In: *Methods of Soil Analysis*. Part 3 – Chemical Methods. Editor: D.L Sparks. SSSA Book Series no 5. Soil Science Society of America, American Society of Agronomy, Madison, Wisconsin, USA, pp 648–649.

LUO, Y.M. and CHRISTIE, P. 1997. Choice of extraction technique for soil reducible trace metals determines the subsequent oxidizable metal fraction in sequential extraction schemes. *International Journal of Environmental Analytical Chemistry,* 72:59–75.

McKENZIE, R.M. 1989. Manganese oxides and hydroxides. In: *Minerals in the Soil Environment.* Second edition. Edited by Dixon, J.B. and Weed, S.B. SSSA Book Series: 1. Soil Science Society of America, Madison, Wisconsin, p 459.

NOWACK, B. and SIGG, L. 1997. Dissolution of Fe(III) (hydr)oxides by metal-EDTA Complexes. *Geochimica et Cosmochimica Acta*, 61:951–967.

PELTIER, E., ALLADA, R., NAVROTSKY, A. and SPARKS, D.L. 2006. Nickel solubility and precipitation in soils: A thermodynamic study. *Clay and Clay Minerals,* 54:153–164.

PRASANNA, S.V., PADMANABHA, P.R. and KAMATH, P.V. 2006. Layered double hydroxides as potential chromate scavengers. *Journal of Colloid and Interface Science*, 304:292–299.

RENGASAMY, P. and OADES, J.M. 1978. Interactions of aluminium (III) and chromium(III). *Australian Journal of Soil Resources,* 16:53–66.

SALEH, F.Y., PARKENTON, T.F., LEWIS, R.V., HUANG, J.H. and DICKSON, K.L. 1989. Kinetics of chromium transformation in the environment. *Science of the Total Environment,* 86:25–41.

SCHECKEL, K.G., SCHEINOST, A.C., FORD, R.G. and SPARKS, D. 2000. Stability of layered Ni hydroxide surface precipitates: A dissolution kinetic study. *Geochimica et Cosmochimica Acta,* 64:2727–2735.

SCHEIDEGGER, A.M., FENDORF, M. and SPARKS, D.L. 1996. Mechanisms of nickel sorption on pyrophillite: Macroscopic and microscopic approaches. *Soil Science Society of America Journal,* 60:1763–1772.

SCHEINOST, A.C., FORD, R.G. and SPARKS, D. L. 1999. The role of Al in the formation of secondary precipitates on pyrophyllite, gibbsite, talc, and amorphous silica: A DRS study. *Geochimica et Cosmochimica Acta,* 63:3193–3203.

SCHWERTMANN, U. 1991. Solubility and dissolution of Fe oxides. In: *Iron Nutrition and Interaction with Plants*. Edited by Chen, Y. and Hadar, Y. Dordrecht, Netherlands: Kluwer, pp 3–27.

SINGER, A., KIRSTEN, W. and BUHMANN, C. 1994. Fibrous clay minerals in the soils of Namaqualand, South Africa: Characteristics and formation. *Geoderma* 66:43–70.

SPARKS, D.L., 2004. *Environmental Soil Chemistry*. 2nd edition. Academic Press, pp 54, 60, 67, 177, 259.

STEPNIEWSKA, Z., BUCIOR, K. and BENNICELLI, R.P. 2004. The effect of MnO_2 on sorption and oxidation of Cr(III) by soils. *Geoderma,* 122:291–296.

TAYLOR, R.M. and McKENZIE, R.M. 1966. The association of trace elements with manganese minerals in Australian soils. *Australian Journal of Soil Research* 4:29–39.

THOMAS, G.W. 1996. Soil pH and soil acidity. In: *Methods of Soil Analysis*. Part 3 – Chemical Methods. Editor: D.L Sparks. SSSA Book Series no 5. Soil Science society of America, American Society of Agronomy, Madison, Wisconsin, USA, p 487.

TRIVEDI, P., AXE, L. and DYER, J. 2001. Adsorption of metal ions onto goethite: Single-adsorbate and competitive systems. *Journal of Colloid and Surface Chemistry,* 191:107–121.

WEHRLI, B., IBRIC, S. and STUMM, W. 1990. Adsorption kinetics of vanadyl(VI) and chromium(III) to aluminium oxide: Evidence for two-step mechanism. *Colloidal Surfaces,* 51:77–88.

YAVUZ, O., ALTUNKAYNAK, Y. and GŰZEL, F. 2003. Removal of copper, nickel, cobalt and manganese from aqueous solution by kaolinite. *Water Research,* 37:948–952.

XU, Y. and AXE, L. 2004. Synthesis and characterization of iron oxide-coated silica and its effect on metal sorption. *Journal of Colloid and Interface Science*, 282:11–19.

ZELAZNY, L.W., HE, L. and VANWORMHOUDT, A. 1996. Charge analysis of soils and anion exchange. In: *Methods of Soil Analysis*. Part 3 – Chemical methods. Editor: D.L. Sparks. SSSA Book Series no 5. Soil Science Society of America, American Society of Agronomy, Madison, Wisconsin, USA, pp 1231–1252.

Chapter 4 Chromium(III) and nickel extractability as influenced by rewetting and drying cycles and an external source of silicon

4.1 Abstract

The use of steel plant slag which contains chromium(III) and nickel in the agricultural region of South Africa's Eastern Highveld necessitates an investigation into the extractability of Cr(III) and Ni. Apart from determining whether Cr(III) and Ni are further immobilised over a period of five rewetting and drying cycles, this study aims to investigate the effect of an external silicon source on Cr(III) and Ni mobility. In addition, easily determinable soil characteristics (colour and texture) that could possibly aid the prediction of Cr(III) and Ni extractability in the natural soil environment are evaluated. Three mineralogically contrasting soils were treated with 15 $mg.kg^{-1}$ Cr(III) and 10 $mg.kg^{-1}$ Ni and subjected to five rewetting and drying cycles. Apart from the Cr(III) and Ni concentrations, a treatment receiving 20 $mg.kg^{-1}$ Si was included. The extractability of Cr(III) and Ni was determined using 0.1 M $Mg(NO_3)_2$ and 0.02 M diammonium EDTA. Three main findings emerged: (i) Although a substantial difference in Cr(III) and Ni mobility was noted, contradictory evidence was gathered regarding the immobilisation of both elements with time; (ii) an amorphous Ni silicate phase seems to render Ni less mobile in soils exhibiting a low affinity for the metal, but more mobile in soils that would otherwise sequester the element more effectively; (iii) rather than using field characteristics as a means to predict metal mobility, laboratory determinable characteristics should be further researched.

Key words: Cr(III), Ni, Si, rewetting-drying cycles, amorphous Ni silicate precipitate

4.2 Introduction

Currently steel plant slag is being used as an agricultural liming agent on the Eastern Highveld of South Africa. Although slag has been found to be an effective neutralising agent in the agricultural environment, the potential detrimental effect of heavy metals such as Cr and Ni, contained within the matrixes of slag, on human health and environmental quality has not been investigated. Cr(VI) and Ni are both known carcinogens (Baytak and Tűrker, 2005; Banks, Scwab and Henderson, 2005; Staunton, 2004). Although not toxic in itself, Cr(III), especially in concretionary subsoils, can be oxidised to the hazardous Cr(VI) ion by an array of Mn oxides (Cooper, 2002; Fendorf, 1994; Bartlett and James, 1979), thereby warranting an investigation into the trivalent ion's mobility.

The study entailed an investigation into, first, the extractability of Cr(III) and Ni over a period of five rewetting and drying cycles and, second, the influence of an external Si source, as found in steel plant slag, on Cr(III) and Ni extractability in particular. Third, the study aimed to determine whether field classifiable soil characteristics (colour and texture) can be used as a means to predict Cr(III) and Ni extractability.

The sorption of Cr(III) and Ni depends, among others, on the hydrolyses of each element within common environmental pH ranges (pH 3–9); on ionic radii; on the nature of the mineral and organic constituents; on the soil solution composition and subsequent ion competition; on soil solution ionic strength; on soil pH; on soil redox conditions; on rhizosphere conditions; on microbial activity; and on an array of soil physical properties such as preferential water flow and soil temperature (Bradl, 2004; Dubbin, 2004; Sparks, 2004; Staunton, 2004; Echeverria *et al.*, 1998; Fendorf, 1994; Dixon and Weed, 1989; Bartlett and James, 1988; Bartlett and James, 1979).

Whereas Cr(III) is known to be rapidly and specifically sorbed, forming polydentate inner-sphere complexes and $Cr(OH)_3.nH_2O$ or $Fe_xCr_{1-x}(OH)_3$ precipitates (Dubbin, 2005; Wittbrodt and Palmer, 1995; Fendorf, Li and Gunter, 1996; Fendorf, 1994; Fendorf and Sparks, 1994), Ni is thought to be much more mobile under alkaline to slightly acidic conditions (Christensen *et al.*, 1996). Sorption of Ni has been shown to be reversible, although rapid, and ionic strength dependent at pH values less than 7 (Scheidegger, Fendorf and Sparks, 1996), indicating the formation of outer-sphere complexes or monodentate inner-sphere complexes (Sparks, 2003; Ford, Scheinost and Sparks 2001). At more alkaline pH values, Ni-Al layered double hydroxides (LDH) precipitated in the presence of Al-containing minerals (Scheinost, Ford and Sparks, 1999), whereas α-$Ni(OH)_2$ precipitated in the presence of minerals that did not contain Al (Scheckel *et al.*, 2000; Scheinost *et al.,* 1999).

Furthermore, these precipitates were stabilised by Si released through the dissolution of Si-containing minerals onto which Ni precipitated (Scheckel *et al.*, 2000; Ford *et al.*, 1999b; Scheidegger, Lamble and Sparks, 1996). Si has been shown to be incorporated into the crystal structure of the Al-Ni LDH and α-Ni(OH)$_2$ precipitates. It seemed plausible that the Si exchanged for nitrate, carbonate, sulphate and other anions in the interlayers of the precipitates, thereby cementing the precipitate to form a phyllosilicate precursor (Peltier *et al.*, 2006; Scheckel *et al*, 2000). In addition, Williams and Crerar (1985) indicated that metal hydroxides (Fe, Al, Mn) in the natural soil environment may act as templates or catalysts to initiate monomeric silicic acid condensation into Si polymers, which in turn might act as reactive sites for subsequent poorly ordered Si precipitation. This reaction results in the formation of negatively charged, open-framework silica polymers, which might show an affinity with positively charged ions such as Cr(III) and Ni. Although Ernst and Calvest (1969) postulated that the transformation of an amorphic Si phase to quartz may take up to 180 million years at 20 °C and 4–5 million years at 50 °C, it is known that amorphous Si phases transform to more stable microcrystalline Si phases in a relatively short time frame (Senkayi *et al.*, 1985; Kastner and Gieskes, 1983). Furthermore, cations may co-precipitate with silica hydrogels or xerogels, forming impurities in the crystal lattices of these phases (Drees *et al.*, 1989).

It is further hypothesised that soil colour and texture can be used to predict the mobility of Cr(III) and Ni in the natural soil environment. According to Brady and Weill (1999), soil colour is derived mainly from sesquioxide and organic matter coatings, and can be viewed as an indication of dominating mineralogy, while soil texture may be used to indicate the cation exchange capacity of soils. Subsoils exhibiting low organic content clearly display the colours of sesquioxide minerals, such as the red of hematite, the yellow of goethite and the brown of maghemite. Mn oxide minerals often colour the soil black.

4.3 Materials and methods

Three South African Eastern Highveld soils – with relief and drainage being the only differing soil-forming factors – to be amended with steel plant slag containing Cr and

Ni were identified and collected from profile pits. The soils were passed through a 2 mm sieve and pH adjusted to 6.0, using 0.02M $Ca(OH)_2$.

4.3.1 Soil characterisation

These three soils were categorised according to the South African Soil Classification System (1991) and the colour determined from the Munsell soil colour chart. The texture was determined from the "feel" technique described by Brady and Weill (1999).

The three soils consisted of an E-horizon, a yellow brown apedal B-horizon, and a red apedal B-horizon. All three horizons exhibited uniform colouration and contained neither mottles nor concretions. The soil form, colour and texture as determined under field conditions are listed in table 4.1.

Table 4.1 Soil form, colour and texture as determined under field conditions

Soil form	Colour	Texture
E-horizon	7.5YR 8/1 (**White**)	Sand
Yellow brown apedal B	7.5 YR 5/8 (**Yellow**)	Sand clay loam
Red apedal B	2.5 YR 3/6 (**Red**)	Sand loam

According to the South African Soil Classification System (1991), reducing conditions, coupled with lateral water movement and the subsequent removal of sesquioxides, clays and organic matter, lead to the characteristic bleached colour and coarser texture of the E-horizon. Yellow brown apedal and red apedal B-horizons are indicative of well-drained, oxidising environments in which Fe-oxide-coated soil particles dominate. Predominantly 1:1 type clays are encountered, although 2:1 type clays, such as smectites, may be present. The red colour dominating the red apedal B-horizon is attributed to at least 15 % hematite composing the total Fe oxide content, whereas goethite dominates the colour in the yellow brown apedal B-horizons (Grondklassifikasiewerkgroep, 1991).

Laboratory characterisations of the soils identified were conducted as follows:

(i) To determine clay content and mineralogy, the clay fraction from each soil was separated through sedimentation and pre-treated, using peroxide, CDB treatment and Mg-saturation. Peroxide was used to facilitate the removal of organic matter, while the latter two treatments removed the free iron oxide mineral phases. To determine the clay mineralogy, XRD analysis was performed on random, oriented, glycolated, and heated clay samples (Singer, Kirsten and Buhmann, 1994). The clay content and mineralogy as determined are presented in table 4.2.

Table 4.2 Soil clay content and mineralogy expressed as a percentage of the bulk soil composition

Soil	**Clay content (%)**	**Clay mineralogy (%)**				
		Smectite (montmorrilonite)	**Kaolinite**	**Mica**	**Goethite**	**Quartz**
White	4.7	-	1.8	0.9	-	2.0
Yellow	23.2	1.9	4.6	1.4	1.2	14.2
Red	16.3	-	9.3	0.6	1.0	5.4

(ii) Determining the cation exchange and anion exchange capacities for each soil consisted of the addition of 25 ml of 1.0 M KCl to 2.5 g soil weighed off in 45 ml polyethylene centrifuge tubes. After shaking for one hour on a reciprocal shaker at 100 oscillations per minute, the suspensions were centrifuged for 15 minutes at 3 500 revolutions per minute (rpm) and the supernatant discarded. The samples were then washed five times, using 0.01 M KCl. At the final washing, the suspension pH values were adjusted to span the expected PZNC range for each soil, using 0.01 M KOH and 0.01 M HCl (Zelazny, He and Vanwormhoudt, 1996). Attempts to adjust the pH values to 4.0, 5.0, 6.0, 7.0 and 8.0 for the yellow brown apedal B-horizon (Yellow) and to 3.0, 4.0, 5.0, 6.0 and 7.0 for the E-horizon (White) and red apedal B-horizon (Red) failed. After shaking the suspension for four hours at 100 oscillations per minute, centrifuging for 15 minutes at 3 500 rpm and recording the suspension pH values, it was noted that the soils still expressed a certain degree of buffering. Final pH values therefore ranged from approximately 4.5 to 6.5, as indicated by figure 3.1. It is hypothesised that a degree of mineral dissolution occurred during the final washing as the red apedal B-horizon (Red) in particular yielded a turbid supernatant, even after 0.2 µg membrane filtering. The supernatant centrifuged from each sample was nonetheless decanted and stored for K^+ and Cl^- determination (C_1). To obtain the entrained solution (V_1), each centrifuge tube was weighed and it was assumed that the K^+ and Cl^- concentrations equalled those of the final washing. The samples were then washed four times with 10 ml of 0.5 $NaNO_3$ and centrifuged as before. The supernatant after each washing was decanted into 50 ml volumetric flasks (V_2), brought to volume, and analysed for K^+ and Cl^- (C_2). The point of zero charge, where the cation exchange capacity CEC) equals the anion exchange capacity (AEC) (Zelazny *et al.*, 1996), for each soil could not be determined. Nonetheless, the final solution pH values and calculated CEC and AEC values can still be used to indicate surface charge characteristics to some extent. The experiments were conducted in triplicate and the K^+ concentrations read on a Jobin Yvon Horiba, model: Ultima ICP-AES fitted with a sequential, radial torch at 766.490 nm. Cl^- concentrations were determined with a Dionex DX 120 Ion Chromatograph (chemically suppressed IC detector).

The following formulas were used to calculate CEC and AEC:

$$\text{CEC (cmol}_c\text{kg}^{-1}) = 0.1\ (C_2V_2 - C_1V_1) / 39\ W$$

$$\text{AEC (cmol}_c\text{kg}^{-1}) = 0.1\ (C_2V_2 - C_1V_1) / 35.5\ W$$

where
C_1 = concentration (mg.L^{-1}) of K^+ and Cl^- in the final washing solution of 0.01 M KCl,
C_2 = concentration (mg.L^{-1}) of K^+ and Cl^- in the displacing solution of 0.5 M $NaNO_3$,
V_1 = volume (ml) of the solution entrained in the soil after the final washing with 0.01 M KCl,
V_2 = total volume (ml) of the displacing solution of 0.5 M $NaNO_3$,
39 = atomic weight of K^+,
35.5 = atomic weight of Cl^- and,

W = oven dried soil sample weight (g).

Table 4.3 Cation exchange and anion exchange capacity determined at three pH values for each of the soils investigated

	pH	**CEC ($cmol_c.kg^{-1}$)**	**AEC ($cmol_c.kg^{-1}$)**
White	4.74	12.1	-0.06
	5.6	12.2	-0.02
	5.9	13.6	-0.18
Yellow	3.95	22.4	3.19
	4.75	25.4	2.04
	6.9	29.7	1.67
Red	4.78	12.1	6.23
	5.57	13.7	5.05
	5.93	15.4	4.96

Negative AEC values, as found for the E-horizon (White) in table 3.1, have also been reported by numerous authors (including Anderson and Sposito, 1992, and Laverdiere and Weaver, 1977). These errors are attributed by Zelansky *et al.* (1996) to disregarding negative adsorption and its influence on ion concentrations in the entrained solution. The surface charge requirements of electroneutrality are satisfied by positive adsorption of counterions (opposite charge) and negative adsorption (exclusion) of coions (same charge). The electric double layer therefore exhibits both counterions and coions, the latter increasing in concentration with distance from the charged mineral surface. The values contained in table 3.1 may thus be regarded as an underestimation of CEC and AEC, but serve nonetheless as an indication of surface charge characteristics.

4.3.2 Batch equilibrium study

A 100 g sample of each soil was treated with 15 $mg.kg^{-1}$ Cr(III) and 10 $mg.kg^{-1}$ Ni, using chromium(III) nitrate nonhydrate and nickel(II) nitrate hexahydrate, respectively. The soil samples were water saturated, left to dry in a constant temperature room at 35 ℃ and rewetted to saturation. The rewetting-drying cycle was conducted five times over a six-week period. Each rewetting and drying cycle constituted a treatment, and each treatment was replicated four times. The Si-added treatment followed the same methodology. Together with 15 $mg.kg^{-1}$ Cr(III) and 10 $mg.kg^{-1}$ Ni, 20 $mg.kg^{-1}$ Si, using sodium silicate, was added. The concentrations of Cr(III) and Ni were chosen so that precipitation was not induced owing to over-saturation in the water-saturated soil.

After the six-week period, 5 g of each soil sample were weighed into a 45 ml polyethylene centrifuge tube and 10 ml of 0.1 M $Mg(NO_3)_2$ was added. The samples were placed on a reciprocal shaker for two hours at 180 rpm, after which all samples were centrifuged for 10 minutes at 1 500 rpm. The supernatant was then passed through an ashless Whatman no 42 filter paper and read on a Spectro Genesis, axially viewed ICP-AES. Blank, as well as reference samples, were included.

0.1 M $Mg(NO_3)_2$ was used as an indication of ions adsorbed and bound through electrostatic forces onto the exchange complex of the soil (Amacher, 1996), as well as an indication of neutral salt soluble precipitates.

Extraction using 0.02 M diammonium EDTA consisted of the addition of 30 ml diammonium EDTA to 10 g soil in a 45 ml polyethylene centrifuge tube. The samples were placed on a reciprocal shaker for two hours at 180 rpm, after which all samples were centrifuged for 20 minutes at 2 500 rpm. The supernatant was then passed through an ashless Whatman no 42 filter paper and read on a Spectro Genesis, axially viewed ICP-AES. Blank as well as reference samples were included. Prior to extraction, all glassware and equipment used were acid washed with 1:10 HNO_3 to limit contamination.

Diammonium EDTA promotes ligand dissolution, and is thought to indicate the plant availability of ions in soils of low organic content. Ca^{2+} and Mg^{2+} ions, however, may interfere with EDTA complexation of Ni and therefore yield lower estimated Ni values (Suarez, 1996).

Statistical analysis entailed the use of SAS 9.1. To investigate significant differences between Cr(III) and Ni extracted levels, soil type sequestration capacities, the influence of rewetting and drying cycles on metal mobility, as well as the effect of an external source of Si on Cr(III) and Ni mobility, analysis of variance (ANOVA) tables were compiled and Tukey's t-test conducted. The respective Least Squares Difference (LSD) values were derived at five percent confidence interval levels.

4.4 Results and discussion

4.4.1 0.1 M $Mg(NO_3)_2$ extractable Cr(III) and Ni

The Cr(III) values extracted using $Mg(NO_3)_2$ were found to be below the method detection limit for the specified extractant, even though the standard range against which Cr(III) levels were read on the ICP-AES reached into the parts per billion range. Using $Mg(NO_3)_2$ as an extractant, the potential further immobilisation of Cr(III) over a five-rewetting-drying-cycle period could not be determined. Neither could any judgment be made on Cr(III) mobility correlated with field classifiable soil characteristics. The low Cr(III) fraction extracted after each of the five rewetting and drying cycles is attributed to polynucleation and stable precipitate formation. It does seem plausible, however, that Cr(III) precipitated on the quartz-dominated E-Horizon (White) should be more mobile than the precipitates formed in the sesquioxide-dominated yellow brown apedal (Yellow) and red apedal B-horizons (Red).

Table 4.4 summarises the extractable Cr(III) and Ni fraction after five rewetting and drying cycles. As expected, a substantially higher exchangeable Ni fraction was extracted using $Mg(NO_3)_{2,}$ owing to the ion's inclination to form outer-sphere complexes, weaker inner-sphere complexes and more soluble precipitates. Apart from the first wetting and drying cycle for the E-horizon (White) and red apedal B-horizon (Red) being significantly higher ($P<0.001$) than rewetting and drying cycles 2 to 5, Ni seemed not to be rendered less mobile over a five rewetting and drying cycle period.

It is hypothesised that Ni precipitates as either a $Ni(OH)_2$ or a Ni-layered double hydroxide (LDH). If precipitated as a Ni-LDH, the newly formed phase will exhibit the composition $[M^{II}_{1-x}M'^{III}_{x}(OH)_2]^{x+}$; where M denotes Ni, and M$'$ may comprise Al, V, Cr(III), Fe(III) and Ga; and $0.15 < x < 0.33$. These Ni-LDH phases, especially those containing Al^{3+} and Fe^{3+}, have been shown to be rather soluble (Prassanna, Padmanabha and Kamath, 2006). Peltier *et al.* (2006) showed that, regardless of anion interlayers, the Ni-LDH phases exhibited substantially more negative enthalpy of formation ($\Delta H_f°$) values than were found for $Ni(OH)_2$. Evidently Ni and Cr(III) may also co-precipitate to form a Ni-Cr(III) LDH phase.

Table 4.4 0.1 M $Mg(NO_3)_2$ extractable Cr(III) and Ni after five rewetting and drying cycle

	Cr(III)			**Ni**		
	Added ($mg.kg^{-1}$)	**Extracted ($mg.kg^{-1}$)**	**Percentage (%)**	**Added ($mg.kg^{-1}$)**	**Extracted ($mg.kg^{-1}$)**	**Percentage (%)**
White	15	-	-	10	1.83a	18.3
Yellow	15	-	-	10	0.43b	4.3
Red	15	-	-	10	1.80a	18
LSD(.05)					0.243	

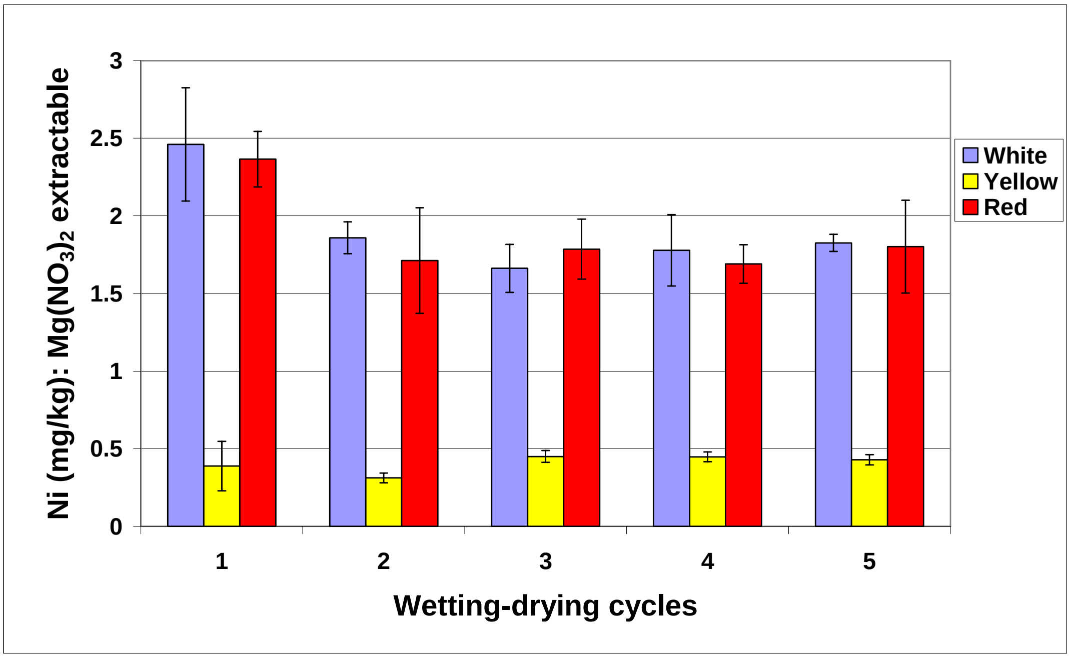

Figure 4.1 $Mg(NO_3)_2$ extractable Ni

When regarding soil colour and texture as an indication of soil mineralogy, it would seem plausible that Ni would be significantly more mobile in the E-horizon (White), than in either the yellow brown apedal (Yellow) or the red apedal B-horizons. Ni has been shown to precipitate as a α-$Ni(OH)_2$ onto quartz surfaces (Scheckel *et al.*, 2000; Scheinost *et al.*, 1999), but to form inner-sphere complexes and rather stable precipitates in the presence of sesquioxide and clay minerals (Jeon *et al.*, 2003;

Trivedi, Axe and Dyer, 2001; Dixon and Weed, 1989). Coupled with the higher clay content and believed higher cation exchange capacity of both the yellow brown apedal (Yellow) and red apedal (Red) B-horizons, the E-horizon (White) should yield higher Ni concentrations than both of the other soils. The stability of sorbed and precipitated Ni in the yellow-brown apedal B-horizon is therefore expected. It is not expected that the red apedal B-horizon would yield significantly higher ($P<0.001$) levels of Ni than the other two soils.

From figure 4.2, as well as table 4.2, it seems clear that Ni extractability cannot be explained by field-classifiable soil characteristics. As expected, the 18.3 % of the added Ni concentration extracted from the E-horizon (White) after five rewetting and drying cycles was significantly higher ($P<0.001$) than the 4.3 % extracted from the yellow-brown apedal B-horizon (Yellow). It was not expected, though, that the 18 % Ni extracted from the red apedal B-horizon (Red) would rival that of the E-horizon.

4.4.2 0.02 M diammonium EDTA extractable Cr(III) and Ni

As indicated by figures 4.2 and 4.3, the findings derived from the $Mg(NO_3)_2$ extraction study are substantiated by the EDTA extraction study. Although higher levels of Cr(III) were extracted using EDTA, these concentrations are still relatively low compared with the Ni concentration extracted (figure 4.3), and would suggest the formation of stable polydentate complexes and polymerised surface precipitates in particular. No clear trend in Cr(III) mobility over the rewetting and drying cycle period could be deduced for the E-horizon (White) and red apedal B-horizon (Red). However, the yellow brown apedal B-horizon (Yellow) showed a significantly decrease ($P<0.001$) between rewetting and drying cycles 1 to 3 and 4 to 5. The significantly higher ($P<0.001$) extractable Cr(III) fraction from the yellow brown apedal B-horizon (Yellow) as opposed to the E-horizon (White) and red apedal B-horizon (Red) for cycles 1 to 3 was not expected.

As discussed in chapter 3, the more pronounced polymerisation of Cr(III) in the yellow brown apedal B-horizon (Yellow) is thought to lead to a more stable Cr(III) precipitate. This should be the case even after a single wetting and drying cycle (as illustrated by figure 3.2, chapter 3) at -3100 $J.kg^{-1}$. It is therefore hypothesised that Cr(III) precipitation is owing to bulk-solution precipitation initially and is not mineral induced. Nonetheless, a decrease in Cr(III) extractability with time was observed for the yellow brown apedal B-horizon (Yellow). The decrease in extractability is attributed to a partial remobilisation of the precipitated Cr(III) phase after being rewetted and a subsequent more effective sorption and polymerisation of the dissolved Cr(III) fraction. The polymerised Cr(III) fraction will form more stable precipitates as the soil dries out, thus explaining the trend in figure 4.2. The data presented in figure 4.2, however, should be seen as contradictory to the findings in chapter 3, as well as the logical deduction from studies conducted on single mineral systems.

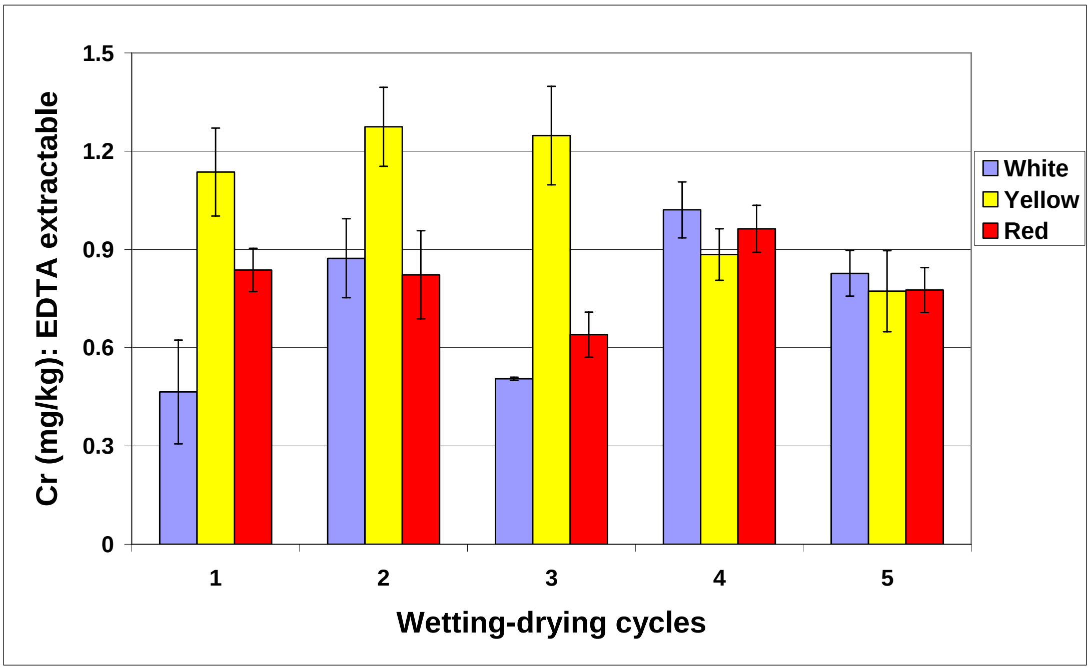

Figure 4.2 0.02 M diammonium EDTA extractable Cr(III)

The morphologies and consequential stabilities of Cr(III) precipitates on soil mineral surfaces, determined through X-ray adsorption fine structure spectroscopy (XAFS) by numerous authors, can be summarised as follows:

(i) Cr(III) precipitates as soluble clusters and moieties onto quartz (Fendorf, Li and Gunter, 1996; Fendorf and Sparks, 1994; Charlet and Manceau, 1992) but ...

(ii) distributes evenly over the goethite surface, adopting its mineral structure (Fendorf, Li and Gunter, 1996; Charlet and Manceau, 1992).

(iii) Cr(III) is effectively sorbed by montmorillonite and the same hydrous chrome oxide (HCO) phase precipitated upon quartz and goethite identified in the interlayers of smectite clays (Sparks, 2003; Abollino *et al.*, 2002; Kraepiel, Keller and Morel, 1999).

(iv) Sesquioxides have been shown to effectively sequester Cr(III) (Eggleston and Stumm, 1993; Charlet and Manceau, 1992; Wehrli, Ibric and Stumm, 1990).

When considering these, it would seem plausible that the Cr(III) sorbed and precipitated by the quartz-dominated E-horizon (White) would be less stable and more mobile than the Cr(III) sequestered by either the yellow brown apedal (Yellow) or red apedal (Red) B-horizons. Furthermore, the higher smectite clay content and cation exchange capacity of the yellow brown apedal B-horizon (Yellow) should lead to a more effective sequestering of Cr(III). The fact that the hypothesis is not met substantiates the thought that Cr(III) precipitation is dominated by bulk-solution precipitation and that mineral-induced precipitation does not contribute as pronouncedly.

Figure 4.2 also denounces, for the time being at least, the notion that soil colour alone, as an indication of mineralogy and clay content, can be used as an indication of Cr(III) mobility.

Table 4.5 illustrates the extractability of Cr(III) and Ni from the three treated soils after five rewetting and drying cycles. EDTA extracted 6.5 % of the initial amount of Cr(III) added to the E-horizon (White), 5.3 % from the yellow-brown apedal B-horizon (Yellow) and 5.5 % from the red apedal B-horizon (Red). Although the E-horizon (White) yielded a significantly higher ($P<0.001$) Cr(III) concentration than either the yellow-brown apedal B-horizon (Yellow) or the red apedal B-horizon (Red) after five rewetting and drying cycles, this was not the case for rewetting and drying cycles 1 to 3.

Figure 4.3 and table 4.5 clearly indicate a rather high EDTA soluble Ni fraction, especially as opposed to Cr(III). Substantiated by findings discussed in chapter 3, it would seem that Ni is associated mainly through electrostatic forces and weak inner-sphere complexes with soil minerals. Precipitation is clearly mineral induced, although bulk-solution precipitation will contribute and dominate as the soils near air dried conditions. Evidently Ni precipitates are quite soluble and should not be regarded as substantially lowering the risk of Ni in the environment.

Table 4.5 0.02 M diammonium EDTA extractable Cr(III) and Ni after five rewetting and drying cycles

	Cr(III)			Ni		
	Added (mg.kg^{-1})	Extracted (mg.kg^{-1})	Percentage (%)	Added (mg.kg^{-1})	Extracted (mg.kg^{-1})	Percentage (%)
White	15	0.98a	6.5	10	3.1b	31
Yellow	15	0.8b	5.3	10	1.21c	21.1
Red	15	0.83b	5.5	10	4.46a	44.6
LSD(0.5)		0.12			0.382	

LSD(.05) values calculated separately for Cr(III) and Ni

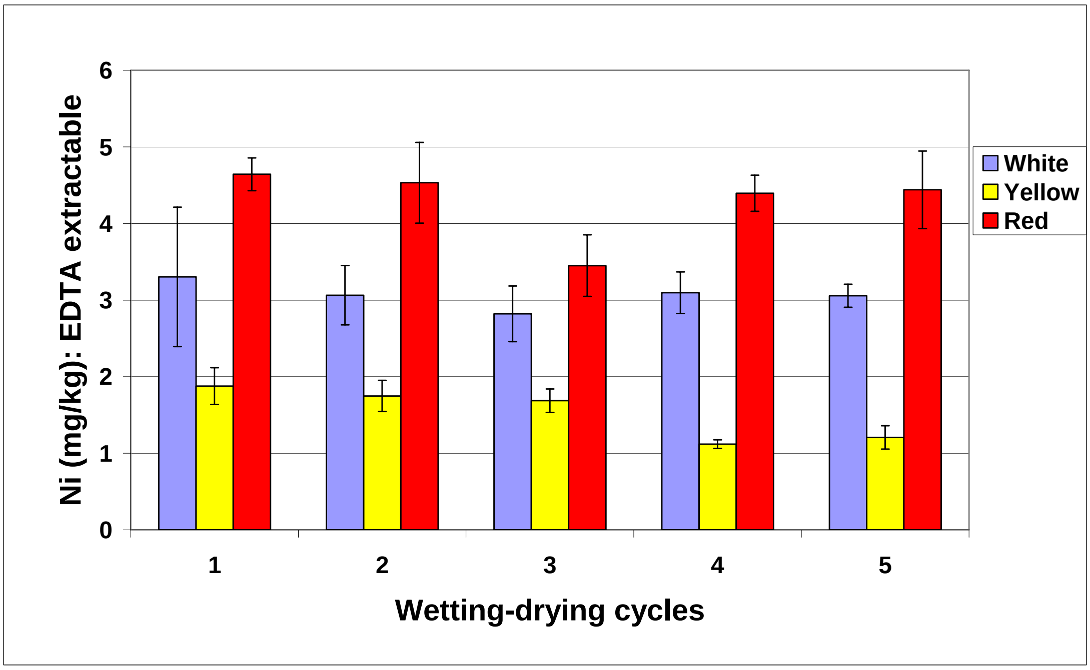

Figure 4.3 0.02 M diammonium EDTA extractable Ni

Ni mobility (figure 4.3), apart from rewetting and drying cycle 3, showed no significant increase or decrease over the five rewetting and drying cycles for both the E-horizon (White) and red apedal B-horizon (Red). Ni levels extracted from the yellow brown apedal B-horizon (Yellow), however, did decrease over the rewetting and drying cycle time period. Whereas no significant difference was observed between rewetting and drying cycles 1 to 3, significantly lower ($P<0.001$) Ni concentrations were extracted after rewetting and drying cycles 4 and 5.

The decrease in Ni mobility is in accordance with the decrease in Cr(III) mobility exhibited by the same soil, and illustrated by figure 4.2. Soils exhibiting a higher montmorillonite clay content and cation exchange capacity may therefore render sorbed cations less available with time. In contrast, soils that do not sequester heavy metals as effectively would seem not to render these elements less mobile over a short time period either. The remobilised Cr(III) and Ni fraction in the yellow brown apedal B-horizon (Yellow) owing to the rewetting of the soil may therefore be sorbed more effectively, where at first it was not. The resulting precipitate will be more polymerised and less soluble. The latter precipitation can occur as a result of the dielectric constant near the soil mineral surfaces being lower than that of the solution owing to ion sorption (Sparks, 2003), and/or of the precipitation of sorbed polymers and polynuclear species owing to local bulk saturation (Ford *et al*., 2001). Furthermore, thermodynamics may dictate the transformation of thermokinetically favoured phases to more stable precipitates such as LDH phases (Peltier *et al*., 2006; Prassanna, Padmanabha and Kamath, 2006). Additionally, sorbed and precipitated metals may diffuse into the crystal structure of the mineral surface onto which it had been sorbed initially (Sparks, 2003; Ford *et al*., 2001).

An alternative explanation of the observed trend is that Cr(III) and Ni may co-precipitate to form a thermokinetically favoured product in the yellow brown apedal B-horizon (Yellow), thus explaining the significantly higher ($P<0.001$) extractability of Cr(III) and Ni over rewetting and drying cycles 1 to 3 as opposed to less extractable levels over cycles 4 and 5. The thermokinetically favoured phase might dissolve all the more as the soil is rewetted, leading to the differentiation of the Cr(III) and Ni phase, and the subsequent formation of separate, thermodynamically stable Cr(III) and Ni phases. It should be remembered, however, that probably no single mechanism is solely responsible for the observed trends in any of the soils investigated.

Clearly indicated by figure 4.3, Ni mobility, throughout the EDTA extractable study, could not be predicted by using soil colour and soil texture as parameters. As indicated by table 4.5, 31 % of Ni added to the E-horizon (White) was extracted after five rewetting and drying cycles. Whereas a significantly lower ($P<0.001$) 21.1% of Ni could be extracted from the yellow brown apedal B-horizon (Yellow), 44.6 % of Ni was extracted from the red apedal B-horizon (Red). The latter's EDTA extractable Ni is significantly ($P<0.001$) higher than values yielded by both the E-horizon (White) and the yellow brown apedal B-horizon (Yellow).

4.4.3 Cr(III) and Ni mobility linked to cation exchange and anion exchange capacity

Clearly much higher concentrations of Ni were extracted from the red apedal B-horizon (Red) and E-horizon (White), as opposed to the yellow brown apedal B-horizon (Yellow). This seem to indicate the formation of easily solubilised $Ni(OH)_2$ precipitates on the quartz surfaces of the E-horizon (White), but more pronounced polymerisation and subsequently more stable precipitated phases in the yellow brown apedal B-horizon (Yellow) owing to its higher smectite clay content and cation exchange capacity. Soils exhibiting a higher clay content, however, do not necessarily sequester Ni more effectively. The notion that the higher clay content of the red apedal B-horizon (Red), as opposed to the E-horizon (White), will also lead to the soil exhibiting a higher cation exchange capacity is denounced by table 4.3. The cation exchange capacity of the red apedal B-horizon (Red) was found not to differ substantially from that of the E-horizon (White), but did show a substantially higher anion exchange capacity than either the E-horizon (White) or the yellow brown apedal B-horizon (Yellow). Soils exhibiting the same cation exchange capacity, but differing in anion exchange capacity, cannot be regarded as having the same affinity for cations such as Ni. It is hypothesised that Ni cations will be able to approach more closely to the exchange complex in a soil with a lower anion exchange capacity because the less negatively charged sites found on the exchange complex will lead to a weaker opposing force, thus increasing the possibility of polymerisation or precipitation to local saturation.

This theory, however, is an oversimplification of the sorption phenomena and probably does not contribute solely to the high EDTA extractable Ni fraction from the red apedal B-horizon (Red). It should be remembered that positively and negatively charged reactive sites are not distributed evenly across the surface of soil minerals under natural conditions. More effective sorption of Ni may be found when Cr(III) is not added to the system, although this requires further investigation. As discussed in chapter 3, the association of Ni with the amorphous Mn oxide mineral phase in the red apedal B-horizon and its dissolution by diammonium EDTA (substantiated by Hlavay *et al.,* 2004), may also contribute to the phenomena. Not only does the red apedal B-horizon contain the highest amorphous Mn oxide phase, but it also exhibits less sorption of Ni by the amorphous Al and Fe oxide phase than found for the yellow brown apedal B-horizon (Yellow).

4.4.4 Effect of Si on Cr(III) stability

Although no specific mechanism regarding Cr(III) immobilisation – as is the case for Ni – has been mentioned by literature or researched, it is thought that the precipitation of the Si oxyanion from solution may render cations less mobile in the soil environment. This may be facilitated through the sequestration of the ion by negatively charged, open-framework silica polymers (Williams and Crerar, 1985) and subsequent stabilisation to microcrystalline Si precipitates (Senkayi *et al.*, 1985), or through the co-precipitation of cations and silica hydrogels or xerogels (Drees *et al.*, 1999).

The $Mg(NO_3)_2$ Cr(III) fraction extracted from the soils investigated yielded values below the method detection limit, and could not even be read against a parts per billion standard range. Although data derived for the E-horizon (White) and yellow brown apedal B-horizon (Yellow) – except after rewetting and drying cycle 5 in the case of the latter – showed no indication of decreased EDTA extractable Cr(III), positive results were obtained for the red apedal B-horizon (Red). Figures 4.4 and 4.5 represent analyses of the E-horizon (White) and yellow brown apedal B-horizon (Yellow), while figure 4.6 represents analyses of the red apedal B-horizon (Red).

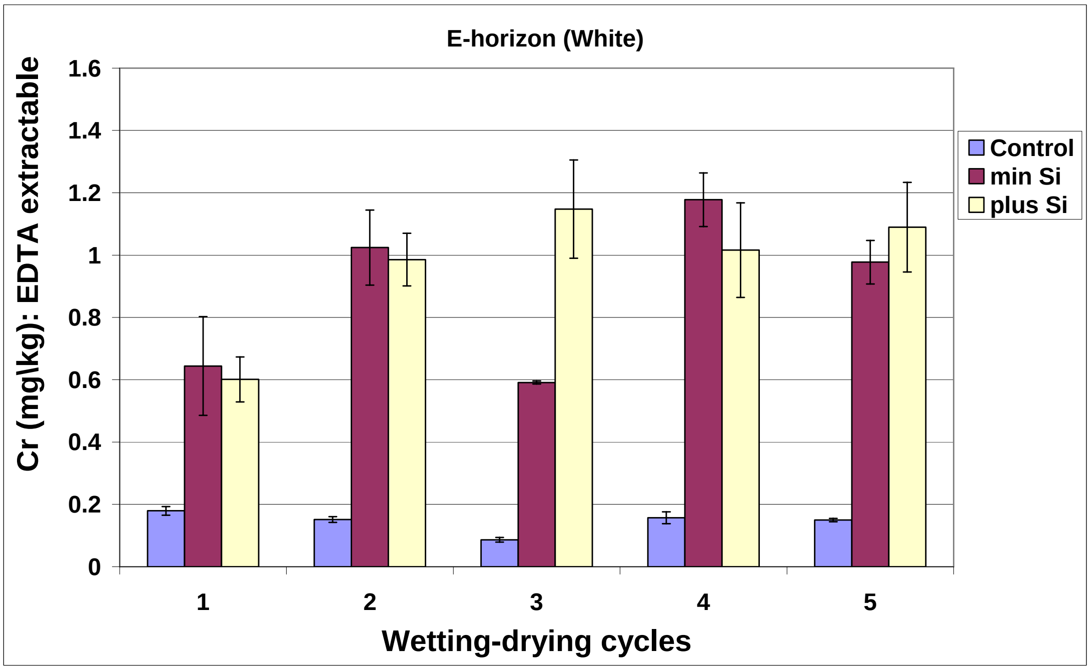

Figure 4.4 0.02 M diammonium EDTA extractable Cr(III) from the E-horizon (White)

The low 0.02 M diammonium EDTA extractable Cr(III) value exhibited by the third rewetting and drying cycle (min Si treatment) of figure 4.4, as well as the drastic decrease of Cr(III) mobility after Si addition, portrayed by rewetting and drying cycle 5 of figure 4.5, may be due to experimental error. In the case of the low Cr(III) concentration extracted using diammonium EDTA (rewetting-drying cycle 3, figure 4.4) not quite 15 mg.kg^{-1} Cr(III) might have been added. The Cr(III) value exhibited by figure 4.5, rewetting-drying cycle 5, does not differ substantially from the control sample values. This would enforce the notion that an experimental error crept in.

Fortunately, these anomalies do not deduct value from the data presented. Figure 4.6 indicates a significant decrease ($P<0.001$) in Cr(III) mobility between the treatment that did not receive Si and the Si-amended treatment after rewetting and drying cycles 3, 4 and 5. This might be owing to the formation of an amorphous or microcrystalline Cr(III) silicate phase. The observed trend, however, is not regarded as conclusive evidence to prove the beneficial effect of an external source of Si on Cr(III) mobility, because the Cr(III) levels extracted from neither E-horizon (White) nor yellow brown apedal B-horizon (Yellow) substantiated the formation of a Cr(III) silicate phase.

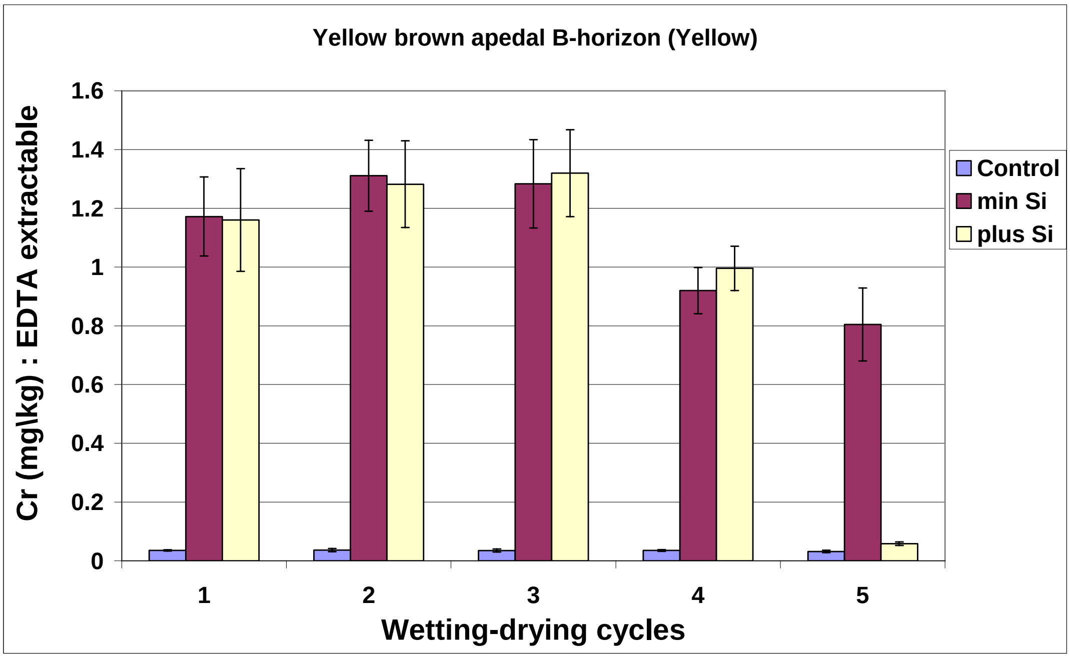

Figure 4.5 0.02 M diammonium EDTA extractable Cr(III) from the yellow brown apedal B-horizon (Yellow)

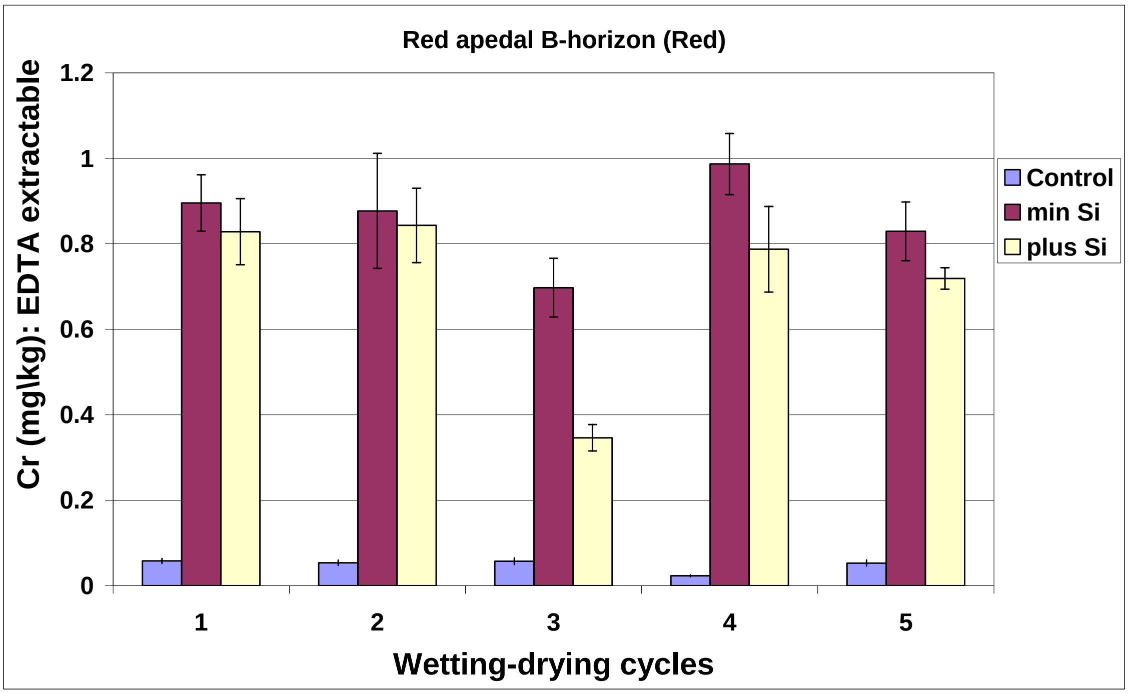

Figure 4.6 0.02 M diammonium EDTA extractable Cr(III) from the red apedal B-horizon (Red)

4.4.5 Effect of Si on Ni stability

Although postulated to substitute for anions locked in the interlayers of Ni precipitates (Peltier *et al.,* 2006; Scheckel *et al,* 2000), the marked influence of Si on Ni mobility as observed in figures 4.7, 4.8 and 4.9 is attributed to the formation of a Ni-silicate precipitate; granted that the more effective sequestration of Ni by negatively charged, open-framework silica polymers may also be responsible for these tendencies. Not only does the interpretation of the data lend itself to either of these mechanisms, but numerous authors (Scheckel *et al.*, 2000; Ford, Scheinost, Sheckel and Sparks, 1999; Scheidegger, Lamble and Sparks, 1996) found the effect of Si on Ni mobility through the mechanism of Si for anion substitution (Peltier *et al.,* 2006; Scheckel *et al,* 2000), to be profound only after a one-year period.

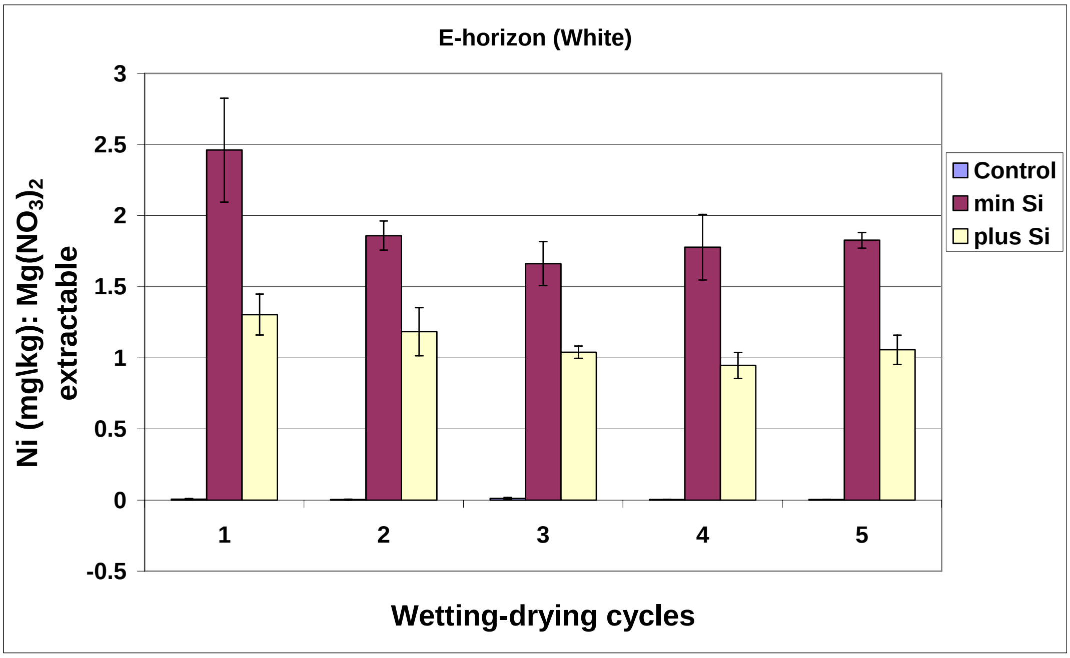

Figure 4.7 0.1 M Mg(NO$_3$)$_2$ extractable Ni from the E-horizon (White) – plus Si treatment

The Mg(NO$_3$)$_2$ extractable Ni fraction show a significant decrease ($P<0.001$) when an external source of Si is added to the E-horizon (White) (figure 4.7) and red apedal B-horizon (Red) (figure 4.8). In the case of the latter, a decrease in Ni mobility was observed only after rewetting and drying cycles 3 to 5 ($P<0.001$). Because both these soils sequester Ni poorly (figure 4.2), it is postulated that the Ni, concentrated in the diffuse double layer surrounding soil particles and the soil solution, precipitates as a Ni-silicate phase in the presence of the added Si. The decrease in mobility exhibited by figure 4.8 is attributed to the stabilisation of the newly formed Ni-silicate precipitate phase owing to Ostwald ripening.

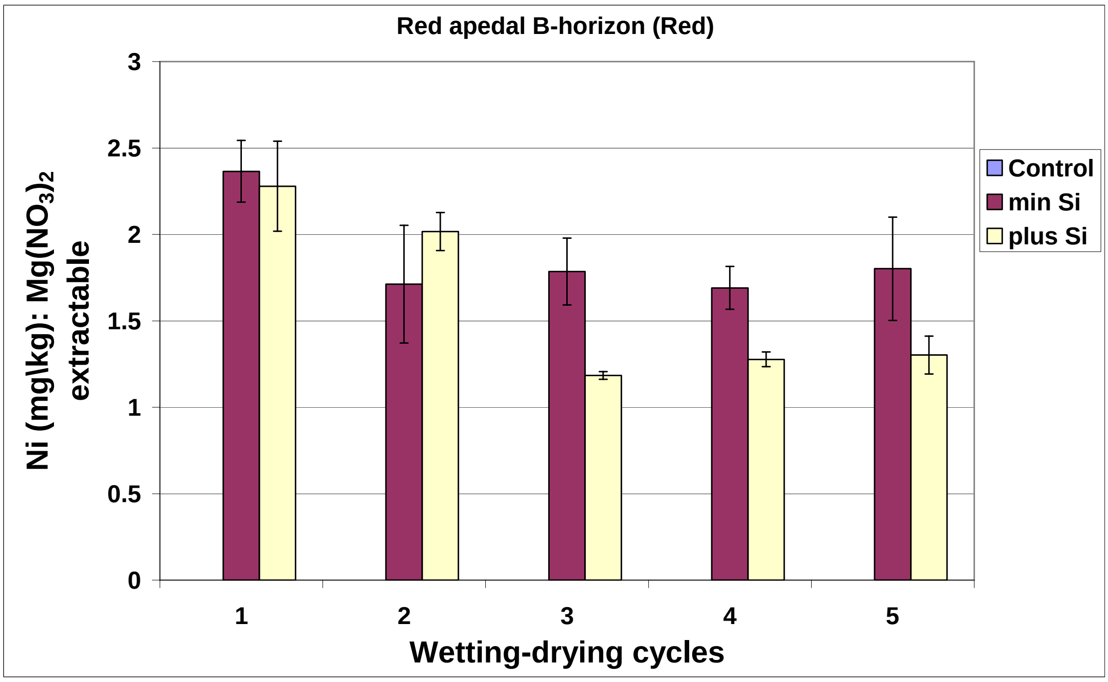

Figure 4.8 0.1 M Mg(NO_3)$_2$ extractable Ni from the red apedal B-horizon (Red) – plus Si treatment

A number of pathways, starting with Si in solution as a precursor, may lead to the neoformation of quartz and, especially, disordered polymorphs in the soil environment. The condensation and polymerisation of monomeric silicic acid to coherent three-dimensional gel networks is influenced by an array of factors, including pH and salt concentration in the soil solution (Drees *et al*., 1985; Williams and Crerar, 1985). Although observed to precipitate onto quartz surfaces in seawater, coatings of organic matter, clay minerals, and sesquioxides in the soil environment may inhibit the precipitation of quartz from solution (Drees *et al*., 1985; Mackenzie and Gees, 1971). The observed immobilisation of Ni in Si-amended soils may therefore be brought about by the precipitation of an amorphous or poorly crystalline Ni-silicate phase, rather than the neoformation of a quartz phase.

However, from the work of Williams and Crerar (1985) a second mechanism can be proposed. The condensation of Si polymers and subsequent precipitation of poorly ordered Si phases onto metal hydroxides may result in the sorption of cations onto the negatively charged, open-framework silica polymers. But Ni is seldom known to form stable complexes with negatively charged functional groups and, moreover, is found to be one of the most mobile of all transition elements (Christensen *et al.*, 1996). This, coupled with the fact that the Ni and Si were added simultaneously to the soil samples, would give preference to the proposed mechanism of a newly formed amorphous or microcrystalline Ni-precipitate. It is thought that Ni and Si would co-precipitate, rather than Si preferentially precipitating to form an open framework polymeric system, which would then sequester Ni and render it less mobile.

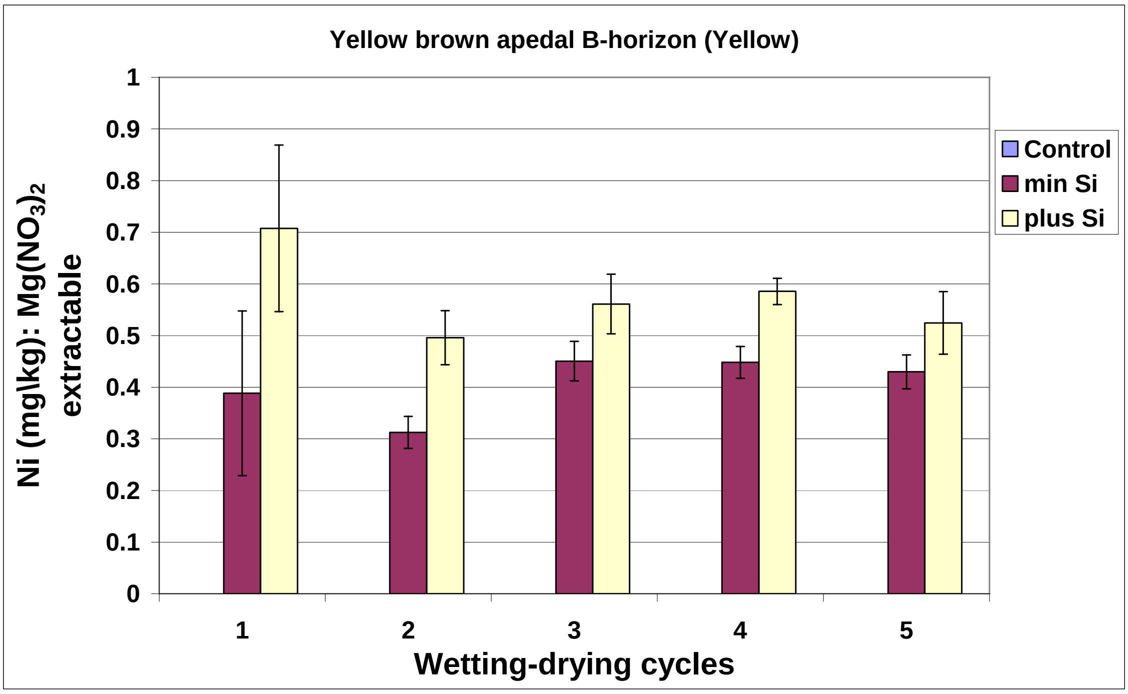

Figure 4.9 0.1 M $Mg(NO_3)_2$ extractable Ni from the yellow brown apedal B-horizon (Yellow) – plus Si treatment

The postulated formation of an amorphous or microcrystalline Ni-silicate phase is further substantiated by the significantly ($P<0.001$) more mobile $Mg(NO_3)_2$ extractable Ni fraction as observed for the yellow brown apedal B-horizon (Yellow) (figure 4.9) when reacted with both Ni and Si. The yellow brown apedal B-horizon (Yellow) sequestered Ni much more effectively than either the E-horizon (White) (figure 4.1) or red apedal B-horizon (Red) (figure 4.1) ($P<0.0001$). Therefore, once the Si was added to the Ni-amended soil, Ni precipitated as an amorphous Ni-silicate before it could be sequestered effectively by the soil particles. The newly formed Ni-silicate phase is thought to be thermokinetically favoured above the formation of inner-sphere complexes, $Ni(OH)_2$ surface precipitation and/or layered double hydroxide phases.

Substantiated by figures 4.7, 4.8 and 4.9, an external source of Si might immobilise Ni to a certain extent in soils exhibiting a low affinity for Ni, but the thermokinetically favoured Ni-silicate phase is not necessarily the more stable product in soils that could otherwise sequester Ni more effectively.

However, when extracted with EDTA, no significant difference between the Si-reacted treatment and the Si-unreacted treatment with regards to Ni mobility were found for all three soil types. Figure 4.10 exemplifies this tendency. The hypothesis that Ni precipitates as an amorphous or microcrystalline Ni silicate phase, rather than impurities in a neoformed quartz phase, is thus substantiated. It is thought that the precipitation of a quartz phase would withstand extraction using EDTA.

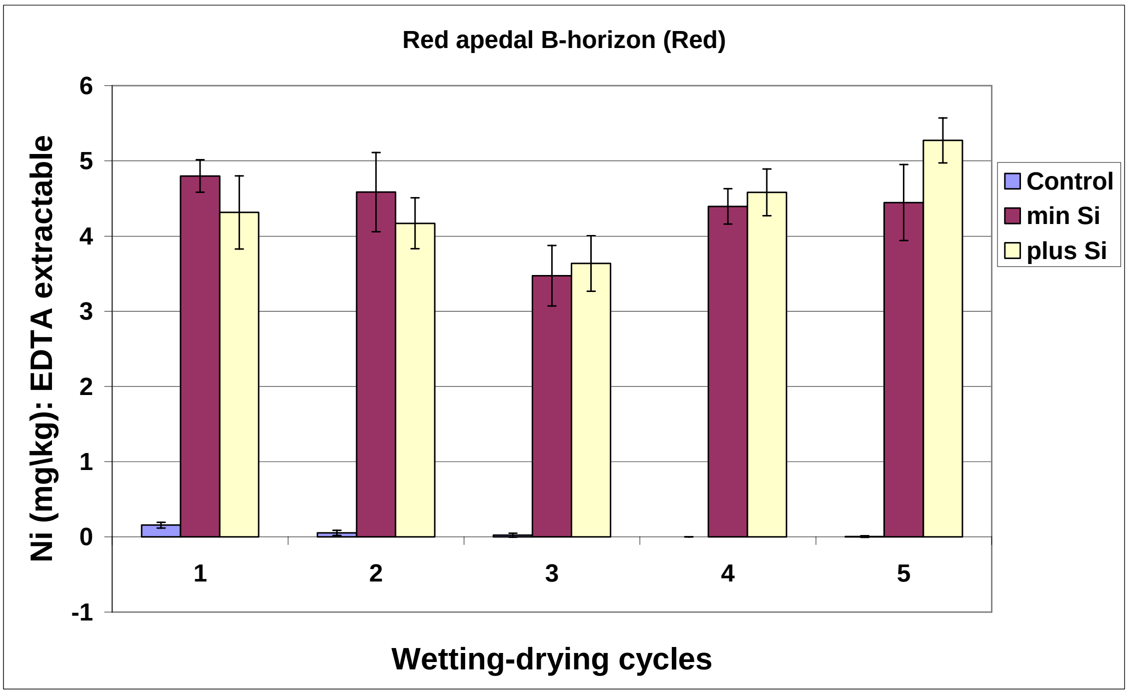

Figure 4.10 0.02 M diammonium EDTA extractable Ni – plus Si treatment

The effect of an external source of Si on Ni extractability might seem to be of academic value only. It is doubtful whether Si, in the short run, will have a major influence on Ni mobility under field scale conditions. Furthermore, the $Mg(NO_3)_2$ extractable Ni fraction is rather low, irrespective of Si addition. But heavy metal mobility in the environment can be predicted only if the mechanisms by which these elements are sequestered are fully understood. Currently these mechanisms are not all known and not clearly comprehended. The study on the effect of Si on Ni extractability thus contributes to a better understanding of Ni dynamics in the soil environment. In addition, it has been shown that the effect of Si on heavy metal mobility is pronounced only after a one-year period (Scheckel *et al.*, 2000; Ford *et al.*, 1999b; Scheidegger *et al.*, 1996). Long-term studies on the further transformation and stabilisation of the amorphous Ni silicate phase must therefore be conducted. It is hypothesised that the amorphous Ni silicate phase, initially precipitated owing to thermokinetic favourability, will transform to less soluble phases that might have an influence on the EDTA extractable Ni fraction.

4.5 Conclusion

From this study three main findings could be concluded:

(i) Cr(III) is sequestered substantially more effective than Ni by all soils investigated.

(ii) A decrease in metal extractability over time was observed for Ni in the soil exhibiting the highest cation exchange capacity.

(iii) Although the influence of an external source of Si on Cr(III) stability could not be determined, Si did influence the mobility of Ni. It is postulated that the amorphous Ni-silicate precipitate, which forms in the presence of an external Si source, may decrease Ni mobility in soils exhibiting a low sequestering capability for Ni, but will have the opposite effect in soils of higher clay content and subsequent cation exchange capacity. This influence of Si on Ni extractability, however, is not substantiated by stronger extractants and may therefore not be of utmost relevance over the period mentioned under field scale conditions.

Furthermore, field-classifiable soil characteristics, such as soil colour and texture, cannot be used as a means to predict Cr(III) and Ni mobility. Although an indication of mineralogy, soil colour predicts neither the charge characteristics of a soil nor the subsequent removal of Cr(III) and Ni from solution. Soil texture might in turn comment on the clay content of soils, but does not specify whether 2:1 clay minerals make up a substantial fraction of it. In addition, the overall charge at a certain pH value is again not reckoned with. Predicting Cr(III) and Ni mobility in particular should therefore rather be modelled on a detailed laboratory soil characterisation which includes an investigation into soil charge.

Even though found to be immobilised within a single wetting and drying cycle, the oxidation of Cr(III) to Cr(VI) in soils dominated by Mn oxides warrants investigation. The high levels of Ni extracted should raise concern regarding the addition of Ni rich products to the environment. This is especially alarming when considering that water will preferentially flow through the path of lowest obstruction through the landscape. As this may have been the case for decades, even centuries, mobile elements may be found to accumulate further down the soil profile or in depressions in the landscape, reaching toxic levels.

4.6 References

ABOLLINO, O., ACETO, M., MALANDRINO, M., SARZANINI, C. and MENTASTI, E. 2002. Adsorption of heavy metals on na-montmorillonite. Effect of pH and organic substances. *Water research*, 37:1619–1627.

AMACHER, M.C. 1996. Nickel, cadmium and lead. In: *Methods of Soil Analysis. Part 3 – Chemical Methods*. Editor: D.L. Sparks. SSSA Book Series no 5. Soil Science Society of America, American Society of Agronomy, Madison, Wisconsin, USA, pp 749–750.

ANDERSON, S.J. and SPOSITO, G. 1992. Proton surface charge density in soils with structural and pH-dependent charge. *Soil Science Society of America Journal* 56:1437–1443.

BANKS, M.K., SCWAB, A.P. and HENDERSON, C. 2005. Leaching and reduction of chromium in soil as affected by soil organic content and plants. *Chemosphere,* (forthcoming, article in press).

BARTLETT, R.J. and JAMES, B. 1979. Behaviour of chromium in soils: III. Oxidation. *Journal of Environmental Quality*, 5:31–35.

BARTLETT, R.J. and JAMES, B.R. 1988. Mobility and bioavailability of chromium in soils. In: Nraigu, J.O., Nieborer, E. (eds). *Chromium in the Natural and Human Environments*. New York: Wiley, pp 267–303.

BAYTAK, S. and TűRKER, R.A. 2005. Determination of lead and nickel in environmental samples by flame atomic absorption spectrometry after column solid-phase extraction on ambersorb-572 with EDTA. *Journal of Hazardous Material,* 129:130–136.

BRADL, H.B. 2004. Adsorption of heavy metal ions on soils and soil constituents. *Journal of Colloid and Interface Science,* 277:1–18.

BRADY, N.C. and WEILL, R.P. 1999. *The Nature and Properties of Soils*. Twelfth edition., Upper Saddle River, New Jersey: Prentice Hall, pp119, 126, 202–204, 311.

CHRISTENSEN, T.H., LEHMANN, N., JACKSON, T. and HOLM, P.E. 1996. Cadmium and nickel distribution coefficients for sandy aquifer materials. *Journal of Contaminant Hydrology,* 24:75–84.

CHARLET, L. and MANCEAU, A.A. 1992. X-ray adsorption spectroscopy study of the sorption of Cr(III) at the oxide-water interface: I. Molecular mechanisms of Cr(III) oxidation by Mn oxides. *Journal of Colloidal Interface Science,* 148:425–442.

COOPER, G.R.C. 2002. Oxidation and toxicity of chromium in ultramafic soils of Zimbabwe. *Applied Geochemistry,* 17:981–986.

DREES, R.L., WILDING, L.P., DMECK, N.E. and SENKAYI, A.L. 1989. Silica in soils: Quartz and disordered silica polymorphs. In: *Minerals in the Soil Environment.* Edited by Dixon, J.B. and Weed, S.B. Second edition. SSSA Book Series: 1. Soil Science Society of America, Madison, Wisconsin, pp 943–949.

DUBBIN, W.E. 2004. Influence of organic ligands on Cr desorption from hydroxyl-Cr intercalated montmorillonite. *Chemosphere* 54:1071–1077.

ECHEVERRIA, J.C., MORERA, M.T., MAZKIARAN, C. and GARRIDO, J.J. 1998. Competitive sorption of heavy metals by soils. Isotherms and fractional factorial experiments. *Environmental Pollution,* 101:275–284.

EGGLESTON, C.M. and STUMM, W. 1993. Scanning tunneling microscopy of Cr(III) chemisorbed on α-Fe_2O_3 (001) surface from aqueous solution: Direct observation of surface mobility and clustering. *Geochimica et Cosmochimica Acta,* 57:4843–4850.

ERNST, W.G, and CALVEST, S.E. 1969. An experimental study of the recrystalization of porcelinite and its bearing on some bedded cherts. *American Journal of Science*, 267A:114–133.

FENDORF, S.E. 1994. Surface reactions of chromium in soils and waters. *Geoderma,* 67:55–71.

FENDORF, S.E., LI, G. and GUNTER, M.E. 1996. Micromorphologies and stabilities of chromium(III) surface precipitates elucidated by scanning force microscopy. *Soil Science Society of America Journal*, 60:99–106.

FENDORF, S.E. and SPARKS, D.L. 1994. Mechanisms of chromium(III) sorption onto silica. II: Effect of reaction conditions. *Environmental Science and Technology,* 28:290–297.

FORD, R.G., SCHEINOST, A.C., SCHECKEL, K.G. and SPARKS, D.L. 1999. The link between clay mineral weathering and structural transformation in Ni surface precipitates. *Environmental Science and Technology* 33(18):3140–3144.

FORD, R.G., SCHEINOST, C.S. and SPARKS, D.L. 2001. Frontiers in metal sorption/precipitation on soil mineral surfaces. *Advances in Agronomy*, 74:41–61.

GRONDKLASSIFIKASIEWERKGROEP 1991. Grondklassifikasie: ‘n Taksonomiese sisteem vir Suid-Afrika. Memoirs oor die natuurlike landbouhulpbronne van Suid-Afrika Nr. 15. ‘n Verslag oor ‘n Navorsingsprojek wat Uitgevoer is onder Beskerming van die Navorsingsinstituut vir Grond en Besproeiing. Departement van Landbou-Ontwikkeling, Pretoria, bl 19–21, 22–25.

HLAVAY, J., PROHASKA, T., WEISZ, M., WENZEL, W.W. and STINGEDER, J.G. 2004. Determination of trace elements bound to soil and sediment fractions. IUPAC Technical Report. *International Union of Pure and Applied Chemistry*, 76 (2):425–442.

JEON, B.H., DEMPSEY, B.A., BURGOS, W.D. and ROYER, R.A. 2003. Sorption kinetics of Fe(II), Zn(II), Co(II), Ni, Cd(II) and Fe(II)/Me(II) onto hematite. *Water Research,* 37:4135–4142.

KASTNER, M. and GIESKES, J.M. 1983. Opal-A to opal-CT transformation: A kinetic study. In: *Siliceous Deposits in the Pacific Region*. Edited: A. Ijima, J.R. Hen, and R. Siever. Amsterdam: Elsevier Science, pp 211–228.

KRAEPIEL, A.M.L., KELLER, K. and MOREL, F.M.M. 1999. A model for metal adsorption on montmorillonite. *Journal of Colloidal Interface Science,* 210(1):43–54.

LAVERDIERE, M.R. and WEAVER, R.M. 1977. Charge characteristics of spodic horizons. *Soil Science Society of America Journal* 41:505–510.

MACKENZIE, F.T. and GEES, R. 1971. Quartz: Synthesis at earth surface conditions. *Science* (Washington, DC), 175:533–535.

PELTIER, E., ALLADA, R., NAVROTSKY, A. and SPARKS, D.L. 2006. Nickel solubility and precipitation in soils: A thermodynamic study. *Clay and Clay Minerals,* 54:153–164.

PRASANNA, S.V., PADMANABHA, P.R. and KAMATH, P.V. 2006. Layered double hydroxides as potential chromate scavengers. *Journal of Colloid and Interface Science*, 304: 292–299.

SCHECKEL, K.G., SCHEINOST, A.C., FORD, R.G. and SPARKS, D. 2000. Stability of layered Ni hydroxide surface precipitates: A dissolution kinetic study. *Geochimica et Cosmochimica Acta,* 64:2727–2735.

SCHEIDEGGER, A. M., FENDORF, M. and SPARKS, D.L. 1996. Mechanisms of nickel sorption on pyrophillite: Macroscopic and microscopic approaches. *Soil Science Society of America Journal,* 60:1763–1772.

SCHEIDEGGER, A. M., LAMBLE, G. M. and SPARKS, D.L. 1996. Spectroscopic analysis for the formation of mixed cation hydroxide phases upon metal sorption on clay and aluminum oxides. *Journal of Colloid and Interface Science,* 186:118–128.

SCHEINOST, A.C., FORD, R.G. and SPARKS, D. L. 1999. The role of Al in the formation of secondary precipitates on pyrophyllite, gibbsite, talc, and amorphous silica: A DRS study. *Geochimica et Cosmochimica Acta,* 63:3193–3203.

SENKAYI, A.L, DIXON, L.R., HOSNER, B.P.K.,YERIMA, and WILDING, L.P. 1985. Replacement of quartz by opaline silica during weathering of petrified wood. *Clays and Clay Mineralogy*, 33:525–531.

SINGER, A., KIRSTEN, W. and BUHMANN, C. 1994. Fibrous clay minerals in the soils of Namaqualand, South Africa: Characteristics and formation. *Geoderma* 66:43–70.

SPARKS, D.L., 2003. *Environmental Soil Chemistry*. 2nd edition. Academic Press, pp 54, 60, 67, 177, 259.

STAUNTON, S. 2004. Sensitivity analysis of the distribution coefficients, Kd, of nickel with changing soil chemical properties. *Geoderma*, 122(2004):281–290.

STUMM, W. and MORGAN, J.J. 1996. *Aquatic Chemistry*. *Chemical Equilibria and Rates in Natural Waters*. Third edition., New York: John Wiley & Sons, pp 309, 367.

SUAREZ, D.L., 1996. Beryllium, magnesium, calcium, strontium, and barium. In: *Methods of Soil Analysis*. Part 3 – Chemical Methods. Editor: D.L Sparks. SSSA Book Series no 5. Soil Science Society of America, American Society of Agronomy, Madison, Wisconsin, USA, p 593.

TRIVEDI, P., AXE, L. and DYER, J. 2001. Adsorption of metal ions onto goethite: Single-adsorbate and competitive systems. *Journal of Colloid and Surface Chemistry,* 191:107–121.

VAN DER WAALS, J.H. 2001. Slag as agricultural limes: Reactivity, heavy metal and phosphorous bio-availability. Unpublished MSc dissertation, Department of Plant Production and Soil Science, University of Pretoria.

WEHRLI, B., IBRIC, S. and STUMM, W. 1990. Adsorption kinetics of vanadyl(VI) and chromium(III) to aluminium oxide: Evidence for two-step mechanism. *Colloidal Surfaces,* 51:77–88.

WILLIAMS, L.A. and CRERER, D.A. 1985. Silica diagenesis. II. General mechanisms. *Journal of Sedimentology and Petrology*, 55:312–321.

WITTBRODT, T. and PAKMER, C.D. 1995. Reduction of Cr(VI) in the presence of excess soil fulvic acid. *Environmental Science and Technology* 29:1–25.

ZELAZNY, L.W., HE, L. and VANWORMHOUDT, A. 1996. Charge analysis of soils and anion exchange. In: *Methods of Soil Analysis*. Part 3 – Chemical methods. Editor: D.L. Sparks. SSSA Book Series no 5. Soil Science Society of America, American Society of Agronomy, Madison, Wisconsin, USA, pp 1231–125

Chapter 5 Steel plant slag reactivity and heavy metal release in a highly buffered soil

5.1 Abstract

The use of steel plant slag as an agricultural liming agent on the Eastern Highveld of South Africa necessitates an investigation into slag reactivity and heavy metal release. Two commercially available slag liming agents, known to contain high levels of specific heavy metals, and a highly buffered soil were used in the investigation. The acid neutralising capacity of the slag samples relative to $CaCO_3$ was determined using the soil suspension method described by Bornmann (1985) and soil pH adjusted to near neutral conditions. The soil was then subjected to five rewetting and drying cycles and the environmental extractable of chromium and nickel determined. The following extractants were used to assess the latter: 0.1 M $Mg(NO_3)_2$, 0.02 M diammonium EDTA, pH 2.0, 0.1 M $NH_2OH.HCl$, pH 3.0, 0.175 M $(NH_4)_2C_2O_4$ + 0.1 M $H_2C_2O_2$ (Tamm's reagent) and 1.0 M HNO_3. The method proposed by Bornmann (1985) proved to underestimate the reactivity of the slag samples and to lead to varying results regarding pH adjustment of the soil. This enabled an investigation into the effect of pH on these heavy metals. Both slag samples almost doubled the extractability of Cr from the soil. Ni dissolved from the slag samples was found to be sequestered rather effectively by the soil, but showed pH sensitivity. Cr extractability was not substantially affected by pH change.

Key words: Steel plant slag, Cr, N, environmental extractability.

5.2 Introduction

The South African statutory requirements to register and sell a liming material are stipulated in Part III of Annexure A of Government Notice R.250: Act 36 of 1947 (Government Gazette no 29720). These mainly require an estimation of the acid neutralising capacity (ANC) of liming materials in soil and consist of the "calcium carbonate equivalent" (CCE) as determined by strong acid (HCl) and resin suspension methods as well as particle size distribution (sieve test) and moisture content.

No specifications for maximum heavy metal contents of liming materials (in fact, of any fertilisers) appear in the act, except those stipulated for wastewater sludge. Since steel plant slag has been used as a liming agent on South Africa's Eastern Highveld agricultural soils for more than a decade, and contains appreciable levels of certain heavy metals, an assessment of the environmental risk associated with slag use is imperative.

Internationally, slag characterisation generally entails a variety of test procedures for elemental composition (XRF, ICP), phase composition (XRD), ANC (long- and short-term batch titrations) and environmental risk associated with hazardous substances (leaching with various extractants). These investigations usually focus on the use of slag in cement manufacturing and road construction applications. Serious investigations into the possible detrimental effects from slag use in agriculture, and especially into the dynamics of hazardous substances (heavy metals) in soil, are few and far between. Slag reactivity as well as the release and in particular the sequestration of Cr and Ni in soil are addressed in this study.

Chromium may be present in either its +3 or +6 oxidation state, the latter being toxic (Fendorf, 1994). Although an essential nutrient, Cr(III) can be oxidised to Cr(VI) by numerous Mn oxide minerals (Stepniewska, Bucior and Bennicelli, 2004; Cooper, 2002; Fendorf, 1994; Charlet and Manceau, 1992; Saleh *et al.*, 1989; Eary and Rai, 1987; Bartlett and James, 1979, etc.), oxidation being especially pronounced at low pH conditions and in poorly aerated subsoils containing easily reducible Mn oxides (Cooper, 2004: Fendorf, 1994). Cr(VI) is sorbed by all soil minerals containing surface hydroxyl groups, especially Al and Fe oxides, kaolinite and montmorillonite (Zachara *et al.*, 1989; Zachara *et al.*, 1987), but is easily reduced to Cr(III) by sulphides, organic matter and ferrous iron (Fendorf, 1994).

Cr(III) has been shown to form inner-sphere complexes and precipitate as a hydrous chrome oxide phase (HCO) on goethite (Fendorf, Li and Gunter, 1996; Charlet and Manceau, 1992), quartz (Fendorf *et al.*, 1996; Fendorf and Sparks, 1994; Charlet and Manceau, 1992) and smectite clays (Fendorf, 1994; Rengasamy and Oades, 1978). Multinuclear Cr(III) species was also identified on hydrous ferric oxide (Charlet and

Manceau, 1992), hematite (Eggleston and Stumm, 1993) and Al_2O_3 (Wehrli, Ibric and Stumm, 1990).

Ni, being present as a divalent cation in soil solution, is believed to be one of the most mobile heavy elements (Christensen *et al.*, 1996) and has been postulated to be specifically sorbed at near neutral pH values onto goethite, hematite (Jeon *et al.*, 2003; Trivedi, Axe and Dyer, 2001) and all of the cryptocrystalline oxides of Mn. Sorption onto Al oxide minerals was found to be significant at pH values between 5.8 and 6.5 (Ho Hsu, 1989). The solubility of Ni sorbed onto synthesised amorphous $Fe(OH)_3$ increased sharply with decreasing pH, and reached a maximum at pH 3.0 (Kedziorek and Bourg, 1996). Scheidegger, Fendorf and Sparks (1996) found Ni sorption onto pyrophyllite to be highly dependent on ionic strength and reversible at pH values less than 7, but not dependent on ionic strength at pH values above 7, indicating nucleation processes at higher pH values. Ni sorption onto montmorillonite is dominated by cation exchange and hindered at low pH values owing to protonated functional groups on the clay sheet edges (Abollino *et al.,* 2002). Because kaolinite exhibits minor permanent charge, sorption of Ni takes place mainly at the exposed $Si-O^-$ and $Al-O^-$ functional groups (Yavuz, Altunkaynak and Gűzel, 2003). Ni desorption from kaolinite was found to be most pronounced at pH 5.0 (Kedziorek and Bourg, 1996).

The aim of this study is to investigate the reactivity of two commercially available slag liming materials, the release of Cr and Ni from these, and the environmental extractability of these elements from slag-amended soil. ‘Environmental extractability’ is quantified by a range of extractants that emulate the distribution of heavy metals among different soil phases in order to assess their potential short- and long-term mobility.

5.3 Materials and methods

For the purpose of this study an acidic (pH 4.33) dolerite-derived soil with high pH buffer capacity was identified, collected and passed through a 2 mm sieve. The slag liming materials used were the < 250 micron (0.25mm) fraction of Highveld steel and Columbus steel slag.

5.3.1 Slag reactivity

A pH buffer curve was compiled, using 0.02 M $Ca(OH)_2$ and the required amount of analytical grade $CaCO_3$ to adjust the soil pH to 6.5 was calculated. The ANC of the slag samples relative to $CaCO_3$ was determined, using the soil suspension method described by Bornmann (1985): to 50 g soil, 50 mg $CaCO_3$ or slag and 125 ml deionised water were added to obtain a 1:2.5 suspension. The suspension was stirred, equilibrated for a 24-hour period (standing) and the pH determined after stirring the suspension again. The relative acid neutralising capacity (in soil suspension) (RS value) was calculated as follows:

$$\frac{\Delta pH(slag)}{\Delta pH(CaCO3)} \times 100$$

5.3.2 Slag heavy metal content

To determine the heavy metal content, each slag sample was subjected (in triplicate) to extraction according to the EPA 3051A method, as well as extraction (in triplicate) using a 1 M HNO_3 solution. The methodology for the latter entailed the addition of 40 ml HNO_3 to 1 g of slag weighed off in a 45 ml polyethylene centrifuge tube. The suspension was placed on a reciprocal shaker for 24 hrs at 180 rpm and then centrifuged at 40 rpm for 15 minutes. The supernatant was membrane filtered (0.25 μm) and metal content determined on an ICP-AES. The HNO_3 extractable heavy metal fraction can be regarded as the upper limit of environmental availability, while the EPA 3051AA values are regarded as a pseudo-total for the purpose of this study.

5.3.3 Batch equilibration study: slag-amended soil

The batch equilibration study entailed the adjustment of 140 g soil samples to a calculated pH of 6.5 using $CaCO_3$, the Highveld steel slag and the Columbus steel slag. A pH buffer curve using 0.02 M $Ca(OH)_2$ was compiled and the required analytical grade $CaCO_3$ to adjust the soil pH to 6.5 was calculated. Calculations amounted to the addition of 0.23 g $CaCO_3$, 0.67g Highveld steel slag, and 0.48 g Columbus steel slag. The latter two calculations were based on Bornmann's RS calculations. A control treatment that received none of the liming agents was included. Each treatment consisted of three replications. The samples were subjected to five rewetting and drying cycles over a three-month period. Each rewetting and drying cycle involved the saturation of each soil sample, entailing the addition of 55 ml ultra pure water.

After the three-month equilibration period, pH (H_2O) for each sample was determined. To determine the soil pH, 10 g of soil was weighed off and 25 ml deionised, distilled H_2O was added. The pH meter was calibrated at 25 °C with commercially available pH 4.0 and pH 7.0 buffer solutions. The soil:water suspension was stirred rapidly for approximately five seconds and left to settle. After a 50 min period the suspension was stirred again and left to settle for 10 min, after which the supernatant pH was determined and recorded (Non-Affiliated Soil Analysis Work Committee, 1990).

The following extractants and methodology were used to investigate the environmental extractability of Cr and Ni:

(i) 10 ml of a 0.1 M $Mg(NO_3)_2$ solution was added to 5 g soil weighed off in a 45 ml polyethylene centrifuge tube. The solution was placed on a reciprocal shaker for two hours at 180 revolutions per minute, and centrifuged for 10 minutes at 1 500 rpm. The supernatant was passed through an ashless Whatman no 42 filter paper (Amacher, 1996). $Mg(NO_3)_2$ is thought to indicate the electrostatically bound and neutral salt dissolvable metal fraction of the soil (Amacher, 1996) which is in constant equilibrium with the soil solution (Sparks, 2004; Brady and Weill, 1999).

(ii) To 10 g of soil weighed off in a 45 ml polyethylene centrifuge tube, 30 ml of a 0.02 M diammonium EDTA solution was added. Afterwards the centrifuge tube was placed on a reciprocal shaker for two hours at 180 rpm and centrifuged for 20 minutes at 2 500 rpm. The supernatant was passed through an ashless Whatman no 42 filter paper (Jean, Bordas and Bollinger, 2006). EDTA promotes ligand dissolution, and thus extracts inner-sphere complexes and metals bound to silanol and aluminol functional groups (Nowack and Sigg, 1997). It has been shown, however, that EDTA dissolves a fraction of the amorphous sesquioxide mineral phase, especially after a 90 min reaction time.

(iii) Of a pH 2.0, 0.1 M $NH_2OH.HCl$ solution, 25 ml was added to 5 g soil. The soil was weighed off in a 45 ml polyethylene centrifuge tube and the solution placed on a reciprocal shaker for 30 min at 180 rpm and centrifuged for 15 minutes at 1 500 rpm. The supernatant was passed though an ashless Whatman no 42 filter paper (Jean, Bordas and Bollinger, 2006; Balasoiu, Zagury and Deschênes, 2000; Gambrell, 1996). $NH_2OH.HCl$ is a mild reducing reagent, which is commonly used to mobilise Mn from its amorphous oxides, or trace metals sorbed onto or occluded in these oxides (Luo and Christie, 1997; Amacher, 1996; Gambrell, 1996), and are reported to minimally attack coexisting Fe oxides (Krasnodebska-Ostrega, Emons and Golimowski, 2001; Luo and Christie, 1997; Gambrell, 1996).

(iv) A pH 3.0, 0.175 M $(NH_4)_2C_2O_4$ and 0.1 M $H_2C_2O_2$ solution, known as Tamm's reagent, was used to estimate the Cr, Ni, and V fraction associated with the amorphous Fe (Loeppert and Inskeep, 1996) and Al (Bertsch and Bloom, 1996) oxide mineral component in soil. To 1 g soil weighed off in a 45 ml polyethylene tube, 30 ml Tamm's reagent was added, placed on a reciprocal shaker for two hours at 180 rpm and centrifuged at 25 rpm for 15 minutes. The supernatant was passed though an ashless Whatman no 42 filter paper. This procedure was conducted in the dark to prevent photoreduction and retard the crystalline Fe oxide dissolution rate (Loeppert and Inskeep, 1996; Bertsch and Bloom, 1996).

Although crystalline Fe oxide minerals will also react with ammonium oxalate, the reaction is rate dependent and the preferential dissolution of poorly crystalline Fe oxides phases (including ferrihydrate) confirmed (Schwertmann, 1991). The acid ammonium oxalate solution has little effect on kaolinite, montmorillonite, vermiculite and illite (Hodges and Zelansky, 1980), but does dissolve trioctahedral layered silicates such as biotite and chlorite (Loeppert and Inskeep, 1996).

(v) 40 ml of a 1.0 M HNO_3 solution was added to 1 g soil and the 45 ml polyethylene tube, into which the soil was weighed off, placed on a reciprocal shaker for two hours at 180 rpm and centrifuged at 25 rpm for 15 minutes. The supernatant was passed though an ashless Whatman no 42 filter paper. Extraction using HNO_3, as described, is thought to be an indication of the upper-limit of environmental heavy metal availability.

All samples were read on a Spectro Genesis, axially viewed ICP-AES. Blank as well as reference samples were included. Prior to extraction all glassware and equipment used were suspended in a 1:10 HNO_3 solution for 24 hours and washed using ultra-pure water to limit contamination. Throughout the study only ultra-pure water and reagents of analytical grade were used. Supernatant pH was determined on an additional three samples for each extractant and subjected to the extraction methodology as described.

Statistical analysis entailed the use of SAS 9.1. To investigate significant differences, analysis of variance (ANOVA) tables were compiled and the Tukey t-test conducted. The respective Least Squares Difference (LSD) values were derived at 5 % confidence interval levels.

5.4 Results and discussion

5.4.1 Slag reactivity

The relative neutralising capacity (RS) and degree to which the initial soil pH of 4.33 was influenced by each slag are summarised in table 5.1. Clearly, the proposed method for calculating slag's capacity to neutralise soil predicts both the Highveld steel slag and Columbus steel slag to be less effective in neutralising soil pH than analytical grade $CaCO_3$. Table 5.2, however, indicates that the neutralising capacities of both slag samples were underestimated. While $CaCO_3$ adjusted the soil pH to 6.52, amendment using the slag samples led to pH value of almost one pH unit higher than aimed for. The method proposed by Bornmann (1985), therefore, needs to be further researched and the necessary adjustments made to enable a more accurate calculation of final soil pH.

Table 5.1 Relative neutralising capacity (RS) of the slag samples used

Treatment	*pH (H_2O)	RS (%)
Soil	4.33 (0.03)	-
$CaCO_3$	5.96 (0.04)	100
Highveld slag	5.01 (0.04)	41.8
Columbus slag	5.29 (0.03)	58.7

*** Value in brackets indicates STdev**

Table 5.2 Determined pH for each treatment after an equilibration period of three months

Treatment	*pH (H_2O)
Control	4.33 (0.03)
$CaCO_3$	6.52 (0.08)
Highveld steel slag	7.47 (0.08)
Columbus steel slag	7.55 (0.07)

***Value in brackets indicates STdev**

The EPA 3051A derived values of Cr and Ni can be regarded as pseudo-total values, while HNO_3 extraction gives an estimate of the long-term environmental availability of the elements investigated when the inherent slag alkalinity is neutralised (equilibrium pH after extraction below one). Table 5.3 summarises the EPA 3051A and HNO_3 extractable heavy metal levels from the slag.

Table 5.3 1.0 M HNO_3 extractable metals from the slag samples used

Slag samples	*Cr (mg.kg^{-1})	*Ni (mg.kg^{-1})	*pH (H_2O)
Highveld (EPA)	793 (171)	31 (5.5)	-
Highveld (HNO_3)	544 (9.87)	10.3 (1.04)	0.41 (0.01)
Columbus (EPA)	934 (73.2)	232 (75.6)	-
Columbus (HNO_3)	1091 (65.7)	203 (21.8)	0.29 (0.01)

*** Value in brackets indicates Stdev**

Some discrepancies were noticed in the results obtained from the EPA 3051A and HNO_3 extraction methods. Table 5.3 illustrates that higher levels of Cr were extracted by HNO_3 than through the EPA 3051A method from the Columbus steel slag. Because a repetition of the HNO_3 extraction yielded similar results to these presented, it is believed that the EPA 3051A results (which were outsourced) are suspect. For the purposes of this study, only the HNO_3 extracted levels of Cr and Ni are considered.

From table 5.3 it is evident that the Columbus steel slag contains high Cr and Ni levels. It should be kept in mind, however, that none of the slag samples will dissolve completely within a three-month period and that not all of the heavy metals contained by these slag matrixes will yet have been released into the soil environment. It is therefore important not to be tempted to express the extracted Cr and Ni fractions from the soil-slag mixture as a percentage of the values listed in table 5.3.

5.4.2 Heavy metal release

Although the difference in pH between treatments does not allow such a clear-cut comparison of heavy metal release from the slag samples as was hoped for, the extent to which Cr and Ni released from the slag matrixes is sequestered by the soil can still be assessed. Furthermore, this difference does allow an investigation into the influence of pH on heavy metal release.

Figure 5.1 and table 5.4 depict Cr extractability using the various extractants discussed. Table 5.4 further indicates the contribution of each slag to the extractable Cr fraction. This is calculated by subtracting the values derived for each slag from the $CaCO_3$ amended treatment values. Owing to the difference in pH between the slag-soil mixture and the $CaCO_3$-soil mixture, these values should be seen as possibly an underestimation of the contribution of slag to the cationic heavy metal values, but an overestimation of the anionic heavy metal values. The higher pH of the slag-soil mixture should lead to a more effective sequestration of cationic species, as opposed to the $CaCO_3$-soil mixture, but a less effective sequestration of anionic species. The same principles are applied to the contribution of the slag samples to the environmental extractability of Ni.

Figure 5.1 and table 5.4 show $Mg(NO_3)_2$ extractable Cr to be below the method detection limit, even when read against a parts per billion standard range. Although extracting higher concentrations, EDTA did not yield Cr levels that can be regarded as substantially higher. Nonetheless, the concentrations of Cr mobilised by $NH_2OH.HCl$ and Tamm's reagent should be taken seriously. As $NH_2OH.HCl$ and Tamm's reagent are said to predominantly dissolve amorphous Mn oxide minerals and amorphous Al and Fe oxide minerals, respectively (Hlavay *et al*., 2004), the Cr fraction dissolved by these extractants can be regarded as being associated with the amorphous sesquioxide content of the soil. The hypothesised affinity of oxalate for Cr(III) (as investigated in chapter 3) should be kept in mind.

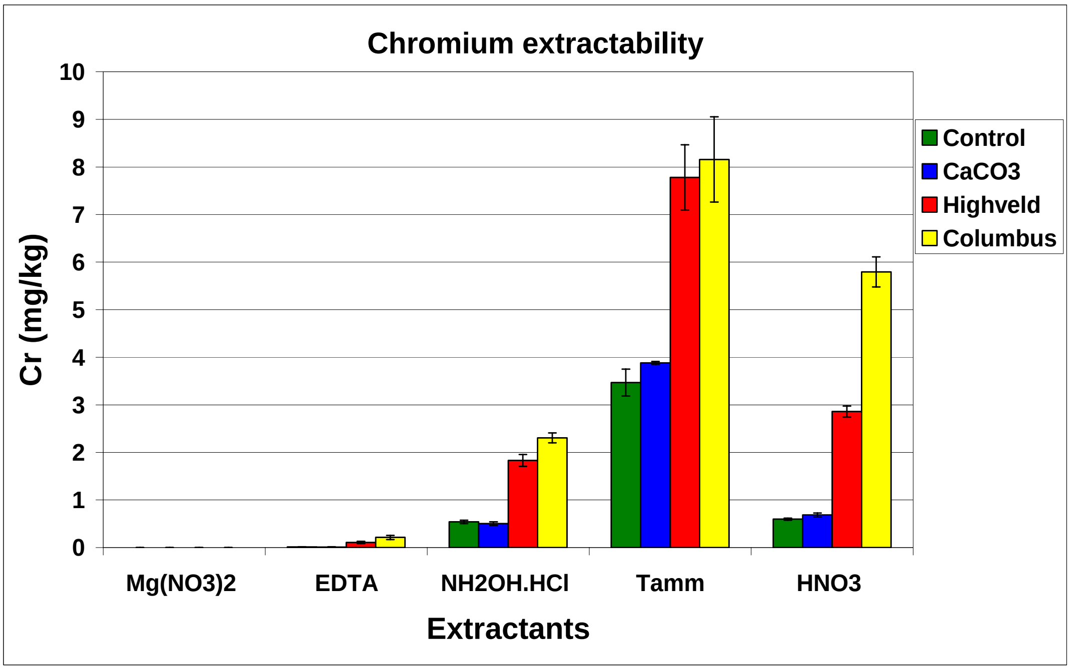

Figure 5.1 Environmental extractability of Cr

Between the Cr values derived from the control and $CaCO_3$ treatment, no significant difference could be noted for any of the extractants, Tamm's reagent being the exception. The similar values between the control and $CaCO_3$ treatment can either be ascribed to Cr being held in a relative inert mineralogical structure or to pH not contributing as significantly to Cr mobility. The substantially higher Cr fraction yielded by Tamm's reagent compared with HNO_3 seem to suggest the latter.

The oxalate in Tamm's reagent is thought to show a high affinity for Cr, thus mobilising the element not solely through the dissolving of amorphous Al and Fe oxide minerals, but especially through specific binding and ligand promoted dissolution. Extraction of Cr by HNO_3 can be ascribed to the exchange of H^+ for

Cr(III), but in particular the dissolution of sesquioxide, clay minerals and the precipitated Cr phase. The fact that the pH 3.0, Tamm's reagent solution extracted significantly more ($P<0.001$) Cr than the pH 0.0, HNO_3 solution substantiates the notion that Cr is rather mobilised through specific binding by agents such as oxalate and a weakening of the Cr-mineral bond, but is not as sensitive to pH change.

Tamm's reagent extracted a mean Fe concentration of 1206 $mg.kg^{-1}$ and Al concentration of 815 $mg.kg^{-1}$, whereas HNO_3 extracted a mean Fe concentration of 326 $mg.kg^{-1}$ and Al concentrations of 1621 $mg.kg^{-1}$. Data derived from previous studies (chapter 3) that suggested an affinity of amorphous Fe oxide minerals for Cr seem to be substantiated. But the oxidation of Cr(III) to Cr(VI) should not be disregarded as a possibility in Mn oxide dominated soils. An investigation into the extent to which Cr(III) is oxidised to Cr(VI) under natural soil environments is therefore a necessity.

Furthermore, an investigation into Cr speciation in slag and slag-amended soil is important. Although first or second hydrolysis Cr(III) species is the most stable form of Cr between pH 4 and 8 (Bradl, 2004; Fendorf, 1994) and Eh values of -200 to 500 mV (Stepnieskwa, Bucior and Bennicelli, 2004), Cr(VI) may still dominate the soil solution if this were the species predominantly dissolved from the slag samples and not reduced by organic matter, sulphides or Fe(II). Whereas Cr(III) is specifically sorbed by most soil mineral surfaces (Fendorf, Li and Gunter, 1996; Fendorf and Sparks, 1994; Fendorf, 1994; Charlet and Manceau, 1992; Rengasamy and Oades, 1978), Cr(VI) is much more mobile and less effectively sorbed at higher pH conditions (Fendorf, 1994).

Table 5.4 exhibits the contribution of the Highveld steel and Columbus steel slag to extractable Cr levels in the soil. When comparing these results with table 5.3, it is clear that the higher the Cr content of the slag, the more Cr is extracted from the soil. Although the extracted Cr levels comprised only a small fraction of the levels contained by the slag samples, oxidised to Cr(VI) these levels will pose a threat to the environment when leached and accumulated deeper down the soil profile or lower lying areas (if not already constituting a major Cr(VI) fraction). Being a strong oxidising agent, corrosive, and a potential carcinogen, coupled with its ability to penetrate biological membranes, Cr(VI) is toxic to all living organisms (Hu and Deming, 2005; Reddy *et al*., 1997; Turner and Rust, 1971) in concentrations as low as 0.5 mg.kg^{-1} in solution and 5 mg.kg^{-1} in soils (Fendorf, 1994). It is a matter of concern that the Cr levels extracted from the soil were more than doubled when adding either of the slag samples, regardless of the extractant used. When considering that more than 5 mg.kg^{-1} Cr has been extracted from the Columbus steel slag using HNO_3, the leaching and accumulation of Cr from soil amended with slag for a number of decades may become a hazard.

Table 5.4 Environmental extractability of Cr and the contribution of slag

Extractant	**Treatment (mg.kg^{-1})**				***Slag contribution (mg.kg^{-1})**	
	Control	**$CaCO_3$**	**Highveld**	**Columbus**	**Highveld**	**Columbus**
$Mg(NO_3)_2$	- j	- j	- j	- j	-	-
EDTA	0.015j	0.012j	0.109ij	0.213hij	0.097	0.2
$NH_2OH.HCl$	0.54ghi	0.504ghi	1.83f	2.31e	1.33	1.8
Tamm's reagent	3.47c	3.88c	7.78a	8.16a	3.9	4.27
HNO_3	0.597gh	0.688g	2.86d	5.8b	2.17	5.11
LSD (.05)	0.455					

*** Calculated by subtracting the slag treatment from the $CaCO_3$ treatment**

Figure 5.2 and table 5.5 summarise the environmental extractability of Ni. With the exception of the Ni extracted with Tamm's reagent, significantly higher ($P<0.001$) Ni concentrations were extracted from the control treatment compared with the $CaCO_3$ treatment. Keeping in mind that the control treatment exhibited a pH of 4.33 and the $CaCO_3$ treatment a pH of 6.52 prior to analyses, it becomes clear that pH has a major effect on Ni mobility.

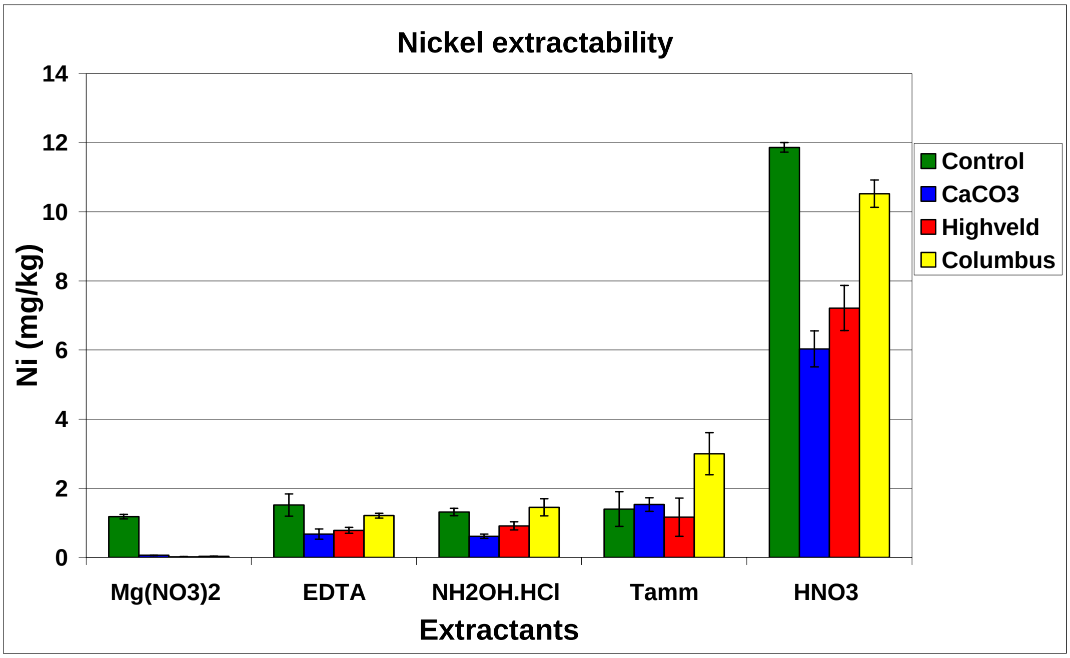

Figure 5.2 Environmental extractability of Ni

The significantly higher ($P<0.001$) fraction of Ni extracted by both $Mg(NO_3)_2$ and EDTA from the control treatment as opposed to the liming treatments suggests that a major fraction of Ni is bound through electrostatic forces, inner-sphere complexation and easily dissolvable precipitates at lower pH values. At higher pH values the extractable Ni decreased significantly ($P<0.001$), even after the addition of Ni containing slag. This is an indication that an increase in pH and negatively charged binding sites will render Ni less mobile. Note that no substantial difference between $Mg(NO_3)_2$, EDTA, $NH_2OH.HCl$ or Tamm's reagent extractable Ni was observed when comparing the control treatment of each, thus suggesting that less Ni in the soil, prior to amendment with liming agents, is found imbedded in the crystal structures of sesquioxide and clay minerals or precipitated as stable phases.

It was initially thought that the greater mobilisation of Ni from the control treatment as opposed to the liming treatments was owing to a difference in after-extraction soil pH between treatments. It would seem logical that the control sample would buffer a change in pH induced by the extractants less effectively than the liming treatments, thus rendering Ni more mobile in the former treatment. Table 5.6, however, denounces the notion. While lesser extractants [$Mg(NO_3)_2$, EDTA and $NH_2OH.HCl$], as predicted, could not overcome the buffer capacity of the soil and liming agents, pH values measured for each treatment after using Tamm's reagent and HNO_3 as extractants were found to be close to the extractant pH values. Although overcoming the buffering capacity of the soil and liming agents, the inclination of Tamm's reagent to dissolve a specific fraction of the soil and slag phase renders this extractant unsuitable as an indicator of the effect of pH on Ni extractability.

Table 5.5 Environmental extractability of Ni and the contribution of slag

Extractant	**Treatment ($mg.kg^{-1}$)**				***Slag contribution ($mg.kg^{-1}$)**	
	Control	**$CaCO_3$**	**Highveld**	**Columbus**	**Highveld**	**Columbus**
$Mg(NO_3)_2$	1.18fghi	0.064k	0.022k	0.031k	-	-
EDTA	1.52f	0.677ij	0.785hij	1.21fgh	0.107	0.532
$NH_2OH.HCl$	1.31fghij	0.613j	0.913ghij	1.45f	0.3	
Tamm's reagent	1.4fg	1.15fghi	1.16fghi	3e	-	1.47
HNO_3	11.9a	6.03d	7.22c	10.5b	1.15	4.49
LSD (.05)	0.519					

*** Calculated by subtracting the slag treatment from the $CaCO_3$ treatment**

HNO_3, however, exemplifies the effect of pH on Ni extractability owing to its unspecified dissolution of mineral phases, as well as desorption through proton substitution. The environmental extractability of Ni is, therefore, governed by the soil pH where chemical equilibrium is induced and not influenced (in the short run) by a sudden drop in pH. As Ni is sequestered most effectively at pH values between 5.5 and 6.5 (Schwertmann and Taylor, 1989), it can be hypothesised that Ni sequestration below pH 5.5 will lead to more readily displaceable or dissolvable phases, as opposed to Ni phases formed at pH values above 6.5.

Table 5.6 Supernatant pH determined for each treatment after being subjected to the various extractants

Treatment	***$Mg(NO_3)_2$**	***EDTA**	***$NH_2OH.HCl$**	***Tamm's reagent**	***HNO_3**
Control	3.71 (0.03)	3.99 (0.01)	2.27 (0.02)	3.54 (0.02)	0.46 (0.02)
$CaCO_3$	5.62 (0.08)	4.24 (0.01)	2.67 (0.04)	3.55 (0.02)	0.48 (0.02)
Highveld steel	6.42 (0.08)	4.48 (0.01)	3.39 (0.02)	3.57 (0.02)	0.47 (0.02)
Columbus steel	6.57 (0.01)	4.50 (0.05)	3.43 (0.03)	3.56 (0.01)	0.48 (0.01)

***Value in brackets indicates STdev**

Only when using Tamm's reagent as an extractant was no significant decrease noted between Ni extracted from the control treatment and that from the $CaCO_3$ treatment. It is thought that Ni associates with the amorphous Fe oxide mineral phase, but does not show the same affinity for the amorphous Mn oxide phase, as indicated by the difference between the control treatment and $CaCO_3$ treatment when subjected to extraction using $NH_2OH.HCl$. Findings regarding the association of Ni with the amorphous Fe oxide phase (chapter 3) are, therefore, substantiating.

From table 5.5 it is clear that the Ni levels extracted by Tamm's reagent were doubled by the Columbus steel slag, compared with the $CaCO_3$ treatment. The difference in pH between these treatments may, however, lead to an underestimation of the Columbus steel slag's contribution, although the maximum sequestration capacity of the soil for Ni may have been reached at pH 6.5. Deduced from data derived from the HNO_3 extractable Ni fraction, it is clear that both Highveld steel and Columbus steel slag contribute to a loading of the soil with Ni. Unlike the influence of the Highveld steel slag, the Columbus steel slag does increase the environmental extractable Ni fraction substantially when compared with the $CaCO_3$ treatment. Although (as mentioned) the HNO_3 extractable Ni level increased by a potentially underestimated 174 % after amendment with Columbus steel slag, the control treatment Ni concentrations still overshadowed this increase. A substantial amount of Ni is therefore sequestered effectively by the soil at high pH levels. In addition, and as demonstrated using HNO_3 as an extractant, Ni phases precipitated at high pH values (greater than 6.5) seem not to be remobilised owing to a sudden drop in pH.

The risk Ni-rich steel plant slag – such as the Columbus steel slag – poses to environmental and human health may thus only become significant in a slag-amended soil that has been left to acidify, and has not been tended to for a certain period. This period cannot be specified without further research. It can be hypothesised, however, that the chemical and physical weathering of Ni phases in the acidified soil would lead to a release of Ni into the soil solution, and that these molecules would not be sequestered effectively under low pH conditions. The high levels of Ni extracted from the control sample, which represents the natural state of the soil, is enough evidence to substantiate the notion that Ni released through weathering, albeit from rock, slag or secondary formed minerals, will be sequestered effectively only under neutral to alkaline pH conditions. Because South African soils do tend to acidify if not limed regularly, Ni mobility may become pronounced in untended soils that have been amended with slag for years or decades.

5.5 Conclusion

When investigating the reactivity of the Highveld steel and the Columbus steel slag and their heavy metal release, a highly buffered, acid soil was identified, and a pH adjustment to 6.5 was attempted, using the slag. The relative neutralising capacity of both slag samples was underestimated by a method used regularly to determine the liming capabilities of slag. The method proposed by Bornmann (1985) should therefore be investigated and reassessed. Owing to the subsequent difference in pH between control and liming treatments, the release of Ni from the slag samples was underestimated. Nonetheless, the effect of pH on Cr and Ni, as well as the contribution of slag to heavy metal levels in the soil, could be investigated.

Cr extractability was found not to be significantly affected by pH. Ni extractability, however, was substantially influenced by pH and the sequestration of Ni by soil constituents was found to be more effective at higher pH conditions. The long-term application of Ni-containing slag, such as the Columbus steel slag, should therefore be monitored and slag-amended soils should not be allowed to acidify. Ni mobilisation from soil that has been limed by a Ni-containing slag for a few years or decades will become a serious threat once liming is discontinued. Furthermore, Cr speciation and the oxidation of Cr(III) to Cr(VI) under natural soil conditions should be investigated, as both the Columbus steel and Highveld steel slag doubled the extractability of Cr after they have been added.

The effect of heavy metals from slag on environmental and human health will probably be realised only after years and decades of slag addition to the soil. Constant research on heavy metal interaction with soil constituents and the discerning use of slag in the environment is therefore imperative.

5.6 References

ABOLLINO, O., ACETO, M., MALANDRINO, M., SARZANINI, C. and MENTASTI, E. 2002. Adsorption of heavy metals on na-montmorillonite. Effect of pH and organic substances. *Water research*, 37:1619–1627.

AMACHER, M.C. 1996. Nickel, cadmium and lead. In: *Methods of Soil Analysis.* Part 3 – Chemical Methods. Editor: D.L. Sparks. SSSA Book Series no 5. Soil Science Society of America, American Society of Agronomy, Madison, Wisconsin, USA, pp 749–750.

BALASOIU, C.F., ZAGURY, G.J. and DESHêNES, L. 2000. Partitioning and speciation of chromium, copper and arsenic in CCA-contaminated soils: Influence of soil composition. *The Science of the Total Environment*, 280:239–255.

BARTLETT, R.J. and JAMES, B. 1979. Behaviour of chromium in soils: III. Oxidation. *Journal of Environmental Quality,* 5:31–35.

BERTSCH, P.M. and BLOOM, P.R. 1996. Aluminium. *Methods of Soil Analysis*. Part 3 – Chemical Methods. Editor: D.L Sparks. SSSA Book Series no 5. Soil Science Society of America, American Society of Agronomy, Madison, Wisconsin, USA, p 530.

BORNMANN, J.J. 1985. ‘n Suspensiemetode vir die evaluering van landboukalk. MSc thesis. University of Pretoria.

BRADL, H.B. 2004. Adsorption of heavy metal ions on soils and soil constituents. *Journal of Colloid and Interface Science,* 277:1–18.

BRADY, N.C. and WEILL, R.P. 1999. *The Nature and Properties of Soils*. Twelfth edition. Prentice Hall, Upper Saddle River, New Jersey, pp 119, 126, 202–204, 311.

CHARLET, L. and MANCEAU, A.A. 1992. X-ray adsorption spectroscopy study of the sorption of C(III) at the oxide-water interface: I. Molecular mechanisms of Cr(III) oxidation by Mn oxides. *Journal of Colloidal Interface Science,* 148:425–442.

CHRISTENSEN, T.H., LEHMANN, N., JACKSON, T. and HOLM, P.E. 1996. Cadmium and nickel distribution coefficients for sandy aquifer materials. *Journal of Contaminant Hydrology,* 24:75–84.

COOPER, G.R.C. 2002. Oxidation and toxicity of chromium in ultramafic soils of Zimbabwe. *Applied Geochemistry,* 17:981–986.

DoE 1996. *Code of Practice for the Agricultural Use of Sewage Sludge*. Second edition. UK: Department of Environment.

EARY, L.E. and RAI, D. 1989. Kinetics of chromate reduction by ferrous ions derived from hematite and biotite at 25°C. *American Journal of Science,* 289:180–213.

EGGLESTON, C.M. and STUMM, W. 1993. Scanning tunneling microscopy of Cr(III) chemisorbed on α-Fe_2O_3 (001) surface from aqueous solution: Direct observation of surface mobility and clustering. *Geochimica et Cosmochimica Acta,* 57:4843–4850.

FENDORF, S.E. 1994. Surface reactions of chromium in soils and waters. *Geoderma,* 67:55–71.

FENDORF, S.E., LI, G. and GUNTER, M.E. 1996. Micromorphologies and stabilities of chromium(III) surface precipitates elucidated by scanning force microscopy. *Soil Science Society of America Journal,* 60:99–106.

FENDORF, S.E. and SPARKS, D.L. 1994. Mechanisms of chromium(III) sorption onto silica. II: Effect of reaction conditions. *Environmental Science and Technology,* 28:290–297.

GAMBRELL, R.P. 1996. Manganese. In: *Methods of Soil Analysis.* Part 3 – Chemical Methods. Editor: D.L Sparks. SSSA Book Series no 5. Soil Science Society of America, American Society of Agronomy, Madison, Wisconsin, USA, pp 678, 750.

HLAVAY, J., PROHASKA, T., WEISZ, M., WENZEL, W.W. and STINGEDER, J.G. 2004. Determination of trace elements bound to soil and sediment fractions. IUPAC Technical Report. *International Union of Pure and Applied Chemistry*, 76(2):425–442.

HODGES, S.C. and ZELANSKY, 1980. Determination of noncrystalline soil components by weight difference after selective dissolution. *Clays and Clay Mineralogy*, 28:35–42.

HO HSU, PA. 1989. Aluminium oxides and oxyhydroxides. In: *Minerals in the Soil Environment.* Edited by J.B. Dixon and S.B. Weed. SSSA Book Series no 1. Soil Science Society of America, Madison, Wisconsin, USA, pp 331–371.

HU, G. and DEMING, R.L. 2005. Speciation of bio-available chromium in soils by solid-phase extraction and graphite furnace atomic absorption spectrometry. *Analytica Chimica Acta,* 535:237–242.

JEAN, L., BORDAS, F. and BOLLINGER, J.C. 2006. Chromium and nickel mobilization from a contaminated soil. *Environmental Pollution*, 147:729–739.

JEON, B.H., DEMPSEY, B.A., BURGOS, W.D. and ROYER, R.A. 2003. Sorption kinetics of Fe(II), Zn(II), Co(II), Ni, Cd(II) and Fe(II)/Me(II) onto hematite. *Water Research,* 37:4135–4142.

KABATA-PENDIAS, A. and PENDIAS, H. 1984. *Trace elements in soils and plants*. Bacon Raton, Florida: CRC, p 178.

KEDZIOREK, M.A.M. and BOURG, A.C.M. 1996. Acidification and solubilisation of heavy metals from single and dual-component model solids. *Applied Geochemistry,* 11:299–304.

KRASNODEBSKA-OSTREGA, B., EMONS, H. and GOLIMOWSKI, J. 2001. Selective leaching of elements associated with Mn–Fe oxides in forest soil, and comparison of two sequential extraction methods. *International Journal of Environmental Analytical Chemistry*, 371:385–390.

LOEPPERT, R.H. and INSKEEP, W.P. 1996. Iron. In: *Methods of Soil Analysis*. Part 3 – Chemical Methods. Editor: D.L. Sparks. SSSA Book Series no 5. Soil Science Society of America, American Society of Agronomy, Madison, Wisconsin, USA, pp 648–649.

LUO, Y.M. and CHRISTIE, P. 1997. Choice of extraction technique for soil reducible trace metals determines the subsequent oxidizable metal fraction in sequential extraction schemes. *International Journal of Environmental Analytical Chemistry,* 72:59–75.

NON-AFFILIATED SOIL ANALYSIS WORK COMMITTEE. 1990. *Handbook of Standard Soil Testing Methods for Advisory Purposes*. Soil Science Society of South Africa, p 3/1.

NOWACK, B. and SIGG, L. 1997. Dissolution of Fe(III) (hydr)oxides by metal-EDTA complexes. *Geochimica et Cosmochimica Acta*, 61:951–967.

REDDY, K.R., PARUPUDI, U.S., DEVULAPALLI, S.N. and XU, C.Y. 1997. Effects of soil composition on the removal of chromium by electrokinetics. *Journal of Hazardous Materials,* 55:135–158.

RENGASAMY, P. and OADES, J.M. 1978. Interactions of aluminium (III) and chromium(III). *Australian Journal of Soil Resources,* 16:53–66.

SALEH, F.Y., PARKENTON, T.F., LEWIS, R.V., HUANG, J.H. and DICKSON, K.L. 1989. Kinetics of chromium transformation in the environment. *Science of the Total Environment,* 86:25–41.

SCHEIDEGGER, A. M., FENDORF, M. and SPARKS, D.L. 1996. Mechanisms of nickel sorption on pyrophillite: Macroscopic and microscopic approaches. *Soil Science Society of America Journal,* 60:1763–1772.

SCHWERTMANN, U. 1991. Solubility and dissolution of Fe oxides. In: *Iron Nutrition and Interaction with Plants*. Edited by Chen, Y. and Hadar, Y. Dordrecht, Netherlands: Kluwer, pp 3–27.

SCHWERTMANN, U, and TAYLOR, R.M. 1989. Iron oxides. In: *Minerals in the Soil Environment.* Second edition. Edited by Dixon, J.B. and Weed, S.B. SSSA Book Series no 1. Soil Science Society of America Madison, Wisconsin, pp 409–415.

SPARKS, D.L., 2003. *Environmental Soil Chemistry*. 2nd edition. Academic Press, pp 54, 60, 67, 177, 259.

STEPNIEWSKA, Z., BUCIOR, K. and BENNICELLI, R.P. 2004. The effect of MnO_2 on sorption and oxidation of Cr(III) by soils. *Geoderma,* 122:291–296.

TRIVEDI, P., AXE, L. and DYER, J. 2001. Adsorption of metal ions onto goethite: Single-adsorbate and competitive systems. *Journal of Colloid and Surface Chemistry,* 191:107–121.

TURNER, M.A. and RUST, R.H. 1971. Effects of chromium on growth and mineral nutrition of soyabeans. *Soil Science Society of America Journal,* 35:2145–2150.

YAVUZ, O., ALTUNKAYNAK, Y. and GŰZEL, F. 2003. Removal of copper, nickel, cobalt and manganese from aqueous solution by kaolinite. *Water Research,* 37:948–952.

ZACHARA, J.M., AINSWORTH, C.C., COWAN, C.E. and RESCH, C.T. 1987. Adsorption of chromate by subsurface soil horizons. *Soil Science Society of America Journal,* 53:418–428.

ZACHARA, J.M., GIRVIN, D.C., COWAN, C.E. and RESCH, C.T. 1989. Chromate adsorption on amorphous iron oxyhydroxide in the presence of major groundwater ions. *Environmental Science and Technology,* 21:589–594.

Chapter 6 Summary and concluding remarks

6.1 Introduction

Heavy metal contamination and pollution are ever-growing concerns. Many of these toxic substances, such as chromium and nickel, not only endanger the equilibrium of natural systems, but also pose a major threat to all living organisms. Although heavy metal ions are frequently found embedded in the crystal lattices of many naturally occurring minerals, it was the Industrial Revolution that brought about production of heavy-metal-rich waste that is still expanding. Great volumes of metallurgical slag, fly-ash, leather tannery waste and electroplating waste, for instance, are being produced annually: discarded onto heaps, used as cements, bricks, road-construction material, and agricultural liming agents.

Since the adsorption of heavy metals onto soil mineral surfaces has been recognised as a significant means of control of metal toxicity in the environment, much has been done to elucidate and predict mechanisms by which these processes occur. Especially in recent years, heavy metal transformation and sorption mechanisms have been researched and reviewed intensely in the hope of finding some basic principles that may be applied without difficulty and controversy.

Nature has not revealed all, however. Although progress is being made, a sufficient understanding of heavy metal sorption and precipitation, especially regarding multi-component systems and soil environments, is still lacking. The logical next step would therefore entail an investigation into heavy metal mobility in the soil environment. This study aimed to contribute to this.

For these purposes Eastern Highveld soils formed the basis. Investigating the interactions of Cr(III) and Ni with certain soil constituents entailed the following areas of research: (i) the environmental extractability of Cr(III) and Ni within a single wetting and drying cycle, as well as the effect of soil water potential on it; (ii) the extractability of Cr(III) and Ni over a period of five rewetting and drying cycles as influenced by an external source of Si; and (iii) the solubility and subsequent release of heavy metals (Cr and Ni) from two commercially available slag samples in a highly buffered soil. The findings are summarised.

6.2 Salt-based study: Cr(III) and Ni extractability

A number of conclusions regarding the environmental extractability of Cr(III) and Ni could be drawn:

(i) Whereas Cr(III) is predominantly sorbed through polydentate inner-sphere complexation and polymerisation at near water saturation, Ni is rather to be found in the diffuse double layer and sorbed through outer-sphere and weak inner-sphere complexes.

(ii) Cr(III) is rendered immobile mainly owing to bulk-solution saturation, although mineral-induced precipitation does contribute.

(iii) Ni precipitation is governed by the effect of mineral phases, although bulk-solution precipitation dominates near air dried conditions.

(iv) Cr(III) and Ni both associate mainly with the Fe fraction in the soils investigated.

(v) Ni – and to a lesser degree Cr(III) – shows a decrease in extractability over a period of five rewetting and drying cycles only in the soil exhibiting a higher 2:1 clay content and cation exchange capacity.

(vi) An external source of Si, as found in the vicinity of dissolving slag, renders Ni less mobile in soils that do not sequester the element effectively, but more mobile in the soil that sequestered the element more effectively. The latter is attributed to the formation of a thermokinetically favoured amorphous or microcrystalline Ni silicate phase. The Ni silicate phase could not withstand extraction using more effective extractants than 0.1 M $Mg(NO_3)_2$.

6.3 Slag-based study: Cr and Ni extractability

Apart from highlighting the reactivity of the Columbus steel and Highveld steel slag as liming agents, the following deductions can be made regarding heavy metal extractability:

(i) Cr extractability is not significantly influenced by pH and seems to be sequestered rather effectively by the soil tested, although the environmental extractability of Cr doubled after the addition of the Columbus steel slag.

(ii) Ni extractability is governed by pH, thus indicating the formation of outer-sphere complexes and weakly held inner-sphere complexes at low pH conditions. Although sequestered effectively at high pH values, the weathering of precipitated Ni phases in acidifying soils once amended with slag for a number of decades may lead to a pronounced leaching of Ni.

6.4 Conclusion

When assessing the use of steel plant slag in agriculture, a characterisation of the slag sample to be used and a detailed knowledge of heavy metal interaction with soil constituents are of utmost importance, and also a clear understanding of water discharge, heavy metal leachability and movement through the landscape. Without a comprehensive knowledge of heavy metal dynamics in the soil environment, predictions regarding the sustainable use of steel plant slag in agriculture cannot be made.

It would seem plausible, however, to reach certain conclusions regarding the prediction of Cr(III) and Ni mobility in the environment:

(i) Field classifiable soil characteristics (soil colour and texture) cannot be used to predict Cr(III) and Ni mobility.

(ii) Laboratory determinable characteristics (i.e. CEC, AEC, mineralogy) should be further researched and may yet yield predictive capabilities. Furthermore, soil water potential levels have been shown to influence the Ni sorption capacity of soil and necessitate an understanding of soil water movement. Soils subject to periodic conditions of reduction may be shown to discharge higher levels of both Cr(III) and Ni as these elements predominantly associate with the amorphous Fe oxide mineral phase in soil. Under conditions of reduction, Fe(III) can be reduced to Fe(II), thus mobilising sorped or precipitated Cr(III) and Ni phases. The effect of newly formed Cr(III) and Ni phases on the reducibility of Fe(III) still needs to be researched.

Although progress is being made, a comprehensive understanding of heavy metal mobility in the natural environment has not been attained. Nonetheless, only by attempting to grasp the complexity of metal sorption onto mineral surfaces and soil constituents can heavy metal pollution be assessed and managed; thereby limiting the environmental risks posed by these elements.